Aus dem Institut für Veterinär-Anatomie
des Fachbereichs Veterinärmedizin
der Freien Universität Berlin

Expression of VIM, TPI and MAT2A and their impact on *in vitro* angiogenesis in human dermal microvascular endothelial cells

Inaugural-Dissertation
zur Erlangung des akademischen Grades eines
Doctor of Philosophy (PhD)
of Biomedical Sciences
an der
Freien Universität Berlin

vorgelegt von
Christina Nicole Herre
Tierärztin aus Bad Neustadt an der Saale

Berlin 2024
Journal-Nr.: 4466

mbvberlin | mensch und buch verlag

Aus dem Institut für Veterinär-Anatomie
des Fachbereichs Veterinärmedizin
der Freien Universität Berlin

Expression of VIM, TPI and MAT2A and their impact on *in vitro* angiogenesis in human dermal microvascular endothelial cells

Inaugural-Dissertation
zur Erlangung des akademischen Grades eines
Doctor of Philosophy (PhD)
of Biomedical Sciences
an der
Freien Universität Berlin

vorgelegt von
Christina Nicole Herre
Tierärztin aus Bad Neustadt an der Saale

Berlin 2024
Journal-Nr.: 4466

Gedruckt mit Genehmigung des Fachbereichs Veterinärmedizin

der Freien Universität Berlin

Dekan:	Univ.-Prof. Dr. Uwe Rösler
Erster Gutachter:	Univ.-Prof. Dr. Mahtab Bahramsoltani
Zweiter Gutachter:	Univ.-Prof. Dr. Robert Klopfleisch
Dritter Gutachter:	Univ.-Prof. Dr. Salah Amasheh

Deskriptoren (nach CAB-Thesaurus):
angiogenesis, endothelial cells, gene expression, cell death, cytoskeleton, metabolism, growth factors, methylation, germany

Tag der Promotion: 09.07.2024

Bibliografische Information der *Deutschen Nationalbibliothek*
Die Deutsche Nationalbibliothek verzeichnet diese Publikation in der Deutschen Nationalbibliografie; detaillierte bibliografische Daten sind im Internet über <http://dnb.ddb.de> abrufbar.

ISBN: 978-3-96729-258-9
Zugl.: Berlin, Freie Univ., Diss., 2024
Dissertation, Freie Universität Berlin
D188

 Choriner Str. 85 - 10119 Berlin
verlag@menschundbuch.de – www.menschundbuch.de

To my family

Table of content

List of tables

Tables of Publication I

Tables of Publication II

List of figures

Figures of Publication I

Figures of Publication II

List of abbreviations

ACT	Actin
ATP	Adenosine triphosphate
BM	Basal medium
CAM	Chick chorioallantoic membrane
ECs	Endothelial Cells
eGFP	Enhanced green fluorescent protein
FDA	US Food and Drug Administration
FGF	Fibroblast growth factor
GAPDH	Glyceraldehyde–3–phosphate dehydrogenase
HD1	Human dermal microvascular endothelial cells derived from neonatal foreskin batch 1
HD2	Human dermal microvascular endothelial cells derived from neonatal foreskin batch 2
HDMECs	Human dermal microvascular endothelial cells
HMBS	Hydroxymethylbilane synthase
MAT2A	S-adenosylmethionine synthetase isoform type 2
N	Native cells of human dermal microvascular endothelial cells
N_1	Native group from batch 1
N_2	Native group from batch 2
RT-qPCR	Reverse transcription-quantitative polymerase chain reaction
SAM	S-adenosylmethionine
SCR	Control cells of human dermal microvascular endothelial cells
SCR_1	Control group from batch 1
SCR_2	Control group from batch 2
SDHA	Succinate dehydrogenase complex, subunit A

sh	Knockdown cells of human dermal microvascular endothelial cells
sh_1	Knockdown group from batch 1
sh_2	Knockdown group from batch 2
TBP	TATA box binding protein
TGF-α and -β	Transforming growth factor alpha and beta
TNF- α	Tumour necrosis factor alpha
TPI	Triosephosphate isomerase
VEGF	Vascular endothelial growth factor
VEGF-A	Vascular endothelial growth factor A
VEGFR-1	Vascular endothelial growth factor receptor 1
VEGFR-2	Vascular endothelial growth factor receptor 2
VIM	Vimentin
VPF/VEGF	Vascular permeability factor/vascular endothelial growth factor

1. Introduction

Since ancient times the cardiovascular system was perceived as a matter of fascination. World-famous scientists e.g. Galen (150) and Leonardo da Vinci (1508), were elaborating and hypothesizing about the anatomy and the development of the heart and the circulatory system (Pasipoularides 2014; Risau 1997). Blood vessels regulate the exchange of nutrients and metabolites between blood and tissue, homeostasis, blood pressure and leukocyte diapedesis. Therefore, blood vessels are crucial for every living system (Makode et al. 2024; Adair and Montani 2010; Mehta and Malik 2006). Until today, major research effort is dedicated to the field of cardiovascular biology and medicine, in particular to the field of angiogenesis, since pathological angiogenesis leads to abnormal vessel formation causing or contributing to numerous diseases (Cao et al. 2023; Dudley and Griffioen 2023). An increased vascularization is mainly related to tumour growth, inflammatory diseases and infectious processes. In contrast, an insufficient vascularization is involved in diverse cardiovascular disorders (Salzinger et al. 2024; Deliyanti et al. 2023; Salewskij and Penninger 2023; Carmeliet and Jain 2000).

Based on its ubiquitous role in physiological and pathological processes, angiogenesis is targeted for treating numerous diseases. In 1971, the concept of anti-angiogenic therapy for cancer treatment was postulated for the first time (Sherwood et al. 1971) (Fig. 1). A decade later, vascular endothelial growth factor (VEGF) was found to be a major angiogenic factor driving angiogenesis in health and disease. Consequently, major research efforts were focusing on inhibiting the VEGF signalling pathway. In 2004, the US Food and Drug Administration (FDA) approved Bevaciziumab (Avastin®), a humanized anti-VEGF monoclonal antibody for treating colorectal cancer as the first anti-angiogenic drug (Yang et al. 2024b; Ferrara et al. 2005; Presta et al. 1997) (Fig.1).

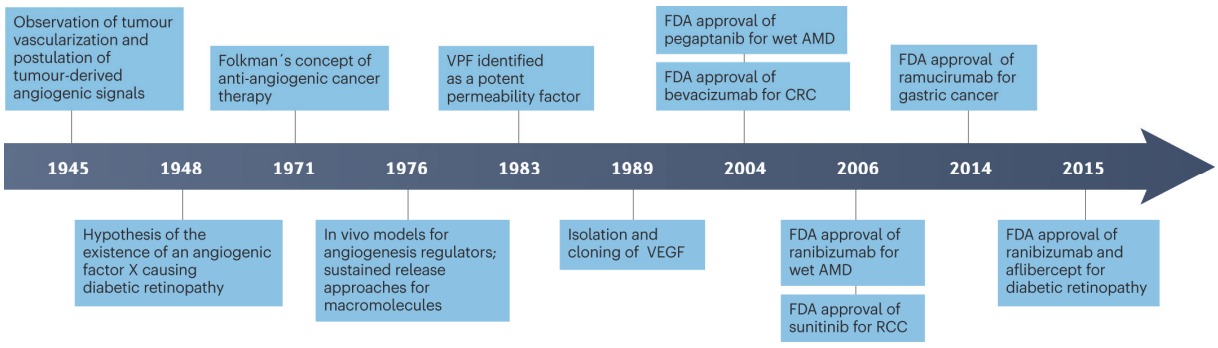

Fig. 1: Key milestones in angiogenesis research and drug discovery. AMD: age-related macular disease; CRC: colorectal cancer; RCC: renal cell carcinoma; FDA: US Food and Drug Administration; VEGF: vascular endothelial growth factor; VPF: vascular permeability factor. Modified (Cao et al. 2023).

Despite the approval of several additional drugs targeting VEGF (Fig. 1), anti-angiogenic medications still struggle with opposed clinical effects, drug resistance, short half-life, unwanted interactions with other drugs and missing biomarkers (Cao et al. 2023; Jayson et al. 2012). For treating ischemic diseases by stimulating angiogenesis, pro-angiogenic factors and pathways were intensely analysed but until today, no successful animal model was shown to be efficient in clinical trials (Zhong et al. 2020; Deveza et al. 2012; Lu et al. 2007).

Even after almost one century of research on angiogenesis, there are still unknown influencing factors on the angiogenic potency of endothelial cells (ECs) which represent one of the most significant components of blood vessels by lining their inner surface and originating angiogenesis (Orozco-Garcia et al. 2024; Ribatti and Crivellato 2012). It is necessary to identify and analyse these factors and involve them in future research. This project is focusing on three target proteins which are expressed in ECs and hypothesized to raise or reduce the angiogenic potency respectively. This study examined the connection between these proteins and *in vitro* angiogenesis in human dermal microvascular endothelial cells (HDMECs).

2. Literature review

2.1 Course of angiogenesis

Angiogenesis is defined as the formation of new blood vessels from pre-existing ones (Shaw et al. 2024; Ribatti and Crivellato 2012; Patan 2000; Risau 1997). The luminal surface of blood vessels is built by a thin layer of ECs which mainly drive angiogenesis. In order to undergo angiogenesis, quiescent ECs can get stimulated by metabolic and mechanical stress, immune response and mainly hypoxia (Orozco-Garcia et al. 2024; Zhou et al. 2024; Fan et al. 2012). Overall, this process is highly regulated and occurs as either endothelial sprouting or intussusceptive growth (Ribatti and Crivellato 2012).

2.1.1 Sprouting angiogenesis

Sprouting angiogenesis is based on the generation of new sprouts from adult vessels. This process involves specific steps of EC stimulation and migration, sprout formation, growth, luminization and finally vessel maturation (Zhou et al. 2024; Patan 2000). Each phase is mediated by accordingly adapted and specialized ECs, i.e. tip, stalk and phalanx cells (Ribatti and Crivellato 2012) (Fig. 2).

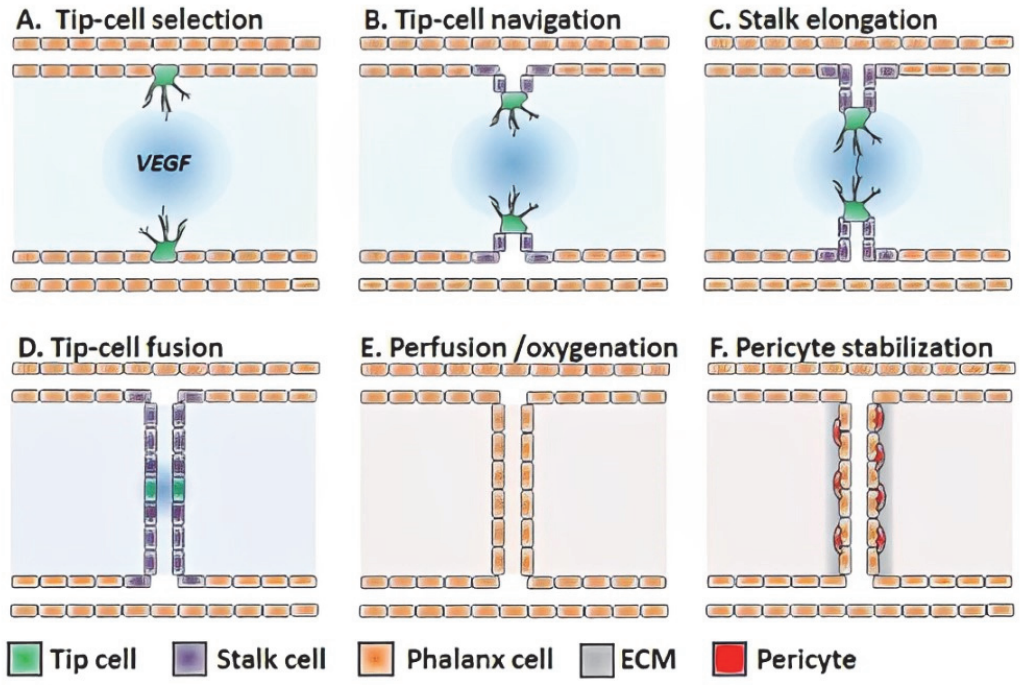

Fig. 2: Schematic overview over the course of sprouting angiogenesis of capillary ECs. A. ECs that are highest exposed to VEGF-A differentiate to tip cells. **B.** Tip cells initiate guidance by extension of filopodia towards angiogenic stimulus. **C.** Stalk cells elongate sprouts by proliferation. **D.** Sprout fusion and luminization. **E.** Initiation of blood flow resulting in oxygenation of tissue. **F.** Maturation of vessel by pericyte recruitment and deposition of basement membrane. Modified (Adair and Montani 2010).

2.1.1.1 Phalanx cells

Blood vessels are mainly lined by quiescent ECs which are thoroughly interconnected by junction proteins and molecules. These cells are termed phalanx cells (Zecchin et al. 2017) (Fig. 2). They are situated in cell cycle arrest and ensure vessel integrity. It was shown that quiescent ECs predominantly express the components of the basement membrane which they are adhesive to (Guo et al. 2024; Ribatti and Crivellato 2012; Kalluri 2003). Generally, this cell specification displays a lower glycolic flux than proliferative ECs (Zecchin et al. 2017). However, only little information has been revealed regarding their metabolism yet. Due to a decrease of nutrients and oxygen, phalanx cells can get stimulated to enter the cell cycle (Guo et al. 2024; De Bock et al. 2009).

2.1.1.2 Tip cells

As soon as an angiogenic stimulus such as hypoxia appears, pro-angiogenic factors are released from the surrounding tissue initiating the “angiogenic switch” of the endothelium (Orozco-Garcia et al. 2024; Zecchin et al. 2017; Fan et al. 2012). Single ECs exposed to the highest amount of vascular endothelial growth factor A (VEGF-A), a key pro-angiogenic factor, differentiate to so-called tip cells (Fig. 2A). Generally, tip cells perform less proliferation but more migration (Guo et al. 2024; Ribatti and Crivellato 2012). They are highly glycolytically active and they use cholesterol turnover and efflux as energy sources. These cells initiate first steps of the sprouting angiogenesis. By the expression of proteolytic cell-surface molecules, they facilitate the degradation of the basement membrane. Furthermore, the turnover of adhesion molecule VE-cadherin leads to the migration towards the stimulus (Zecchin et al. 2017). These cells express a high number of cell-surface receptors, mainly vascular endothelial growth factor receptor 2 (VEGFR-2). VEGF-A binds predominantly to VEGFR-2 which is abundant on filopodia. The sensitivity towards VEGF-A initiates filopodia formation and provides guidance of the migratory sprout towards the angiogenic stimulus (Shaw et al. 2024; Mentzer and Konerding 2014) (Fig. 2B). The activation of VEGFR-2 and the following Notch signalling pathway result in a decreased expression of VEGFR-2 in surrounding cells causing their differentiation to stalk cells (Guo et al. 2024; Fan et al. 2012; Ribatti and Crivellato 2012) (Fig. 2C).

2.1.1.3 Stalk cells

Opposed to tip cells, stalk cells are highly proliferative, display only little filopodia and predominantly express vascular endothelial growth factor receptor 1 (VEGFR-1). VEGF-A binds to VEGFR-1 and initiates the elongation of the sprout towards the angiogenic stimulus by proliferation (Shaw et al. 2024; Ribatti and Crivellato 2012; Patan 2000) (Fig. 2C). For

proliferation, stalk cells generate energy mainly by performing glycolysis and fatty acid metabolism. Sprouts from different origins grow towards each other until they meet, fuse together and luminize (Fig. 2D). Shear stress and several other mechanical signals lead to the synthesis of components of the basement membrane and the association with pericytes. As soon as the vascular supply is reassured and the angiogenic factors are decreased, ECs differentiate to quiescent phalanx cells (Zecchin et al. 2017) (Fig. 2E-F).

2.1.2 Intussusceptive angiogenesis

The non-sprouting or intussusceptive angiogenesis describes the generation of vessels due to the division of pre-existing ones (Diaz-Flores et al. 2024; Patan 2000). Equally to sprouting angiogenesis, this process is stimulated by extraluminal signals. Additionally, intussusception can be triggered by intraluminal signals, e.g. shear stress and turbulences (De Spiegelaere et al. 2012). During non-sprouting angiogenesis, ECs from opposed microvascular walls protrude into the lumen until they meet (Fig. 3a-c, a'-c'). Myofibroblasts and pericytes synthesize collagen fibrils and other components of the extracellular matrix forming a tissue pillar. Possessing an intact basement membrane, the transluminar pillar projects across the vessel and gets invaded by myofibroblasts and pericytes to divide the lumen (Diaz-Flores et al. 2024; Mentzer and Konerding 2014; Djonov et al. 2003) (Fig. 3d, d'). The process of intussusceptive angiogenesis enables vasculature to grow rapidly and extensively. The following remodelling adjusts and organises new vessels according to their hemodynamic forces. The concluding stage of intussusceptive branching remodelling causes changes in branching geometry of supplying branches (Shaw et al. 2024; De Spiegelaere et al. 2012; Djonov et al. 2003). So far, regulatory and intracellular mechanisms of ECs performing intussusceptive angiogenesis are not fully revealed.

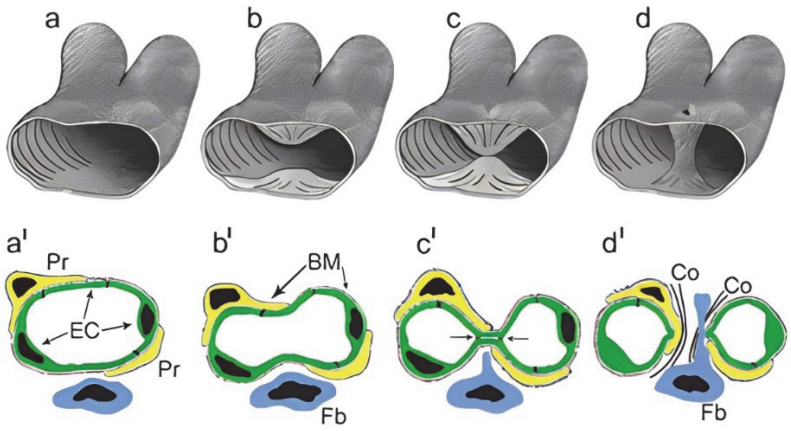

Fig. 3: Schematic overview over the course of intussusceptive angiogenesis of capillary ECs. a-b, a'-b' Protrusion of opposing ECs into vessel lumen. **c-c'** ECs establishing contact and reorganizing junctions. **d-d'** Perforation of EC bilayer perforates and pericytes and fibroblasts form a tissue pillar. Pr: pericyte; EC: endothelial cell; Fb: fibroblast; BM: basement membrane; Co: collagen fibrils. Modified (Adair and Montani 2010).

2.2 Field of angiogenesis research

In 1971 Judah Folkman and his team published the revolutionary hypothesis about the correlation of tumour growth and angiogenesis. They suggested that tumours require blood vessels to grow and survive and that the inhibition of angiogenesis could be therapeutic (Pathak et al. 2024; Ribatti 2008; Sherwood et al. 1971) (Fig. 1). This new approach raised interest all around the world and led to an explosively great research effort in the field of angiogenesis that lasts until today. Currently, major focus is on tissue engineering and wound healing with the aim to improve tissue and organ regeneration and transplantation (Nosrati et al. 2021; Omorphos et al. 2021). The process of angiogenesis can get modelled and evaluated by several existing bioassays which are categorized in three groups: *in vivo*, *ex vivo* and *in vitro* (Omorphos et al. 2021; Stryker et al. 2019; Tahergorabi and Khazaei 2012).

2.2.1 *In vivo* and *ex vivo* models of angiogenesis

By *in vivo* assays involving living organisms and with the aim to minimize the number of animal experiments, most studies are performed first in *in vitro* models. However, it is necessary to execute *in vivo* models subsequently to study effects in living biological systems (Stryker et al. 2019). The most widely used *in vivo* angiogenesis assay is the so-called Chick chorioallantoic membrane (CAM) assay which uses blood vessels of the CAM of fertilized eggs (Stryker et al. 2019; Goodwin 2007) (Table 1). Moreover, angiogenesis can be viewed in zebrafish embryos due to their transparent character (Nathan et al. 2024; Udvadia and Linney 2003). By it being pellucid and all blood vessels being generated by angiogenesis, the cornea is also targeted to evaluate angiogenesis (Cao et al. 2024; Tahergorabi and Khazaei 2012; Gimbrone et al. 1974). Furthermore, Xenograft assay provides information about the effect of drugs on an induced pathological entity in immunodeficient host organs (Nowak-Sliwinska et al. 2018; Jardim-Perassi et al. 2014) (Table 1).

Table 1: Most commonly used *in vivo* and *ex vivo* models of angiogenesis.

Type of assay	Target tissue
In vivo	Chick chorioallantoic membrane (CAM)
	Zebrafish
	Cornea
	Xenograft
Ex vivo	Thoracic aorta ring
	Retinal fragments

Ex vivo assays mimic *in vivo* situations by explanting ECs including their surrounding tissue and cultivating them as units outside the body. Mostly used is the thoracic aorta ring from rats or mice which get cultured in a pro-angiogenic media inducing angiogenesis (Mishra et al. 2024; Ghoochani et al. 2016; Nicosia and Ottinetti 1990). Furthermore, retinal fragments can get seeded in a fibrin gel as part of the *ex vivo* retina angiogenesis model. By supplementing VEGF, angiogenesis gets stimulated and can be monitored (Rezzola et al. 2013) (Table 1).

2.2.2 *In vitro* models of angiogenesis

In the research field of angiogenesis, *in vitro* models are frequently used to provide initial information about morphogenesis, cellular and molecular mechanisms and direct effects of pro- and antiangiogenic agents (Kim et al. 2024; Stryker et al. 2019; Nowak-Sliwinska et al. 2018; Goodwin 2007). In comparison to *in vivo* and *ex vivo* assays, *in vitro* studies are highly efficient regarding time and cost. Experimental setups can be designed less complicated and experiments can be performed under precise standardized conditions (Kim et al. 2024; Nowak-Sliwinska et al. 2018; Sarkanen et al. 2010; Auerbach et al. 2003). Moreover, implementing *in vitro* models reduces the number of animal experiments which raise major ethical concerns and entail experimental disadvantages (Doke and Dhawale 2015; Russell and Burch 1992). Due to their crucial role in metabolite diffusion and originating angiogenesis, microvasculature constitutes 95% of the body mass endothelium. Therefore, researchers were mainly focusing on establishing *in vitro* models with microvascular endothelial cells (Hewett 2016; Pries et al. 2014; Leblanc et al. 2012).

2.2.2.1 Overview of existing in vitro models

Most *in vitro* assays cover only single stages of the angiogenic cascade resulting in the classification of assays into proliferation, migration and differentiation or tube formation assays (Stryker et al. 2019; Nowak-Sliwinska et al. 2018; Tahergorabi and Khazaei 2012; Goodwin 2007) (Table 2). Proliferation assays are commonly used to examine pro-angiogenic or anti-angiogenic effects of a substance on ECs. Therefore, cells get cultivated, labelled and exposed to the substrate of interest. Proliferation can get evaluated by counting manually or electronically using a hemocitometer or coulter counter known as cell counting technique (Stryker et al. 2019; Wei et al. 2017). Alternatively, colorimetric and DNA synthesis techniques monitor and measure biomolecules, such as 3-(4,5-dimethylthiazol-2-yl)-2,5-diphenyltetrazolium bromide and DNA which are directly proportional to cell density (Stryker et al. 2019; Rajabi et al. 2015; Goodwin 2007; Staton et al. 2004). Additionally, angiogenic factors can stimulate ECs to migrate along their gradient. These events are examined by migration assays, such as the wound healing assay. In this assay, a lesion is caused in a confluent monolayer in order to monitor the migration rate of ECs which intend to close the lesion (Wei

et al. 2017). A further assay is the matrix degradation assay which is focusing on the expression and activity of matrix metalloproteases. These enzymes are necessary for ECs to detach from extracellular matrix in order to migrate towards a stimulus (Maurya et al. 2024; Goodwin 2007). Potential angiogenic factors can get analysed using the Boyden chamber. Therefore, the migration of ECs through a central filter gets analysed as a response to an angiogenic factor (Jeanneau et al. 2024; Goodwin 2007; Boyden 1962). In comparison to the Boyden chamber, the phagokinetic track assay is more precise. The movement of cells displace colloidal gold and generate measurable tracks (Stryker et al. 2019; Staton et al. 2004). In tube formation assays, the process of forming new capillaries is of focus. Matrigel is frequently used to analyse angiogenic and non-angiogenic biomolecules based on the capacity of a substrate enabling ECs to build tubules (Esparza et al. 2024; Sacharidou et al. 2012). Finally, co-culture assays examine both angiogenic factors and cell line behaviour by cultivating ECs together with stromal cells (Stryker et al. 2019; Staton et al. 2004) (Table 2).

Table 2: Most commonly used *in vitro* models of angiogenesis.

Specific *in vitro* assay	**Technique**
Proliferation	Cell counting
	Colorimetric
	DNA synthesis
Migration	Wound healing
	Matrix degradation
	Boyden chamber
	Phagokinetic track
Tube formation	Matrigel
	Co-culture

2.2.2.2 Challenges of in vitro models

Even though *in vitro* models of angiogenesis are routinely used in labs all over the world, they still face problems of reproducibility and accurate interpretation. Sources of error are suggested to be based on utilized ECs, reproduction to the living environment and procedure of assays (Stryker et al. 2019; Nowak-Sliwinska et al. 2018; Tahergorabi and Khazaei 2012; Staton et al. 2004; Auerbach et al. 2003). Regarding ECs, most cells used in assays are purchased from specialized distributors which preselect cells by passaging. Therefore, cells are already stimulated to enter a proliferative state unlike quiescent cells of existing vessels of living organisms (Guerrero et al. 2021; Staton et al. 2004). Further, ECs are highly

inhomogeneous regarding their features and phenotypes. Based on their tissue heritage, ECs can differ in size, shape and cell junctions (Tahergorabi and Khazaei 2012). They can also vary tremendously regarding their antigen expression and receptor density, which leads to dissimilar angiogenic responses (Guerrero et al. 2021; Staton et al. 2004). Furthermore, *in vitro* models are not able to identically mimic living environments (Stryker et al. 2019; Nowak-Sliwinska et al. 2018; Tahergorabi and Khazaei 2012). Multiple components are mostly missing, e.g. supporting cells and extracellular matrix, shear stress and components of circulating blood (Nowak-Sliwinska et al. 2018; Tahergorabi and Khazaei 2012). Still, there is no gold standard of angiogenesis assays which led to a huge number of different *in vitro* assays involving various environmental and cultivational alterations (Stryker et al. 2019; Staton et al. 2004). Despite the vast heterogeneity of assays, most *in vitro* assays examine only single stages of angiogenesis. Therefore, the course of angiogenesis is split up into specific steps instead of being analysed as one dynamic process. This represents a huge disadvantage in comparison to *in vivo* assays (Tahergorabi and Khazaei 2012). Focused on solving this challenge, researchers established the so-called all-in-one assay (Bahramsoltani and De Spiegelaere 2016; De Spiegelaere et al. 2011; Bahramsoltani et al. 2010; Bahramsoltani and Plendl 2004).

2.2.2.3 All-in-one assay

When performing the all-in-one angiogenesis assay, microvascular endothelial cells get cultivated long-term in a pro-angiogenic media provoking an angiogenic response (Bahramsoltani and De Spiegelaere 2016; Bahramsoltani et al. 2010; Bahramsoltani and Plendl 2004). While undergoing the *in vitro* angiogenic cascade, ECs change their morphology. Based on these morphological changes, cells get assigned to six defined stages. These stages describe morphological events of confluent monolayer (stage 1), >50% elongated shaped cells (stage 2), >50% linearly arranged cells (stage 3), networking of linearly arranged cells (stage 4), appearance of capillary-like structures (stage 5) and all linearly arranged cells form capillary-like structures as well as the dissolution of the cell layer on the bottom (stage 6) (Bahramsoltani et al. 2010). By monitoring these morphological alterations and assigning respective stages over the whole period of cultivation, *in vitro* angiogenesis can get examined qualitatively and quantitatively. When using the all-in-one assay, researchers revealed tremendous differences in the angiogenic behaviour of ECs from different batches, questioning their angiogenic potency (De Spiegelaere et al. 2011; Sievers et al. 2011; Bahramsoltani et al. 2010; Bahramsoltani and Plendl 2007).

2.3 Angiogenic potency of endothelial cells

Irrespective of cell origins, distributor recommended media composition and cultivation processes, different batches of human microvascular ECs displayed variations in their angiogenic behaviour when performing the all-in-one assay, leading to the classification of ECs into angiogenic and non-angiogenic ECs. Two EC batches derived from heart and skin were running through the *in vitro* angiogenic cascade chronologically within 60 days resulting in them being designated as angiogenic. In comparison, two further EC batches derived from skin and lungs presented much lower angiogenic potency leading to their classification as non-angiogenic. Pulmonal ECs reached stage 3 as the furthest differentiation and regressed subsequently to levels 2 and 1. Furthermore, non-angiogenic ECs from skin could not get stimulated to any stage of the *in vitro* angiogenic cascade and remained in stage 1 (Bahramsoltani et al. 2013; De Spiegelaere et al. 2011; Sievers et al. 2011; Hirschberg et al. 2005; Bahramsoltani and Plendl 2004). Most ECs used in *in vitro* assays, are purchased from certain distributors recommending them explicitly for the use in *in vitro* angiogenesis models. However, it has been shown that their capacity to be used for assays which cover single stages of *in vitro* angiogenesis does not necessarily represent their potency to run through the whole angiogenic cascade (Bahramsoltani and De Spiegelaere 2016; Sievers et al. 2011; Bahramsoltani et al. 2010; Bahramsoltani and Plendl 2007; Bahramsoltani and Plendl 2004).

Mechanisms and influencing factors of the angiogenic potency are not yet fully revealed. So far, the origin of ECs and their location within the organ are described as having a major influence (Maacha et al. 2020; De Spiegelaere et al. 2012; Albertin et al. 2009; Ribatti et al. 2002; Blacher et al. 2001). Furthermore, differences were shown in between EC batches isolated from micro- and macrovasculature. It is suggested that their dissimilar expression profiles result in a divergent angiogenic behaviour regarding their differentiation, response to technical manipulations and interactions with other cells (Bahramsoltani et al. 2014; De Spiegelaere et al. 2012; Burri et al. 2004). Additionally, the process of *in vitro* cultivation, e.g. repeated passaging, coating of culture plates and media composition, was found to highly influence the angiogenic potency of cells (Guerrero et al. 2021; Marrelli et al. 2011; Staton et al. 2009; Auerbach et al. 2003). However, ECs within one culture and being cultivated under the same environmental conditions are able to display differences in their angiogenic behaviour, concluding that major effecting factors derive from both: the environment and each individual EC (Sievers et al. 2015; Sievers et al. 2011).

2.3.1 Non-angiogenic endothelial cells

The appearance of non-angiogenic ECs is still a conundrum in the research field of angiogenesis. Rarely information is given about their cellular characteristics, influencing factors and molecular mechanisms. Regarding extrinsic factors stimulating the non-angiogenic phenotype, it was shown that inflammatory cytokines induce their emergence *in vitro* and *in vivo* (Huinen et al. 2021; Naschberger et al. 2005). Furthermore, it was stated that intense isolation and harvesting procedures carried out in labs affect the *in vitro* angiogenic potency and might lead to a non-angiogenic phenotype (Guerrero et al. 2021; Marin et al. 2001). Additionally, divergent cultivational conditions might cause a phenotypic change to non-angiogenic. Despite them still expressing angiogenic factors, researchers suggest that these ECs are able to undergo a transdifferentiation into other cell types, e.g. monocytes, macrophages and pericytes (Antohe 2006; Zhu et al. 2006; Sommer et al. 2005). Moreover, unknown intrinsic factors of each individual EC affect the angiogenic potency. Even under the same microenvironmental conditions, different ECs showed variations in their angiogenic potency (Sievers et al. 2015; Aird 2012; Sievers et al. 2011; Zhu et al. 2006). Several studies state special features among non-angiogenic ECs. It has been shown that factors, like Rho GTPases inhibitor CDC42GAP is highly expressed in ECs with low angiogenic potency (Engelse et al. 2008). Furthermore, an excessive intracellular storage of lipids was found, indicating a dissimilar lipid metabolism in contrast to angiogenic ECs (Sievers et al. 2015). In order to detect potential marker proteins for angiogenic and non-angiogenic ECs, proteome expression profiles of two batches of angiogenic microvascular ECs and two non-angiogenic batches were determined. Seven proteins were found solely in angiogenic ECs and only one protein exclusively in non-angiogenic ECs (Bahramsoltani et al. 2013).

S-adenosylmethionine synthetase isoform type 2 (MAT2A) represents the protein which was solely detected in non-angiogenic ECs (Bahramsoltani et al. 2013). MAT2A is an essential enzyme related to cell metabolism. Among body tissues, MAT2A is mostly encoded by MAT2A-gene determining the abbreviation “MAT2A”. Only in liver cells, the enzyme is expressed via MAT1A-gene (Wang et al. 2024; Li et al. 2022; Firestone and Schramm 2017; Shafqat et al. 2013). Primarily it catalyses the reaction of methionine and adenosine triphosphate (ATP) in the methionine cycle. Therefore, it is a rate-limiting enzyme synthesizing S-adenosylmethionine (SAM). SAM is an important compound participating in the syntheses of polyamines, homocysteine and reduced glutathione (Yang et al. 2024a; Pascale et al. 2022). Furthermore, it is highly implicated in methyl transfer reactions involving proteins, lipids and nucleic acids, serving as a major methyl donor (Shafqat et al. 2013). Hence, it regulates cellular processes, such as maturation and differentiation of cells induced by DNA-methylation as well as migration and proliferation of cells by DNA-hypomethylation (Pascale et al. 2022; Chen et

al. 2021; Zhang 2018; Sahin et al. 2010). It has been observed accordingly in ECs. They displayed a reduced capacity of migration and proliferation by implementing SAM (Banerjee and Bacanamwo 2010; Sahin et al. 2010). In contrast, an increased VEGF-A expression and differentiation of cells was detected when inhibiting DNA-methylation (Banerjee and Bacanamwo 2010). These findings lead to the suggestion of MAT2A mainly having an anti-angiogenic effect on ECs.

2.3.2 Angiogenic endothelial cells

Most ECs used in labs are considered to be angiogenic, resulting in a frequent use and intense analysis. As already mentioned, most *in vitro* models do not determine the angiogenic potency of ECs. Therefore, results must be taken with caution. Numerous angiogenic factors are identified to directly stimulate cells to differentiate to angiogenic ECs and undergo the angiogenic cascade. Among them, there are members of fibroblast growth factor (FGF) family, angiogenin, transforming growth factor alpha and beta (TGF-α and -β), vascular permeability factor/vascular endothelial growth factor (VPF/VEGF), interleukins, chemokines, tumour necrosis factor alpha (TNF- α) and angiopoietins (Lopes-Coelho et al. 2021; Khoury and Ziyadeh 2011; Kuwano et al. 2001). These extrinsic factors interact mainly with respective intrinsic factors expressed by ECs, such as VEGF-, FGF- and tyrosine kinases-receptors (Zafer et al. 2022; Bouïs et al. 2006; Sato et al. 1995). Furthermore, it was shown that only angiogenic ECs are able to synthesise and effectively secrete certain components of the basement membrane, i.e. collagen type IV and laminin, in comparison to non-angiogenic (Sievers et al. 2015; Bahramsoltani et al. 2014; Sievers et al. 2011). When searching for markers identifying angiogenic ECs, it was found that CD 143 expression is lower in angiogenic ECs in comparison to non-angiogenic ECs (Silva et al. 2014). Moreover, previously mentioned proteomic approach detected seven proteins which were only found in angiogenic EC batches (Bahramsoltani et al. 2013).

Vimentin (VIM) was one of the seven proteins being detected in angiogenic ECs (Bahramsoltani et al. 2013). VIM is a type III intermediate filament protein which is abundant in all major human tissues (Danielsson et al. 2018). As one of the components of the cytoskeleton, it mainly effects cell mechanics and motility. Furthermore, it is highly involved in intracellular and extracellular signalling pathways affecting cell growth, wound healing, and lipogenesis. Extracellular vimentin was found to be a marker of circulating tumour cells and mediate cell invasion of viruses and bacteria (Zhao et al. 2024; Paulin et al. 2022; Patteson et al. 2020; Danielsson et al. 2018). Regarding ECs, VIM was identified as a marker for immature angiogenic blood vessels (Van Beijnum et al. 2006). It was shown that VIM expression decreased in immature precursor cells with maturation (Nowak-Sliwinska et al. 2018; Van

Beijnum et al. 2006). By modulating cell shape and stabilizing cell-matrix adhesion, it is suggested to highly influence early stages of angiogenesis, i.e. cell migration and sprouting (Danielsson et al. 2018; Antfolk et al. 2017; Dave and Bayless 2014; Tsuruta and Jones 2003). Furthermore, in microvascular ECs, VIM expression was shown to be dynamic depending on environmental conditions suggesting that cells adjust their cell adhesion and motility to environmental stress (Cesari et al. 2020; Liu et al. 2010). When knocking down VIM in mice, insufficiencies regarding vessel-remodelling, wound-healing and vasoactivity was detected (Patteson et al. 2020; Danielsson et al. 2018; Dave and Bayless 2014). Until today, VIM is being analysed to reveal further angiogenic processes which are influenced by this protein (Suprewicz et al. 2024; Dayekh and Mequanint 2023).

Triosephosphate isomerase (TPI) was a further protein found solely in angiogenic ECs (Bahramsoltani et al. 2013). TPI is a non-allosteric enzyme which is catalytically active by dimerization (Myers and Palladino 2023; Wierenga et al. 2010). It is mostly known for its involvement in glycolysis and gluconeogenesis. Hereby it catalyses the conversion of the isomers dihydroxyacetone phosphate into D-glyceraldehyde-3-phosphate reversely (Zuo et al. 2024; Myers and Palladino 2023; Wierenga et al. 2010; Qiu et al. 2007). Due to its glycolytic activity, it is interconnected to other metabolic pathways, e.g. lipid metabolism and pentose phosphate pathway. Therefore, TPI is an essential enzyme for cell metabolism and is highly expressed in all human tissues (Orosz et al. 2009). Recently, numerous other functions, so-called moonlighting functions, have been described, e.g. it may serve as autoantigen, a factor of virulence of some organisms and seafood allergen. Additionally, it is suggested to be involved in cell cycle, leading to cell proliferation (Werelusz et al. 2024; Myers and Palladino 2023; Rodríguez-Bolaños and Perez-Montfort 2019; Orosz et al. 2009). In angiogenic ECs, it was shown that glycolic metabolism was increased to generate energy for cell motility and proliferation (Dumas et al. 2020). Furthermore, TPI expression in ECs appeared to be stimulated by VEGF and hypoxia (Yetkin-Arik et al. 2019; Yamaji et al. 2004). So far, only rare information is given about TPI and its connection to angiogenesis.

2.4 Aims and hypothesis of this thesis

The research field of *in vitro* angiogenesis still faces tremendous problems regarding their reproducibility (Nosrati et al. 2021; Stryker et al. 2019; Nowak-Sliwinska et al. 2018; Russell and Burch 1992). A key factor seems to be ECs displaying a vast variety in their angiogenic behaviour during the angiogenic cascade (Bahramsoltani et al. 2010; Bahramsoltani and Plendl 2007; Bahramsoltani and Plendl 2004). The angiogenic potency of different EC batches is mostly unknown and mimicked by the usage of single stage *in vitro* angiogenesis assays. Still, influencing factors raising or reducing the angiogenic potency are unknown and must get investigated (Bahramsoltani and De Spiegelaere 2016; Sievers et al. 2011; Bahramsoltani et al. 2010; Bahramsoltani and Plendl 2007; Bahramsoltani and Plendl 2004).

This study aims to determine whether the expression of VIM, TPI and MAT2A respectively is related to angiogenesis *in vitro* in human dermal microvascular endothelial cells (HDMECs). Therefore, three main questions were pursued:

- How is the native expression profile of each protein individually during the course of angiogenesis *in vitro*?
- Does knocking down each protein solely have an impact on the angiogenic behaviour of ECs *in vitro*?
- Does knocking down each protein solely have an impact on the expression of the other two proteins *in vitro*?

Based on literature research and prior studies, VIM and TPI are hypothesizes to arouse pro-angiogenic effects and raise the angiogenic potency of HDMECs, whereas MAT2A is suggested to cause non-angiogenic effects and reduce the angiogenic potency.

3. Publication I

RESEARCH ARTICLE

Expression of vimentin, TPI and MAT2A in human dermal microvascular endothelial cells during angiogenesis *in vitro*

OPEN ACCESS

Authors: Christina Herre[1], Arpenik Nshdejan[1], Robert Klopfleisch[2], Giuliano Mario Corte[1], Mahtab Bahramsoltani[1]

Affiliations: **1** Department of Veterinary Medicine, Institute of Veterinary Anatomy, Freie Universität Berlin, Berlin, Germany,
2 Department of Veterinary Medicine, Institute of Veterinary Pathology, Freie Universität Berlin, Berlin, Germany

Received: October 29, 2021
Accepted: March 27, 2022
Published: April 28, 2022

Journal: PLoS ONE 17(4): e0266774

DOI: https://doi.org/10.1371/journal.pone.0266774

Editor: Andrea Caporali, University of Edinburgh, UNITED KINGDOM

Contribution of work:

Name	Type of Authorship	Contribution to Publication I
Christina Herre	First author	Correspondence with PLoS ONE Conceptualization Investigation Methodology Data curation Data analysis Writing
Arpenik Nshdejan	Co-author	Conceptualization Methodology Data curation Writing -review and editing
Robert Klopfleisch	Co-author	Supervision Writing -review and editing
Giuliano Mario Corte	Co-author	Formal analysis Supervision Writing -review and editing
Mahtab Bahramsoltani	Co-author	Conceptualization Methodology Formal analysis Project administration Supervision Writing -review and editing

PLOS ONE

RESEARCH ARTICLE

Expression of vimentin, TPI and MAT2A in human dermal microvascular endothelial cells during angiogenesis *in vitro*

Christina Herre[1]*, **Arpenik Nshdejan**[1], **Robert Klopfleisch**[2], **Giuliano Mario Corte**[1], **Mahtab Bahramsoltani**[1]

1 Department of Veterinary Medicine, Institute of Veterinary Anatomy, Freie Universität Berlin, Berlin, Germany, **2** Department of Veterinary Medicine, Institute of Veterinary Pathology, Freie Universität Berlin, Berlin, Germany

* christina.herre@fu-berlin.de

OPEN ACCESS

Citation: Herre C, Nshdejan A, Klopfleisch R, Corte GM, Bahramsoltani M (2022) Expression of vimentin, TPI and MAT2A in human dermal microvascular endothelial cells during angiogenesis *in vitro*. PLoS ONE 17(4): e0266774. https://doi.org/10.1371/journal.pone.0266774

Editor: Andrea Caporali, University of Edinburgh, UNITED KINGDOM

Received: October 29, 2021

Accepted: March 27, 2022

Published: April 28, 2022

Data Availability Statement: All data files are available from the Harvard database (https://doi.org/10.7910/DVN/ZSDUOV).

Funding: The author(s) received no specific funding for this work.

Competing interests: The authors have declared that no competing interests exist.

Abstract

Introduction

In vitro assays of angiogenesis face immense problems considering their reproducibility based on the inhomogeneous characters of endothelial cells (ECs). It is necessary to detect influencing factors, which affect the angiogenic potency of ECs.

Objective

This study aimed to analyse expression profiles of vimentin (VIM), triosephosphate isomerase (TPI) and adenosylmethionine synthetase isoform type–2 (MAT2A) during the whole angiogenic cascade *in vitro*. Furthermore, the impact of knocking down vimentin (VIM) on angiogenesis *in vitro* was evaluated, while monitoring TPI and MAT2A expression.

Methods

A long–term cultivation and angiogenic stimulation of human dermal microvascular ECs was performed. Cells were characterized via VEGFR–1 and VEGFR–2 expression and a shRNA–mediated knockdown of VIM was performed. The process of angiogenesis *in vitro* was quantified via morphological staging and mRNA–and protein–levels of all proteins were analysed.

Results

While native cells ran through the angiogenic cascade chronologically, knockdown cells only entered beginning stages of angiogenesis and died eventually. Cell cultures showing a higher VEGFR–1 expression survived exclusively and displayed an upregulation of MAT2A and TPI expression. Native cells highly expressed VIM in early stages, MAT2A mainly in the beginning and TPI during the course of angiogenesis *in vitro*.

Conclusion

VIM knockdown led to a deceleration of angiogenesis *in* vitro and knockdown cells displayed expressional changes in TPI and MAT2A. Cell populations with a higher number of stalk cells emerged as being more stable against manipulations and native expression profiles provided an indication of VIM and MAT2A being relevant predominantly in beginning stages and TPI during the whole angiogenic cascade *in vitro*.

Introduction

Angiogenesis is described as the growth and remodelling of new blood vessels from pre–existing ones [1–3]. During sprouting angiogenesis *in vivo*, vascular basement membrane degrades and endothelial tip cells migrate towards an angiogenic stimulus such as vascular endothelial growth factor A (VEGF-A). VEGF-A initiates tip cell activation and migration via vascular endothelial growth factor receptor–2 (VEGFR–2), which is abundant on filopodia. Induced by the expression of vascular endothelial growth factor receptor–1 (VEGFR–1), endothelial stalk cells elongate the sprout via proliferation. An internal lumen is being built and endothelial phalanx cells synthesise a new basement membrane, resulting in a mature vessel [3, 4].

The ability to run through these processes is indispensable for many pathological events, like tumour growth, ischemia and cardio vascular diseases [3]. Current effort in the research field of angiogenesis is focusing on tissue engineering and wound healing [5–7]. According to the 3Rs principle of replacing, reducing and refining animal experiments of Russel and Burch [8] and with the aim to reduce time and cost, *in vitro* models of angiogenesis are used frequently. However, due to the absence of a gold standard for these assays and the inhomogeneous character of endothelial cells (ECs), *in vitro* assays still face immense problems considering their reproducibility [6, 9–12].

Most *in vitro* assays cover only single stages of angiogenesis, e.g. migration, proliferation or tube formation [9, 10, 13]. However, the capacity of ECs to get stimulated for specific assays does not necessarily represent their potential to undergo the whole angiogenic cascade. While establishing an all–in–one assay, that comprises all stages of angiogenesis, it was shown that several batches of capillary–derived primary cell cultures of human microvascular endothelial cells display differences in their angiogenic potency. Irrespective of distributor recommended conditions of growth stimulation and cultivation, not all cells were able to undergo all stages of angiogenesis, resulting in the classification of ECs into angiogenic and non–angiogenic [14–17]. In order to investigate molecular differences and determine potential marker proteins, Bahramsoltani et al. [18] generated protein expression profiles of angiogenic and non–angiogenic ECs. By evaluating the expression patterns, seven proteins were found exclusively in angiogenic batches and only one protein in non–angiogenic. For this study, three proteins were determined to undergo further analysis.

Among the seven proteins found in angiogenic ECs, vimentin (VIM) is the most explored protein regarding its role in angiogenesis. The type III intermediate filament protein belongs to a protein family, which is mainly responsible for cell shape and motility. Therefore, VIM is shown to be expressed in all major human tissues, especially in highly proliferative and undifferentiated cells [19]. Besides its influence on the cell skeleton, VIM is described as a multifunctional protein that is involved in intracellular and extracellular signalling pathways and in mediating host cell invasion for viruses, including SARS–CoV, and different bacteria [20]. Considering angiogenesis, VIM is already established as a marker for immature angiogenic

blood vessels [21]. By effecting the cytoskeleton and stabilizing the cell–matrix adhesion, it is highly involved in angiogenesis, especially during cell migration [19, 22] and sprouting [23, 24]. While passing the angiogenic cascade, it was shown that the expression of VIM in immature precursor cells decreased with maturation [10, 21]. Further studies showed the dynamic in VIM expression that may represent an adaptive mechanism of microvascular endothelial cells to stress. It may help cells to adjust their cell adhesion and motility to environmental conditions [25, 26]. Furthermore, knocking down models in mice led to insufficiencies in wound–healing, vessel remodelling and vasoactivity, without exposing the affected components and mechanisms. Up until today, the specific role of VIM in dermal angiogenesis is not fully revealed [19, 20, 23].

As a further protein, triosephosphate isomerase (TPI) was solely expressed in angiogenic ECs [18]. TPI is a glycolytic enzyme, which reaches its full catalytic activity by dimerization. It converts the isomers dihydroxyacetone phosphate into D–glyceraldehyde–3–phosphate reversely [27, 28]. Due to its involvement in glycolysis and gluconeogenesis, TPI establishes a connection to other metabolic mechanisms, i.e. lipid metabolism and pentose phosphate pathway. It represents an essential enzyme for cell metabolism which is highly present in all different kinds of human tissues [29]. It was demonstrated that stimulation of TPI induces an increase in ATP and leads to cell proliferation [28], a pivotal step in angiogenesis. In capillary ECs, it was shown that TPI expression was upregulated by induction of hypoxia [30]. Generally, there is hardly any information about TPI and its role in angiogenesis.

According to the proteomic approach of Bahramsoltani et al. [18], only one protein was found exclusively in non–angiogenic ECs, i.e. S–adenosylmethionine synthetase isoform type–2 (MAT2A). This enzyme is related to cell metabolism and is encoded by two genes, MAT1A–gene and MAT2A–gene. While MAT1A–gene is mostly expressed in liver tissue, MAT2A–gene is widely distributed in human tissues [31]. MAT2A is a highly conserved enzyme synthesising S–adenosylmethionine (SAM) by catalysing the reaction of methionine and adenosine triphosphate (ATP). SAM is a well–established and highly important compound, which serves as the major methyl donor in most methyl transfer reactions, including the methylation of proteins, nucleic acids and lipids [32]. Molecular methylation tends to have mainly regulatory functions, e.g. DNA–methylation results in the activation of cells to undergo maturation and differentiation [33]. Alternatively, hypomethylation of DNA promotes cells to migrate and proliferate. In ECs, the downregulation of DNA–methylation displayed an increase in VEGF–A expression resulting in a higher angiogenic potential [34]. In contrast, by increasing DNA–methylation due to implementation of SAM, ECs show a decreasing capacity to build capillary–like structures. This compound prevents ECs to undergo migration and proliferation [33, 34]. Until today, there is still rarely information about the enzyme S–adenosylmethionine synthetase isoform type–2 relating to ECs.

The aim of the present study was to determine the impact of knocking down VIM in human dermal microvascular endothelial cells (HDMECs) during the angiogenic cascade *in vitro*. Within this process, expressional changes in TPI and MAT2A mRNA and protein levels were analysed. Furthermore, the experimental setup was designed to exhibit time–dependant fluctuations in VIM, TPI and MAT2A expression during angiogenesis *in vitro*.

Cells, materials and methods

Plasmids, primers and shRNA

Initially, five constructs were designed for the expression of short hairpin RNA targeting VIM–mRNA (shVIM). The generation of shVIM was carried out as previously described for FoxP2 [35]. In brief, the linear DNA coding for the constructs of shVIM was structured sense–

loop–antisense. The loop sequence was GTGAAGCCACAGATG. The knockdown efficiency of each hairpin construct was tested in HEK 293T cells *in vitro*. Concurrently, an overexpression of VIM, tagged with V5 epitope was induced (VIM^+, shown in S1 Table). By using V5 antibodies (Abcam, Cambridge, UK, ab15828, 1:5,000) as primary and Rabbit IgG (GE Healthcare, Freiburg, Germany, NA9340, 1:10,000) as secondary antibodies, Western blot analysis determined the construct with the strongest reduction in VIM expression (shVIM target sequence GGCACGTCTTGACCTTGAACG). The DNA fragments were subcloned into the lentiviral expression vector pFUGW, that was modified by the addition of an U6 promotor with the aim to raise its expression efficacy [36]. For visual infection control, the modified vector contained the information for enhanced green fluorescent protein (eGFP). Additionally, a nontargeting hairpin (shSCR target sequence GAGAGCCGTCCCGGTCTATTA) was subcloned into the vector to be used as a control. The generation of lentivirus was implemented as previously published [36]. Viral titers were maintained in the range of 1–3 x 10^7 IU/μl and viral particles were added to the cells in a 50–fold concentration.

Cells, media and cultivation

Two batches of human microvascular endothelial cells derived from neonatal foreskin (HD1 and HD2) were acquired from LONZA Bioscience (Basel, Switzerland, HMVEC–dBl–Neo, Cat. No. CC–2813). Endothelial cell population was guaranteed by the distributor's certified analysis of CD31/105 and von Willebrand Factor VIII expression and positive uptake for acetylated low density lipoprotein. EBM™–2 Endothelial Cell Growth Basal Medium–2 (LONZA, Basel, Switzerland, Cat. No. CC–00190860) was used as a basal medium (BM). For facilitating cell survival and provoking an angiogenic response, EGM™–2 MV Microvascular Endothelial SingleQuots™ Kit (LONZA, Basel, Switzerland, Cat. No. CC–4147) was added to the BM, resulting in a proangiogenic medium including 5% Fetal Bovine Serum, 0.4% Fibroblast Growth Factor–B, 0.1% Vascular Endothelial Growth Factor, 0.1% Epidermal Growth Factor, 0.1% Insulin–like Growth Factor 1, 0.1% Ascorbic Acid, 0.1% Gentamicin sulfate–Amphotericin B and 0.04% Hydrocortisone. Refreshing of media was executed twice weekly.

In vitro angiogenesis assay

12 wells of each 24-well-culture plate (Corning Life Sciences, Amsterdam, Netherlands, Cat. No. 3738) were covered with 0,5μl gelatine (Sigma Aldrich, St. Louis, MO, USA, Cat. No. G6144, 1,5% in PBS) for 20 minutes, before ECs of both batches were seeded, respectively. Cells were used in third passage in a concentration of 4.5 x 10^4 cells per well. In total 4.86 x 10^6 cells were cultured in 108 wells per batch. ECs were incubated for up to 50 days at 37˚C in a 5% CO_2 humidified atmosphere (INCO2/1, Memmert GmbH & Co. KG, Schwabach, Germany). On the first day of cultivation, cells of both batches were divided into three groups each. One third of cultivated ECs were infected with lentiviral particles, initiating the knockdown of VIM (sh_1, sh_2). By using a nontargeting hairpin, the second group represented the control group (SCR_1, SCR_2) and the last group consisted of native cells (N_1, N_2). Phase–contrast microscopy was carried out using an inverted microscope (LEICA DMi8; Leica Microsystems, Wetzlar, Germany). Angiogenesis *in vitro* was quantified according to the previously established all–in–one angiogenesis assay [14–17, 37]. Therefore, two central and two marginal visual fields per well were randomly defined per coordinates on the first day of investigation. Digital pictures of each of these visual fields were taken twice a week by using LEICA MC170 HD video camera (Leica Microsystems, Wetzlar, Germany) and the imaging and analysis software Leica Application Suite X (LAS X Version 3.4.2, Leica Microsystems, Wetzlar, Germany). Based on cell morphology in the micrographs, ECs were assigned to their respective stage of

angiogenesis *in vitro* (Table 1, [16]). In an entire period of 50 days of cultivation, ECs of all groups were staged at 14 investigation days. For each visual field, the sum of allocated stages of all 14 investigation days (S^{group}) was calculated. Within each group in both batches, the arithmetic mean of the sums of the visual fields were computed ($\overline{S^{group}}$).

Quantitative analysis of VIM, TPI, MAT2A, VEGFR–1 and VEGFR–2 transcripts via RT–qPCR

Cells were harvested at days 1, 5, 25 and 50 by using Hydroxyethylpiperazine Ethane Sulfonic acid, Trypsin/EDTA and Trypsin Neutralisation Solution (LONZA, Basel, Switzerland, ReagentPack™ Subculture Reagents, Cat. No. CC–5034). Instantaneously after centrifugation, cell pellets were deeply frozen in liquid nitrogen. Total RNA was isolated using Total RNA Kit, peqGold (Peqlab/VWR, Darmstadt, Germany, Cat. No. 12–6834). Remaining DNA was digested via TURBO™ DNase (ThermoFisher Scientific, Bremen, Germany, Cat. No. AM2238) treatment. Isolated RNA was reverse transcribed using SuperScript IV Reverse Transcriptase (ThermoFisher Scientific, Bremen, Germany, Cat. No. 18091050) and quantitative PCR was performed with Rotor–Gene 6000 (Qiagen, Hilden, Germany) and Rotor–Gene Q 2.3.5 software. All samples were run in triplicates under use of Maxima SYBR Green qPCR Master Mix (2x) (ThermoFisher Scientific, Bremen, Germany, Cat. No K0223). Based on the standard curve method of comparative quantification, a standard curve for every gene was generated to determine the amplification efficiency and the calibrator sample. Initially, four reference genes were tested. Using the GeNorm software [38], SDHA and GAPDH were identified as the most stable reference genes and were used for further normalisation. For the normalisers and the genes of interest, the C_t difference between the test sample and calibrator sample was calculated and normalized to a normalisation factor of the reference genes after adjusting for minute variations in amplification efficacy. The primers were designed using NCBI/Primer–BLAST and are listed in S1 Table.

Western blot analysis

After harvesting at day 5, 15, 25 and 50 as described above, cell pellets were resuspended in M–Per™ Mammalian Protein Extraction Reagent (ThermoFisher Scientific, Bremen, Germany,

Table 1. Definition of stages of angiogenesis *in vitro* and description of cell morphology within the different stages [16].

Stage no.	Morphology of endothelial cells
Stage 1	Confluent monolayer
	Polygonal shaped cells
Stage 2	Endothelial sprouting, late phase
	>50% elongated shaped cells
Stage 3	Linear side–by–side arrangement, late phase
	>50% linearly arranged cells
Stage 4	Networking
	Network of linearly arranged cells
Stage 5	Three-dimensional organisation, early phase
	Appearance of capillary–like structures (linear structures of endothelial cells with a diameter of more than 28 μm; for these structures an internal lumen was shown by electron microscopy)
Stage 6	Three–dimensional organisation, late phase
	All linearly arranged cells form capillary–like structures; dissolution of cell layer on the bottom

https://doi.org/10.1371/journal.pone.0266774.t001

Cat. No. 78501) complemented with Halt™ Protease and Phosphatase Inhibitor Cocktail (ThermoFisher Scientific, Bremen, Germany, Cat. No. 78440). Protein quantity was measured via bicinchoninic acid (BCA) method using Bicinchoninic Acid Kit for Protein Determination (Sigma Aldrich, St. Louis, MO, USA, Cat. No. BCA1). On each detection day, three samples of each group were collected. 20 μg protein per sample was deployed and separated by 12% sodium dodecyl sulfate–polyacrylamide gel electrophoresis, followed by electroblotting onto nitrocellulose paper. Blots were blocked in Tris–buffered saline with 0.1% Tween–20 (TBS–T) for 1 h at room temperature and incubated over night at 4˚C with primary antibodies targeting VIM (DAKO, Hamburg, Germany, M7020, 1:500), TPI (Santa Cruz, Heidelberg, Germany, H–11, 1:200), MAT2A (Santa Cruz, Heidelberg, Germany, B–10, 1:200) and Actin (Novus Biologicals, Centennial, CO, USA, AC–15, 1:5,000). Actin (ACT) served as an internal control. Subsequently, blots were washed in TBST–T buffer solution. For the detection of VIM and ACT, blots were incubated with sheep anti–mouse IgG secondary antibody (GE Healthcare, Freiburg, Germany, NA9310, 1:5,000) for 2 h at room temperature. Considering TPI and MAT2A, further incubation was unnecessary due to horseradish peroxidase being already attached to both antibodies. For visualization of proteins, SignalFire™ ECL Reagent (Cell Signal technology, Frankfurt, Germany, Cat No. 6883), G:BOX Chemi XX6 gel imaging system (Syngene, Cambridge, UK) and image acquisition software GeneSys (GeneSys V1.56.0, Syngene, Cambridge, UK) was used.

Statistics

Statistical analysis was carried out using the software SPSS Statistics (SPSS Statistics 25, IBM Corporation, Armonk, NY, USA). By executing the Shapiro–Wilk test, raw data distributions were tested. Normally distributed data is expressed as mean ± standard deviation and non–normally distributed data is expressed as median ± standard error. The comparison of two independent groups was performed with Student's *t* test for unpaired data or Mann–Whitney U test, respectively. For more than two groups, data was analysed with one–way ANOVA and post hoc Dunn–Bonferroni test. Wilcoxon rang–sum test was used to evaluate changes of two dependant variables within a group. Statistical significance was defined as $p<0.05$.

Results

Gene expression of VEGFR–1 and VEGFR–2

For characterization of the cell population, the gene expression of VEGFR–1 and VEGFR–2 was measured in native cells of both batches at day 1, 5, 15, 25 and 50. Median and standard error of C_t values of all times are shown in the S2 Table. At all points in time, N_1 and N_2 showed a higher expression of VEGFR–2 than VEGFR–1 ($p<0.05$). Analysing the median of VEGFR–1 and VEGFR–2 expression for all points of investigation (Fig 1), VEGFR–2 was significantly upregulated compared to VEGFR–1 in both HD1 ($p<0.001$) and HD2 ($p<0.001$). While expression of VEGFR–2 was equal between HD1 and HD2, VEGFR–1 was significantly higher expressed in HD1 than in HD2 ($p<0.01$).

Angiogenesis *in vitro* in N1 and N2

In the beginning of cultivation, native cells of HD1 showed a high cell density (Fig 2A). At day 8, already more than 50% of N_1 were linearly arranged, representing stage 3. A three–dimensional organisation, which appears in stage 5, was visible from day 25 onwards (Fig 2B). These cells were able to run through the whole angiogenic cascade chronologically in a total of 29 days, resulting in the formation of capillary–like structures and the dissolution from the

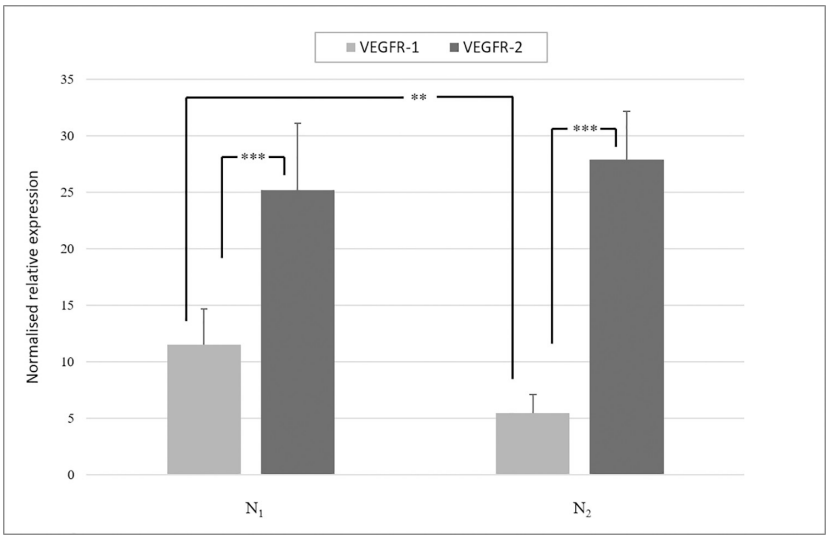

Fig 1. Gene expression of VEGFR–1 and VEGFR–2 in HD1 and HD2. Median and standard error of gene expression of VEGFR–1 and VEGFR–2 at all points of investigation in native ECs of HD1 and HD2 are shown. VEGFR–2 was expressed significantly higher than VEGFR–1 in N_1 and N_2 ($p<0.001$). Between the two batches, VEGFR–2 was expressed equally, whereas VEGFR–1 was expressed significantly higher in HD1 than in HD2 ($p<0.01$). Statistical analysis was carried out using Mann–Whitney U test for unpaired data. $^{*}p<0.05$, $^{**}p<0.01$, $^{***}p<0.001$.

https://doi.org/10.1371/journal.pone.0266774.g001

bottom of the cell culture in stage 6 (Fig 2C). In contrast, native cells of HD2 displayed a lower cell density in the beginning of cultivation and less sprouting activity (Fig 3A). Therefore, more linear side–by–side arrangement was observed. By the networking of linearly arranged cells, N_2 entered stage 4 at day 18. Finally, cells of HD2 reached stage 6 after 25 days of cultivation (Fig 3B and 3C). For quantification of angiogenesis *in vitro*, mean values and standard deviations of sums of assigned stages of angiogenesis (S) were evaluated and compared by using one–way ANOVA and Dunn–Bonferroni post hoc test. N_1 reached a value of $\overline{S^{N_1}}$ = 56.9 ± 4.3 and N_2 of $\overline{S^{N_2}}$ = 50.5 ± 6.5. By comparing the values between the batches, it was shown that $\overline{S^{N_2}}$ is significantly lower than $\overline{S^{N_1}}$ ($p<0.001$).

Angiogenesis *in vitro* in SCR1 and SCR2

The high density of cells of SCR_1 was similar to N_1 at the beginning of cultivation (Fig 2D). SCR_1 reached stage 3 after 11 days and stage 5 from day 29 onwards (Fig 2E). After a chronological course of all stages, SCR_1 entered stage 6 after 32 days (Fig 2F). By detecting eGFP as an infection control, the fluorescent signal in SCR_1 showed a constant infection until the end of cultivation (Fig $2D_{GFP}$–$2F_{GFP}$). Cells of SCR_2 showed a lower cell density in the beginning of cultivation in comparison to SCR_1 (Fig 3D). During the course of angiogenesis *in vitro*, less sprouting but more linear side–by–side arrangement was observed. Cells of the control group entered stage 4 from day 22 onwards (Fig 3E). At day 18, 25, 32 and 39, cells of SCR_2 were less differentiated than native cells ($p<0.05$), whereas no more difference was detectable at day 50. Finally, cells of SCR_2 were able to undergo the whole angiogenic cascade until day 43 (Fig 3F). SCR_2 displayed a constant fluorescent signal over the cultivation period (Fig $3D_{GFP}$–$3F_{GFP}$). By comparing the sums of assigned stages of angiogenesis, it was shown that $\overline{S^{SCR_2}}$ ($\overline{S^{SCR_2}}$ = 49.1 ± 6.6) is significantly lower than $\overline{S^{SCR_1}}$ ($\overline{S^{SCR_1}}$ = 55.1 ± 5.6, $p<0.001$).

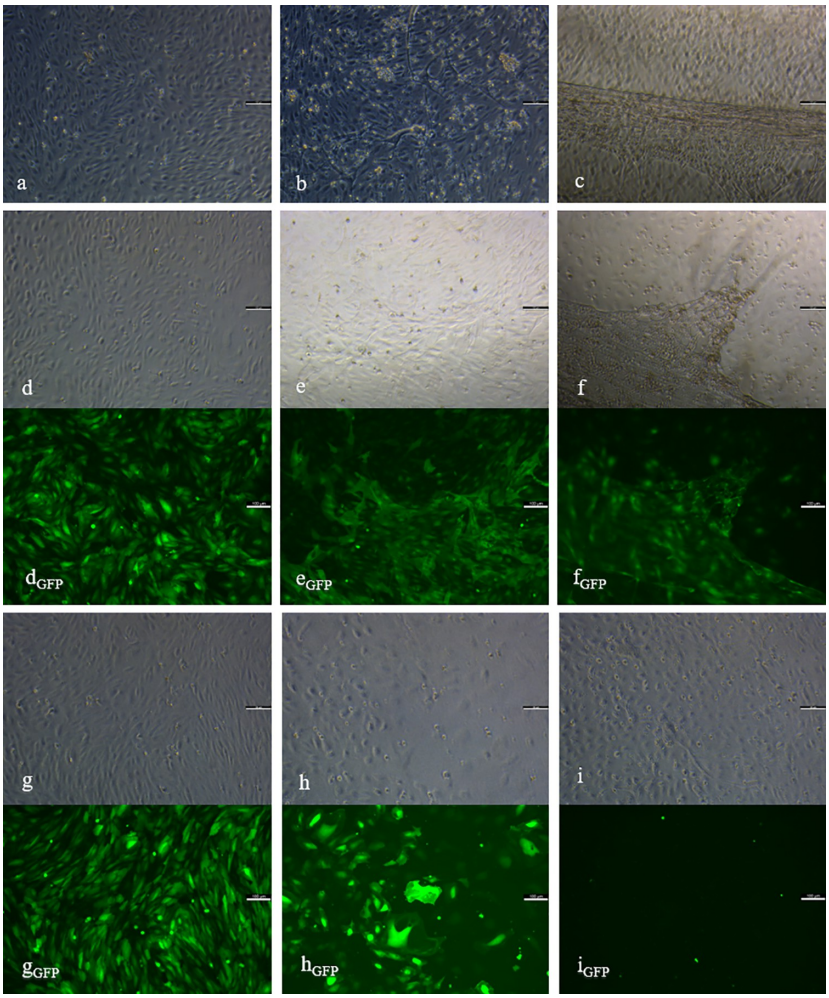

Fig 2. Angiogenesis *in vitro* of ECs of HD1. Native (a-c), control (d-f) and knockdown group (g-i) including the eGFP control of SCR_1 (d_{GFP}, e_{GFP}, f_{GFP}) and sh_1 (g_{GFP}, h_{GFP}, i_{GFP}) at day 5 (a, d, d_{GFP}, g, g_{GFP}), 25 (b, e, e_{GFP}, h, h_{GFP}) and 50 (c, f, f_{GFP}, i, i_{GFP}) of cultivation are presented. Elongated and linearly arranged cells of stage 2–3 (a, d, g) in all groups at day 5, was followed in N_1 and SCR_1 by networking (b, e) and three-dimensional organisation of stage 5–6 (c, f). The knockdown group showed a decrease (h), followed by an increase in cell density, ending up with networking structures of stage 4 (i). Control group showed positive eGFP control during the investigation period (d_{GFP}, e_{GFP}, f_{GFP}), whereas sh_1 displayed a reduction in fluorescent signals (g_{GFP}, h_{GFP}, i_{GFP}). Scale bars = 100 μm.

https://doi.org/10.1371/journal.pone.0266774.g002

Angiogenesis *in vitro* in sh1 and sh2

In the beginning of cultivation, cell density was high in sh_1 (Fig 2G). However, from day 15 onwards a rapid and progressive decline in cell density was visible, with cells remaining in early stages (Fig 2H). At day 29 and following, an increase in cell density was visible. Consequently, cells entered stage 4, visible via the networking of linearly arranged cells. Cells of sh_1 did not enter late stages of angiogenesis *in vitro* during the cultivation period of 50 days (Fig 2I). Detection of eGFP revealed a steady decline over the whole cultivation period. At day 50,

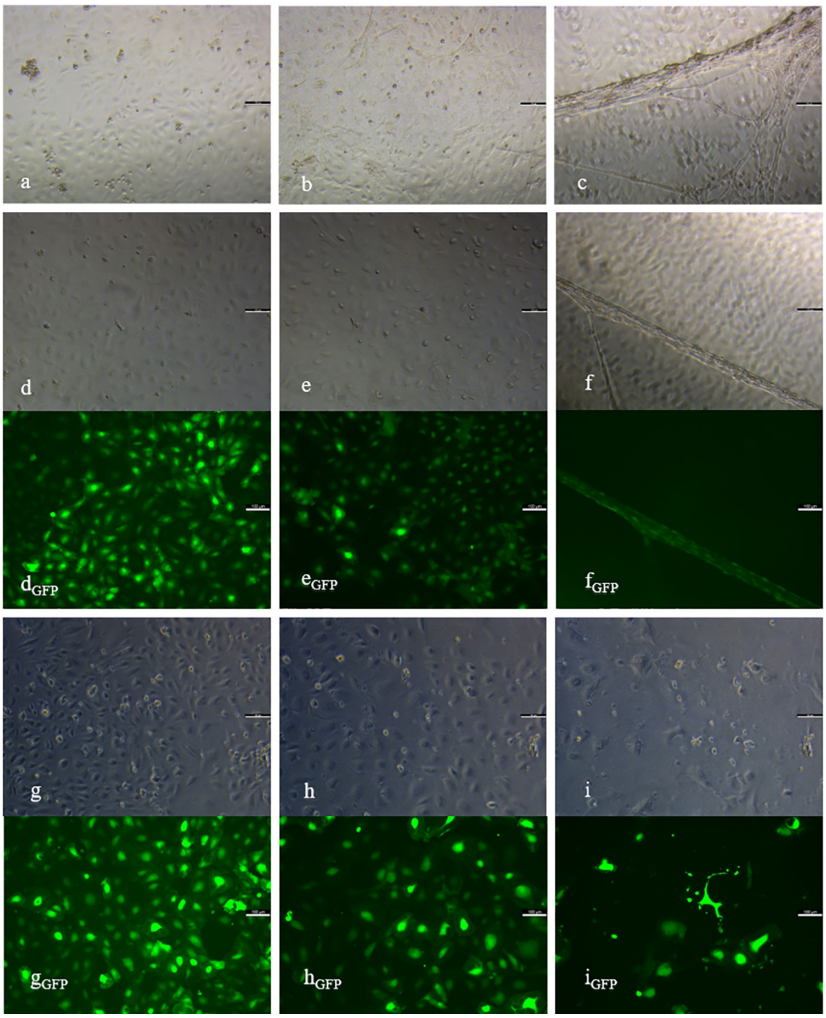

Fig 3. Angiogenesis *in vitro* of ECs of HD2. Native (a-c), control (d-f) and knockdown group (g-i) of HD2 including eGFP control of SCR_2 (d_{GFP}, e_{GFP}, f_{GFP}) and sh_2 (g_{GFP}, h_{GFP}, i_{GFP}) at day 5 (a, d, d_{GFP}, g, g_{GFP}), 25 (b, e, e_{GFP}, h, h_{GFP}) and 50 (c, f, f_{GFP}, i, i_{GFP}) of cultivation. Elongated shaped cells of stage 2 (a, d, g) in all groups at day 5, was followed in N_2 and SCR_2 by networking (b, e) and three-dimensional organisation in stage 5–6 (c, f). The knockdown group showed a persistent decrease in cell density (h, i). Control group showed positive eGFP control during the investigation period (d_{GFP}, e_{GFP}, f_{GFP}), whereas sh_2 displayed a reduction in fluorescent signals (g_{GFP}, h_{GFP}, i_{GFP}). Scale bars = 100 μm.

https://doi.org/10.1371/journal.pone.0266774.g003

eGFP was not verifiable anymore (Fig $2G_{GFP}$–$2I_{GFP}$). While displaying a lower cell density than sh_1 at day one of cultivation, the knockdown of VIM in HD2 resulted in a constant increase in cell death, beginning at day 8 (Fig 3G and 3H). Due to the persistent decrease in cell number, staging of angiogenesis was not feasible from day 36 (Fig 3I). Cells of sh_2 showed networking but no further differentiation. In sh_2, cell death was also detected via eGFP (Fig $3G_{GFP}$–$3I_{GFP}$). The time–dependant mean values and standard deviations of assigned stages are shown in S3 Table and the course of angiogenesis *in vitro* for all groups of both batches

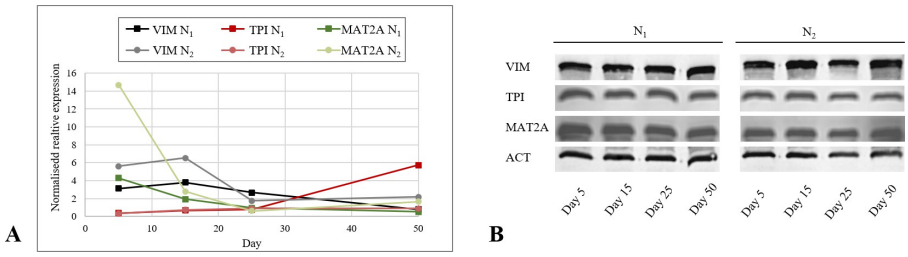

Fig 4. mRNA and protein expression of VIM, TPI and MAT2A in native cells. A. Expression of VIM, TPI and MAT2A in native endothelial cells of both batches during the angiogenic cascade. Decreasing expression in VIM and MAT2A and increasing in TPI was statistically proven under the use of Wilcoxon rang sum test ($p<0.05$). **B.** Western blot analysis of VIM, TPI and MAT2A in native cells of HD1 and HD2 at day 5, 15, 25 and 50. ACT was used as internal control. $^{*}p<0.05$, $^{**}p<0.01$, $^{***}p<0.001$.

https://doi.org/10.1371/journal.pone.0266774.g004

(N_1, SCR_1, sh_1, N_2, SCR_2, sh_2) in S1 Fig. By comparing the values of assigned stages of angiogenesis between both knockdown groups, it was shown that cells of sh_2 reached a sum of $\overline{S^{sh_2}}$ = 33.5 ± 10.1 and thus a significant lower value than sh_1 resulting in $\overline{S^{sh_1}}$ = 40.6 ± 9.1 ($p<0.001$). Further analysis between groups of the same batch showed, that values of N_1 and SCR_1 were significantly higher than sh_1 ($p<0.001$). In HD2, cells of the native group and the control group reached significantly higher values than sh_2 ($p<0.001$). In both batches, native and the control groups did not show differences.

Expression of VIM, TPI and MAT2A in N1 and N2

In order to elucidate the expression status of VIM, TPI and MAT2A in different stages of the angiogenic cascade *in vitro*, native ECs of both batches were harvested at day 5, 15, 25 and 50 and mRNA and protein levels were measured. VIM mRNA expression was initially persistent in N_1. From day 15 onwards, the expression was downregulated significantly on each detection day ($p<0.05$). In N_2, VIM decreased continuously at each detection day ($p<0.05$). Comparing VIM expression between both batches, N_2 displayed a higher expression at day 5, 15 and 50 and a lower expression at day 25 ($p<0.05$, Fig 4A). On protein level, VIM was detectable in both batches at each time point similarly (Fig 4B). Between day 5 and day 15, a significant increase in TPI mRNA expression was observed in N_1 and N_2 ($p<0.05$), followed by a stable expression until day 25. While, N_1 showed an uprise in TPI expression until day 50 ($p<0.05$), N_2 remained stable. TPI on mRNA levels was similar between N_1 and N_2 at day 5, 15 and 25. At day 50 TPI was higher expressed in N_1 ($p<0.05$, Fig 4A). Western blot analysis of TPI showed stable protein levels in N_1 and N_2 (Fig 4B). MAT2A mRNA expression in N_1 was decreasing from day 5 to 25 ($p<0.01$) until it remained at this level. In N_2, MAT2A showed a decline in expression between day 5 and day 25, followed by an increase until day 50 ($p<0.05$). Expression of MAT2A in N_1 was significantly lower at day 5, 15 and 50 and higher at day 25 than in N_2 (Fig 4A). In both batches, protein levels were shown to be stable during the angiogenic cascade (Fig 4B). Median and standard error of protein expression is provided in S4 Table.

Expression of VIM in sh1 and sh2

In addition to eGFP detection, RT–qPCR and Western blot analysis were used as a knockdown control. On mRNA levels, it was shown that VIM expression in sh_1 was significantly downregulated than in SCR_1 on day 5, 15 and 25 ($p<0.001$). At day 50, no difference was measurable

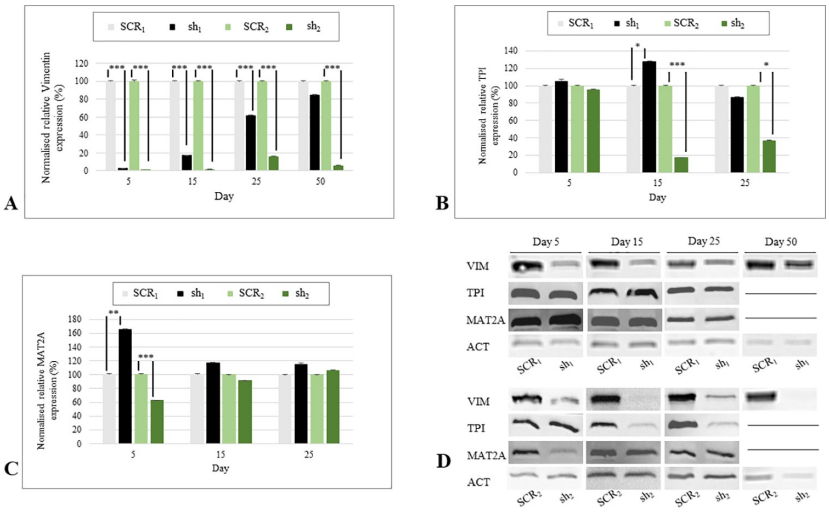

Fig 5. mRNA and protein expression of VIM, TPI and MAT2A in knockdown cells. A. Median and standard error of relative VIM mRNA expression of sh_1, SCR_1, sh_2, SCR_2. VIM was significantly downregulated in sh_1 and sh_2 at each investigation day ($p<0.001$), except of day 50 in sh_1. Statistical analysis was carried out using Mann–Whitney U test for unpaired data. **B.** Relative mRNA expression of TPI of sh_1, SCR_1, sh_2, SCR_2. TPI was significantly upregulated in sh_1 at day 15 ($p<0.05$) and downregulated in sh_2 at day 15 ($p<0.001$), and 25 ($p<0.05$). Statistical analysis was carried out using Mann–Whitney U test for unpaired data. **C.** Median and standard error of relative MAT2A mRNA expression of sh_1, SCR_1, sh_2, SCR_2. MAT2A was significantly upregulated in sh_1 ($p<0.01$), and downregulated in sh_2 at day 5 ($p<0.001$). Statistical analysis was carried out using Mann–Whitney U test for unpaired data. **D.** Western blot analysis of VIM, TPI and MAT2A in sh_1, SCR_1, sh_2, SCR_2 at day 5, 15, 25. ACT was used as internal control. $^{*}p<0.05$, $^{**}p<0.01$, $^{***}p<0.001$.

https://doi.org/10.1371/journal.pone.0266774.g005

(Fig 5A). In addition, on protein levels, the knockdown in HD_1 was not visible at day 50 anymore (Fig 5D). In sh_2 the VIM mRNA and protein levels were significantly lower at all points in time ($p<0.001$, Fig 5A and 5D). Resulting in sh_1 and sh_2 showing a lack in knockdown efficacy based on eGFP detection, mRNA and protein levels, data of both knockdown groups regarding day 50 are excluded from further investigations. The comparison of VIM expression in sh_1 and sh_2 demonstrated a significantly higher mRNA expression in sh_1 at all time points ($p<0.01$).

Expression of TPI and MAT2A in sh1 and sh2

To evaluate expressional changes of TPI and MAT2A occurring during the knockdown, sh_1 and sh_2 mRNA and protein levels were compared with SCR_1 and SCR_2. TPI mRNA levels were higher in sh_1 than in SCR_1 at day 15 ($p<0.05$) and equally at day 5 and 25, whereas sh_2 displayed a decreased expression at day 15 ($p<0.001$) and 25 ($p<0.05$) and no difference at day 5 (Fig 5B). By comparing the knockdown groups of both batches, a higher expression of TPI was detected in sh_1 than in sh_2 at day 5 and 15 ($p<0.05$). Both showed equal amounts of TPI at day 25. On protein levels, TPI was detectable at each day of investigation in both batches. In HD2 protein bands matched the mRNA expression patterns of sh_2 and SCR_2 (Fig 5D). In contrast, the knockdown group of HD1 showed a significantly higher mRNA expression in MAT2A than SCR_1 at day 5 ($p<0.01$), whereas sh_2 displayed a decreased expression ($p<0.001$). At day 15 and 25, no further differences were visible (Fig 5C). These observations were confirmed on protein levels (Fig 5D). MAT2A was higher expressed in sh_2 than in sh_1 at

day 5 ($p<0.05$) and equal at the other investigation days. Median and standard error of protein expression are provided in S4 Table.

Discussion

Up until today, reproducibility is still an issue of concern in the research field of angiogenesis *in vitro* [6, 9–12]. ECs display an immense diversity in their behaviour during the angiogenic cascade [14–16]. It is necessary to investigate influencing factors that raise or reduce their angiogenic potency, respectively. Therefore, in this study the impact of knocking down VIM on angiogenesis *in vitro* was explored, meanwhile expressional changes in TPI and MAT2A were detected. Furthermore, native expression profiles of VIM, TPI and MAT2A were determined during the whole angiogenic cascade *in vitro*.

Native groups of HD1 and HD2 were able to undergo every stage of angiogenesis chronologically, resulting in the classification of both batches as being angiogenic ECs. By comparing the mRNA expression patterns of VEGFR–1 and –2 between both batches, it was notifiable that VEGFR–1 was significantly higher expressed in HD1 than in HD2. While VEGFR–2 is predominantly expressed in tip cells, higher levels of VEGFR–1 mRNA are detectable in stalk cells [4, 16, 39, 40]. Therefore, it can be supposed, that the cell population of HD1 comprised a higher amount of stalk cells than the cell culture of HD2. During the course of angiogenesis, stalk cells are responsible to elongate the sprout by extensive proliferation [4, 41]. Based on the higher proliferative character of HD1, N_1 showed a greater cell density at the beginning of cultivation. Furthermore, it was shown that a low expression level of VEGFR–1 accelerates angiogenesis *in vitro* induced by VEGF–A [16], which was visible by N_2 entering stage 6 earlier than N_1. Additionally, the sum of assigned stages of angiogenesis in N_1 ($\overline{S^{N_1}}$) and N_2 ($\overline{S^{N_2}}$), in SCR_1 ($\overline{S^{SCR_1}}$) and SCR_2 ($\overline{S^{SCR_2}}$) and in sh_1 ($\overline{S^{sh_1}}$) and sh_2 ($\overline{S^{sh_2}}$) showed significantly higher values for all groups of HD1, most likely resulting from the described cell type populations.

In N_1 and N_2, VIM displayed a similar decreasing mRNA expression pattern as previously described in immature precursor cells [10, 21]. It was highest expressed in the beginning stages of angiogenesis in both batches while cells were morphologically staged to phases 2 and 3. This strengthens the assumption of VIM having an impact on early steps of the angiogenic cascade in HDMECs by influencing the cytoskeleton for adhesion, migration and sprouting [19, 22–24]. Mechanisms which are strongly related to endothelial tip cells. So is VIM recently described as a positive marker for epicardial tip cells [42]. By N_2 inheriting a smaller amount of stalk cells within their population, this might be the reason for them displaying a higher mRNA expression of VIM than N_1. Considering TPI, it was found to be upregulated in the beginning of the angiogenic cascade *in vitro*, followed by a stable mRNA expression in N_2 and a final uprise in N_1. TPI is involved in the glycolytic metabolism. In various stages of angiogenesis, e.g. proliferation, migration and tube formation, a high ATP supply is necessary [28, 43, 44], which might have led to the upregulation and constant expression of TPI. Expression levels of TPI were equal between both batches, except of a significantly higher mRNA level in N_1 at day 50 which might be caused due to their higher proliferative character. During these steps, cells require energy for coordinating the formation of tube–like structures while maintaining barrier integrity [45] which was most likely intensified by N_1 displaying a higher number of cells. Furthermore, MAT2A was significantly downregulated considering its mRNA expression in both batches during the angiogenic cascade, most strongly in the beginning. As previously described, MAT2A–activity induces the downregulation of the angiogenic potency of ECs and the initiation of maturation by synthesising SAM [33, 34]. By the cells reducing the expression of MAT2A, they might have intended to increase their angiogenic potency in order to differentiate and undergo the angiogenic cascade. The higher amount of stalk cells in N_1

might have been the reason for the significantly lower expression of MAT2A in N_1 than in N_2. By showing an accelerative course of angiogenesis, N_2 entered stages of maturation earlier than N_1, which might have led to a lower MAT2A mRNA expression level at day 25 followed by a significant uprise at day 50. For validating the impact of TPI and MAT2A on the angiogenic cascade *in vitro*, further investigations must be initiated.

Over the whole cultivation period of 50 days, the infection appeared to be successful and persistent. Both, SCR_1 and SCR_2, were able to enter all stages of the angiogenic cascade, including eGFP positive structures. Additionally, protein levels and quantifying angiogenesis displayed no differences between N_1 ($\overline{S^{N_1}}$) and SCR_1 ($\overline{S^{SCR_1}}$), N_2 ($\overline{S^{N_2}}$) and SCR_2 ($\overline{S^{SCR_2}}$). However, a delay in entering the stages of angiogenesis *in vitro* was detectable in SCR_2, while morphological staging of SCR_1 was mostly equal to N_1, concluding that the infection with viral particles might have affected SCR_2 more intensely than SCR_1. As previously described, lentiviral transduction can have an adverse effect on cell proliferation, depending on the target cell [46]. With SCR_2 having less stalk cells and showing a less proliferative character, this might be the reason for them being influenced more intensely by manipulations.

The downregulation of VIM expression led to cell death of infected cells in both cultures. Via the protein Rudhira/Breast Carcinoma Amplified Seqence 3, VIM is linked to microtubules, resulting in the stabilization of the cytoskeleton, which is essential for focal adhesion and cells migration [20, 47]. ECs are adherent cells, for which it is necessary to create cell–cell and cell–matrix connections for stability, communication and differentiation [19, 48]. By knocking down VIM, ECs were most likely not able to build a stable cell layer for interaction and further developments, resulting in cell death. While cells of sh_2 were dying progressively, sh_1 recovered from cell loss. The higher amount of stalk cells in sh_1 might have facilitated an increase in cell density and enabled further differentiations. It can be supposed that due to their proliferative character, sh_1 showed a greater cell number of uninfected cells which led to a generally higher mRNA expression of VIM in sh_1 than in sh_2. Regarding the angiogenic cascade, a part of the infected cells of both knockdown groups were able to enter stage 4 as a maximum, suggesting that cells still owned native VIM. In sh_1, the number of uninfected cells increased, so that no reliable interpretations about VIM were possible anymore. However, quantitation of angiogenesis stated the deceleration of angiogenesis in both batches, by the sum of assigned stages for the knockdown groups ($\overline{S^{sh_1}}$, $\overline{S^{sh_2}}$) being significantly smaller than the control ($\overline{S^{SCR_1}}$, $\overline{S^{SCR_2}}$) and the native group ($\overline{S^{N_1}}$, $\overline{S^{N_2}}$). This leads to the assumption that VIM raises the angiogenic potency of HDMECs *in vitro* and is essential for cell survival.

Comparing sh_1 and sh_2 with SCR_1 and SCR_2, sh_1 displayed a significantly higher TPI mRNA expression than SCR_1 at day 15. An increase in TPI was already related to a cellular stress response, in order to upregulate cellular energy metabolisms [30]. While TPI is upregulated in sh_1, sh_2 displayed a significant decrease in protein and mRNA levels at day 15 and 25. From day 8 onwards, a persistent death of ECs in sh_2 was detectable. As previously described, cell death leads towards a dysregulation of metabolisms, resulting in no further metabolic activity [49]. This impact on cell metabolism might have caused the lower expression of TPI in sh_2 in comparison with sh_1 at day 5 and 15. Suggesting that MAT2A influences ECs via SAM-mediated methylations, the upregulation in MAT2A expression in sh_1 at day 5 might be a support mechanism to reduce angiogenic activity. Contrarily, the cell population of sh_2might have intended to decrease cellular SAM levels by downregulating MAT2A at day 5. It was shown that SAM inhibits mitogenic effects of growth factors, with the aim of recovering damaged cells [50].

Conclusion

This study stated that different endothelial cell batches, which are isolated from the same tissue, acquired from the same distributor and being cultivated under the same conditions, show different morphologies during the angiogenic cascade *in vitro*. Despite being characterized as angiogenic cultures, both batches vary tremendously in their behaviour of compensating with manipulations. By knocking down of VIM, the cell population with the higher number of stalk cells was able to increase in cell density and upregulated TPI and MAT2A expression. In contrast, cell population with less stalk cells died continuously, going along with the downregulation of TPI and MAT2A expression. Generally, VIM knockdown decelerated angiogenesis *in vitro* and resulted in cell death in both batches, concluding that VIM might be an essential protein for the angiogenic cascade and cell survival of ECs. Additionally, it was shown that VIM and MAT2A were highest expressed in beginning stages of angiogenesis *in vitro*, followed by a low-level expression. Concurrently, TPI was first upregulated and subsequently stably expressed during the course of angiogenesis. In order to validate the connection between the three proteins and to determine the impact of TPI and MAT2A on angiogenesis, it is necessary to do further research, i.e. knocking down of TPI and of MAT2A. Moreover, the specific mechanisms, on how these proteins affect ECs during angiogenesis *in vitro* must be analysed.

Supporting information

S1 Fig. Stages of angiogenesis *in vitro* of HDMECs. Native groups (N_1, N_2), control groups (SCR_1, SCR_2) and knockdown groups (sh_1, sh_2) are presented. Mean values are calculated for 4 visual fields of 4 wells per culture at 14 detection days during a cultivation period of 50 days. Native and control groups of both batches ran through all six stages of angiogenesis chronologically. Cells of sh_1 and sh_2 entered stage 4 as a maximum. Sh_2 displayed a persistence in cell death until no further staging was possible from day 36 onwards.
(TIF)

S1 Table. List of primers used for overexpression (VIM^+) and RT–qPCR. Genes of interest: qVIM, qMAT2A, qTPI, qVEGFR–1 and qVEGFR–2; reference genes: succinate dehydrogenase complex, subunit A (qSDHA), hydroxymethylebilane synthase (qHMBS), glyceraldehyde–3–phosphate dehydrogenase (qGAPDH) and TATA box binding protein (qTBP).
(DOCX)

S2 Table. VEGFR–1 and VEGFR–2 expression in native ECs of HD1 and HD2. Median and standard error was evaluated at day 1, 5, 15, 25 and 50 of cultivation. By using Mann–Whitney U test for unpaired data, it was shown that VEGFR–2 was higher expressed than VEGFR–1 at every point of investigation in both cultures ($p<0.05$).
(DOCX)

S3 Table. Morphologically assigned stages of angiogenesis *in vitro*. Mean values and standard deviation for all groups of both batches at 14 detection days over the cultivation period of 50 days are presented.
(DOCX)

S4 Table. VIM, TPI and MAT2A expression. Median and standard error of VIM TPI and MAT2A expression in N_1, SCR_1, sh_1, N_2, SCR_2 and sh_2 are shown for day 5, 15, 25 and 50.
(DOCX)

S1 Raw images.
(PDF)

Acknowledgments

The authors want to thank Constance Scharff and the research group of Animal Behaviour, Institute of Biology at FU Berlin for supporting the synthesis of viral particles and acknowledges Dr. Ezequiel Mendoza for assistance in RT–qPCR analysis.

Author Contributions

Conceptualization: Christina Herre, Arpenik Nshdejan, Mahtab Bahramsoltani.

Data curation: Christina Herre, Arpenik Nshdejan.

Formal analysis: Giuliano Mario Corte, Mahtab Bahramsoltani.

Investigation: Christina Herre.

Methodology: Arpenik Nshdejan, Mahtab Bahramsoltani.

Project administration: Mahtab Bahramsoltani.

Supervision: Robert Klopfleisch, Giuliano Mario Corte, Mahtab Bahramsoltani.

Writing – original draft: Christina Herre.

References

1. Risau W. Mechanisms of angiogenesis. Nature. 1997; 386:671–4. https://doi.org/10.1038/386671a0 PMID: 9109485
2. Patan S. Vasculogenesis and angiogenesis as mechanisms of vascular network formation, growth and remodeling. J Neurooncol. 2000; 50:1–15. https://doi.org/10.1023/a:1006493130855 PMID: 11245270
3. Arboleda-Velasquez JF, D'Amore PA. Vasculogenesis and Angiogenesis. In: Cellular and Molecular Pathobiology of Cardiovascular Disease: Elsevier; 2014. p. 181–196. https://doi.org/10.1016/B978-0-12-405206-2.00010–7
4. Ribatti D, Crivellato E. "Sprouting angiogenesis", a reappraisal. Dev Biol. 2012; 372:157–65. https://doi.org/10.1016/j.ydbio.2012.09.018 PMID: 23031691
5. Omorphos NP, Gao C, Tan SS, Sangha MS. Understanding angiogenesis and the role of angiogenic growth factors in the vascularisation of engineered tissues. Mol Biol Rep. 2021; 48:941–50. https://doi.org/10.1007/s11033-020-06108-9 PMID: 33393005
6. Nosrati H, Aramideh Khouy R, Nosrati A, Khodaei M, Banitalebi-Dehkordi M, Ashrafi-Dehkordi K, et al. Nanocomposite scaffolds for accelerating chronic wound healing by enhancing angiogenesis. J Nanobiotechnology. 2021; 19:1. https://doi.org/10.1186/s12951-020-00755-7 PMID: 33397416
7. Tanase CE, Sartoris A, Popa MI, Verestiuc L, Unger RE, Kirkpatrick CJ. In vitro evaluation of biomimetic chitosan-calcium phosphate scaffolds with potential application in bone tissue engineering. Biomed Mater. 2013; 8:25002. https://doi.org/10.1088/1748-6041/8/2/025002 PMID: 23343569
8. Russel William and Burch Rex. The Principles of Humane Experimental Technique. Medical Journal of Australia. 1960; 1:500. https://doi.org/10.5694/j.1326-5377.1960.tb73127.x
9. Stryker ZI, Rajabi M, Davis PJ, Mousa SA. Evaluation of Angiogenesis Assays. Biomedicines 2019. https://doi.org/10.3390/biomedicines7020037 PMID: 31100863
10. Nowak-Sliwinska P, Alitalo K, Allen E, Anisimov A, Aplin AC, Auerbach R, et al. Consensus guidelines for the use and interpretation of angiogenesis assays. Angiogenesis. 2018; 21:425–532. https://doi.org/10.1007/s10456-018-9613-x PMID: 29766399
11. Iqbal F, Szaraz P, Librach M, Gauthier-Fisher A, Librach CL. Angiogenic potency evaluation of cell therapy candidates by a novel application of the in vitro aortic ring assay. Stem Cell Res Ther. 2017; 8:184. https://doi.org/10.1186/s13287-017-0631-1 PMID: 28807010
12. Doke SK, Dhawale SC. Alternatives to animal testing: A review. Saudi Pharm J. 2015; 23:223–9. https://doi.org/10.1016/j.jsps.2013.11.002 PMID: 26106269
13. Tahergorabi Z, Khazaei M. A review on angiogenesis and its assays. Iran J Basic Med Sci. 2012; 15:1110–26. PMID: 23653839
14. Bahramsoltani M, Plendl J. A new in vitro model to quantify angiogenesis. [Ein neues in vitro Modell zur Quantifizierung der Angiogenese]. ALTEX. 2004; 21:227–44. PMID: 15586254

15. Bahramsoltani M, Plendl J. Different ways to antiangiogenesis by angiostatin and suramin, and quantitation of angiostatin-induced antiangiogenesis. APMIS. 2007; 115:30–46. https://doi.org/10.1111/j.1600-0463.2007.apm_405.x PMID: 17223849

16. Bahramsoltani M, Spiegelaere W de, Janczyk P, Hiebl B, Cornillie P, Plendl J. Quantitation of angiogenesis in vitro induced by VEGF-A and FGF-2 in two different human endothelial cultures—an all-in-one assay. Clin Hemorheol Microcirc. 2010; 46:189–202. https://doi.org/10.3233/CH-2010-1345 PMID: 21135494

17. Bahramsoltani M, Spiegelaere W de. Quantitation of Tumor Angiogenesis In Vitro: An All-In-One Angiogenesis Assay. Methods Mol Biol. 2016; 1464:185–91. https://doi.org/10.1007/978-1-4939-3999-2_17 PMID: 27858367

18. Bahramsoltani M, Harms T, Drewes B, Plendl J. Searching for markers to identify angiogenic endothelial cells: a proteomic approach. Clin Hemorheol Microcirc. 2013; 55:255–69. https://doi.org/10.3233/CH-2012-1631 PMID: 23089887

19. Danielsson F, Peterson MK, Caldeira Araújo H, Lautenschläger F, Gad AKB. Vimentin Diversity in Health and Disease. Cells. 2018. https://doi.org/10.3390/cells7100147 PMID: 30248895

20. Patteson AE, Vahabikashi A, Goldman RD, Janmey PA. Mechanical and Non-Mechanical Functions of Filamentous and Non-Filamentous Vimentin. Bioessays. 2020; 42:e2000078. https://doi.org/10.1002/bies.202000078 PMID: 32893352

21. van Beijnum JR, Dings RP, van der Linden E, Zwaans BMM, Ramaekers FCS, Mayo KH, et al. Gene expression of tumor angiogenesis dissected: specific targeting of colon cancer angiogenic vasculature. Blood. 2006; 108:2339–48. https://doi.org/10.1182/blood-2006-02-004291 PMID: 16794251

22. Tsuruta D, Jones JCR. The vimentin cytoskeleton regulates focal contact size and adhesion of endothelial cells subjected to shear stress. J Cell Sci. 2003; 116:4977–84. https://doi.org/10.1242/jcs.00823 PMID: 14625391

23. Dave JM, Bayless KJ. Vimentin as an integral regulator of cell adhesion and endothelial sprouting. Microcirculation. 2014; 21:333–44. https://doi.org/10.1111/micc.12111 PMID: 24387004

24. Antfolk D, Sjöqvist M, Cheng F, Isoniemi K, Duran CL, Rivero-Muller A, et al. Selective regulation of Notch ligands during angiogenesis is mediated by vimentin. Proc Natl Acad Sci USA. 2017; 114:E4574–E4581. https://doi.org/10.1073/pnas.1703057114 PMID: 28533359

25. Liu T, Guevara OE, Warburton RR, Hill NS, Gaestel M, Kayyali US. Regulation of vimentin intermediate filaments in endothelial cells by hypoxia. Am J Physiol Cell Physiol. 2010; 299:C363–73. https://doi.org/10.1152/ajpcell.00057.2010 PMID: 20427712

26. Cesari C de, Barravecchia I, Pyankova OV, Vezza M, Germani MM, Scebba F, et al. Hypergravity Activates a Pro-Angiogenic Homeostatic Response by Human Capillary Endothelial Cells. Int J Mol Sci 2020. https://doi.org/10.3390/ijms21072354 PMID: 32231163

27. Wierenga RK, Kapetaniou EG, Venkatesan R. Triosephosphate isomerase: a highly evolved biocatalyst. Cell Mol Life Sci. 2010; 67:3961–82. https://doi.org/10.1007/s00018-010-0473-9 PMID: 20694739

28. Qiu J, Gao H-Q, Zhou R-H, Liang Y, Zhang X-H, Wang X-P, et al. Proteomics analysis of the proliferative effect of low-dose ouabain on human endothelial cells. Biol Pharm Bull. 2007; 30:247–53. https://doi.org/10.1248/bpb.30.247 PMID: 17268060

29. Orosz F, Oláh J, Ovádi J. Triosephosphate isomerase deficiency: new insights into an enigmatic disease. Biochim Biophys Acta. 2009; 1792:1168–74. https://doi.org/10.1016/j.bbadis.2009.09.012 PMID: 19786097

30. Yamaji R, Fujita K, Nakanishi I, Nagao K, Naito M, Tsuruo T, et al. Hypoxic up-regulation of triosephosphate isomerase expression in mouse brain capillary endothelial cells. Arch Biochem Biophys. 2004; 423:332–42. https://doi.org/10.1016/j.abb.2004.01.003 PMID: 15001397

31. Firestone RS, Schramm VL. The Transition-State Structure for Human MAT2A from Isotope Effects. J Am Chem Soc. 2017; 139:13754–60. https://doi.org/10.1021/jacs.7b05803 PMID: 28880543

32. Shafqat N, Muniz JRC, Pilka ES, Papagrigoriou E, Delft F von, Oppermann U, et al. Insight into S-adenosylmethionine biosynthesis from the crystal structures of the human methionine adenosyltransferase catalytic and regulatory subunits. Biochem J. 2013; 452:27–36. https://doi.org/10.1042/BJ20121580 PMID: 23425511

33. Sahin M, Sahin E, Gümüşlü S, Erdoğan A, Gültekin M. DNA methylation or histone modification status in metastasis and angiogenesis-related genes: a new hypothesis on usage of DNMT inhibitors and S-adenosylmethionine for genome stability. Cancer Metastasis Rev. 2010; 29:655–76. https://doi.org/10.1007/s10555-010-9253-0 PMID: 20821252

34. Banerjee S, Bacanamwo M. DNA methyltransferase inhibition induces mouse embryonic stem cell differentiation into endothelial cells. Exp Cell Res. 2010; 316:172–80. https://doi.org/10.1016/j.yexcr.2009.08.011 PMID: 19715692

35. Haesler S, Rochefort C, Georgi B, Licznerski P, Osten P, Scharff C. Incomplete and inaccurate vocal imitation after knockdown of FoxP2 in songbird basal ganglia nucleus Area X. PLoS Biol. 2007; 5:e321. https://doi.org/10.1371/journal.pbio.0050321 PMID: 18052609

36. Lois C, Hong EJ, Pease S, Brown EJ, Baltimore D. Germline transmission and tissue-specific expression of transgenes delivered by lentiviral vectors. Science. 2002; 295:868–72. https://doi.org/10.1126/science.1067081 PMID: 11786607

37. Spiegelaere W de, Cornillie P, van den Broeck W, Plendl J, Bahramsoltani M. Angiopoietins differentially influence in vitro angiogenesis by endothelial cells of different origin. Clin Hemorheol Microcirc. 2011; 48:15–27. https://doi.org/10.3233/CH-2011-1393 PMID: 21876231

38. Olias P, Adam I, Meyer A, Scharff C, Gruber AD. Reference genes for quantitative gene expression studies in multiple avian species. PLoS One. 2014; 9:e99678. https://doi.org/10.1371/journal.pone.0099678 PMID: 24926893

39. Suchting S, Freitas C, Le Noble F, Benedito R, Bréant C, Duarte A, et al. The Notch ligand Delta-like 4 negatively regulates endothelial tip cell formation and vessel branching. PNAS. 2007; 104:3225–30. https://doi.org/10.1073/pnas.0611177104 PMID: 17296941

40. Chappell JC, Bautch VL. Vascular Development. In: Koopman P, editor. Organogenesis in Development: Organogenesis in development. 1st ed. s.l.: Elsevier textbooks; 2010. p. 43–72. https://doi.org/10.1016/S0070-2153(10)90002-1

41. Gerhardt H, Golding M, Fruttiger M, Ruhrberg C, Lundkvist A, Abramsson A, et al. VEGF guides angiogenic sprouting utilizing endothelial tip cell filopodia. J Cell Bio. 2003; 161:1163–77. https://doi.org/10.1083/jcb.200302047 PMID: 12810700

42. Rusu MC, Poalelungi CV, Vrapciu AD, Nicolescu MI, Hostiuc S, Mogoanta L, et al. Endocardial tip cells in the human embryo—facts and hypotheses. PLoS One. 2015; 10:e0115853. https://doi.org/10.1371/journal.pone.0115853 PMID: 25617624

43. Yetkin-Arik B, Vogels IMC, Nowak-Sliwinska P, Weiss A, Houtkooper RH, van Noorden CJF, et al. The role of glycolysis and mitochondrial respiration in the formation and functioning of endothelial tip cells during angiogenesis. Sci Rep. 2019; 9:12608. https://doi.org/10.1038/s41598-019-48676-2 PMID: 31471554

44. Wang X, Ackermann M, Neufurth M, Wang S, Li Q, Feng Q, et al. Restoration of Impaired Metabolic Energy Balance (ATP Pool) and Tube Formation Potential of Endothelial Cells under "high glucose", Diabetic Conditions by the Bioinorganic Polymer Polyphosphate. Polymers. 2017; 9:575. https://doi.org/10.3390/polym9110575 PMID: 30965879

45. Gómez-Escudero J, Clemente C, García-Weber D, Acín-Pérez R, Millán J, Enríquez JA, et al. PKM2 regulates endothelial cell junction dynamics and angiogenesis via ATP production. Sci Rep. 2019; 9:15022. https://doi.org/10.1038/s41598-019-50866-x PMID: 31636306

46. Eekels JJM, Pasternak AO, Schut AM, Geerts D, Jeeninga RE, Berkhout B. A competitive cell growth assay for the detection of subtle effects of gene transduction on cell proliferation. Gene Ther. 2012; 19:1058–64. https://doi.org/10.1038/gt.2011.191 PMID: 22113311

47. Robert A, Hookway C, Gelfand VI. Intermediate filament dynamics: What we can see now and why it matters. Bioessays. 2016; 38:232–43. https://doi.org/10.1002/bies.201500142 PMID: 26763143

48. Bazzoni G, Dejana E. Endothelial cell-to-cell junctions: molecular organization and role in vascular homeostasis. Physiol Rev. 2004; 84:869–901. https://doi.org/10.1152/physrev.00035.2003 PMID: 15269339

49. Kist M, Vucic D. Cell death pathways: intricate connections and disease implications. EMBO J. 2021; 40:e106700. https://doi.org/10.15252/embj.2020106700 PMID: 33439509

50. Lu SC, Mato JM. S-Adenosylmethionine in cell growth, apoptosis and liver cancer. J Gastroenterol Hepatol. 2008; 23 Suppl 1:S73–7. https://doi.org/10.1111/j.1440-1746.2007.05289.x PMID: 18336669

S1 Table. List of primers used for overexpression (VIM+) and RT–qPCR. Genes of interest: qVIM, qMAT2A, qTPI, qVEGFR–1 and qVEGFR–2; reference genes: succinate dehydrogenase complex, subunit A (qSDHA), hydroxymethylebilane synthase (qHMBS), glyceraldehyde–3–phosphate dehydrogenase (qGAPDH) and TATA box binding protein (qTBP).

Target Gene	Orientation	Primer sequence (5' – 3')	Amplicon length (bp)	Annealing Temperature (°C)
VIM$^+$	forward	GCGGGATCCGCCACCATGTCCACCAGGTCCGTGTCC	101	69
	reverse	GCGGAATTCAATTCAAGGTCATCGTGATG		
qVIM	forward	GGCACGTCTTGACCTTGAAC	110	64
	reverse	GTTCCTGAATCTGAGCCTGC		
qTPI	forward	TGGCATCACTGAGAAGGTTG	122	63
	reverse	TTGCAGTCTTGCCAGTACCA		
qMAT2A	forward	CTGGCAGAACTACGCCGTAATG	116	66
	reverse	GTGTGGACTCTGATGGGAAGCA		
qSDHA	forward	CAAACTCGCTCTTGGACCTG	118	64
	reverse	ACAGATTCTTCCCCAGCGTT		
qHMBS	forward	TGCCAGAGAAGAGTGTGGTG	101	62
	reverse	GAGGTTTCCCCGAATACTCC		
qGAPDH	forward	ACACCCACTCCTCCACCTTT	99	62
	reverse	TGCTGTAGCCAAATTCGTTG		
qTBP	forward	GAGCTGTGATGTGAAGTTTCC	118	61
	reverse	TCTGGGTTTGATCATTCTGTAG		
qVEGFR–1 [16]	forward	GACCTGGAGTTACCCTGATGAAA	76	60
	reverse	GGCATGGGAATTGCTTTGG		
qVEGRF–2 [16]	forward	CACCACTCAAACGCTGACATGTA	95	60
	reverse	GCTCGTTGGCGCACTCTT		

S2 Table. VEGFR–1 and VEGFR–2 expression in native ECs of HD1 and HD2. Median and standard error was evaluated at day 1, 5, 15, 25 and 50 of cultivation. By using Mann–Whitney U test for unpaired data, it was shown that VEGFR–2 was higher expressed than VEGFR–1 at every point of investigation in both cultures ($p<0.05$).

	Day 1		Day 5		Day 15		Day 25		Day 50	
	VEGFR–1	**VEGFR–2**	**VEGFR–1**	**VEGFR–2**	**VEGFR–1**	**VEGFR–2**	**VEGFR–1**	**VEGFR–2**	**VEGFR–1**	**VEGFR–2**
N_1	25.92 ± 3.14	54.42 ± 4.43	12.37 ± 5.70	20.98 ± 8.82	11.63 ± 1.16	24.47 ± 2.05	6.16 ± 2.21	14.72 ± 4.55	7.44 ± 1.61	102.94 ± 5.05
N_2	1.55 ± 0.70	8.56 ± 1.77	8.26 ± 1.90	40.26 ± 5.24	10.29 ± 0.83	62.06 ± 3.69	5.24 ± 1.34	18.33 ± 3.67	5.22 ± 1.11	16.09 ± 2.30

S3 Table. Morphologically assigned stages of angiogenesis *in vitro*. Mean values and standard deviation for all groups of both batches at 14 detection days over the cultivation period of 50 days are presented.

	Day 4	Day 8	Day 11	Day 15	Day 18	Day 22	Day 25	Day 29	Day 32	Day 36	Day 39	Day 43	Day 46	Tag50
N_1	2.25	2.63	2.75	2.88	3.13	3.88	4.63	5.63	5.75	5.75	6.00	6.00	6.00	6.00
	± 0.46	± 0.52	± 0.46	± 0.35	± 0.64	± 0.35	± 0.52	± 0.52	± 0.46	± 0.46	± 0.00	± 0.00	± 0.00	± 0.00
SCR_1	2.13	2.38	2.75	3.00	3.50	3.75	4.13	4.75	5.50	5.63	5.75	6.00	6.00	6.00
	± 0.35	± 0.52	± 0.46	± 0.53	± 0.76	± 0.46	± 0.35	± 0.46	± 0.53	± 0.52	± 0.46	± 0.00	± 0.00	± 0.00
sh_1	1.75	2.13	2.13	2.50	2.25	2.38	2.63	3.50	3.63	3.88	4.13	4.13	4.13	4.13
	± 0.46	± 0.35	± 0.35	± 0.53	± 0.46	± 0.52	± 0.74	± 0.76	± 0.74	± 0.83	± 0.35	± 0.35	± 0.35	± 0.35
N_2	1.75	2.00	2.25	2.50	3.75	4.13	5.63	5.75	6.00	6.00	6.00	6.00	6.00	6.00
	± 0.46	± 0.00	± 0.71	± 0.93	± 0.71	± 0.64	± 0.74	± 0.46	± 0.00	± 0.00	± 0.00	± 0.00	± 0.00	± 0.00
SCR_2	1.50	1.63	1.75	2.13	2.50	3.50	4.13	4.75	4.88	5.00	5.13	5.63	5.75	5.88
	± 0.53	± 0.52	± 0.46	± 0.83	± 0.93	± 0.93	± 0.99	± 0.46	± 0.35	± 0.00	± 0.35	± 0.52	± 0.46	± 0.35
sh_2	1.25	1.75	1.88	2.00	2.13	1.88	2.38	3.50	3.50	–	–	–	–	–
	± 0.46	± 0.46	± 0.64	± 0.53	± 0.64	± 0.64	± 0.52	± 0.93	± 0.93	–	–	–	–	–

S4 Table. VIM, TPI and MAT2A expression. Median and standard error of VIM TPI and MAT2A expression in N_1, SCR_1, sh_1, N_2, SCR_2 and sh_2 are shown for day 5, 15, 25 and 50.

		Day 5	Day 15	Day 25	Day 50
	VIM	3.11 ± 1.07	3.80 ± 0.67	2.67 ± 0.64	0.79 ± 0.99
N_1	**TPI**	0.37 ± 0.46	0.68 ± 0.42	0.76 ± 0.67	12.15 ± 3.87
	MAT2A	4.30 ± 1.13	1.93 ± 0.73	0.94 ± 1.79	0.51 ± 1.89
	VIM	3.77 ± 1.25	1.72 ± 1.08	1.77 ± 0.55	0.98 ± 0.56
SCR_1	**TPI**	0.31 ± 0.54	0.73 ± 0.42	0.97 ± 0.87	7.99 ± 1.62
	MAT2A	6.94 ± 1.62	0.48 ± 0.96	0.54 ± 0.35	2.09 ± 0.97
	VIM	0.12 ± 0.26	0.30 ± 0.41	1.04 ± 0.44	0.69 ± 0.46
sh_1	**TPI**	0.85 ± 1.05	0.93 ± 0.57	0.66 ± 0.54	X
	MAT2A	10.56 ± 1.76	0.56 ± 0.97	0.63 ± 1.04	X
	VIM	5.60 ± 1.25	6.53 ± 1.12	1.73 ± 0.49	2.18 ± 0.59
N_2	**TPI**	0.34 ± 0.21	0.74 ± 0.46	0.89 ± 0.31	0.87 ± 0.41
	MAT2A	14.67 ± 1.28	2.79 ± 0.67	0.63 ± 0.46	1.65 ± 1.81
	VIM	7.01 ± 1.35	3.59 ± 0.87	2.12 ± 0.70	1.87 ± 0.60
SCR_2	**TPI**	0.22 ± 0.29	0.92 ± 0.51	1.08 ± 0.90	0.95 ± 0.42
	MAT2A	12.93 ± 1.32	1.57 ± 0.78	0.41 ± 0.37	0.95 ± 0.31
	VIM	0.04 ± 0.10	0.06 ± 0.24	0.34 ± 0.30	0.11 ± 0.22
sh_2	**TPI**	0.21 ± 0.28	0.16 ± 0.32	0.35 ± 0.74	X
	MAT2A	8.13 ± 1.46	1.44 ± 0.71	0.44 ± 0.46	X

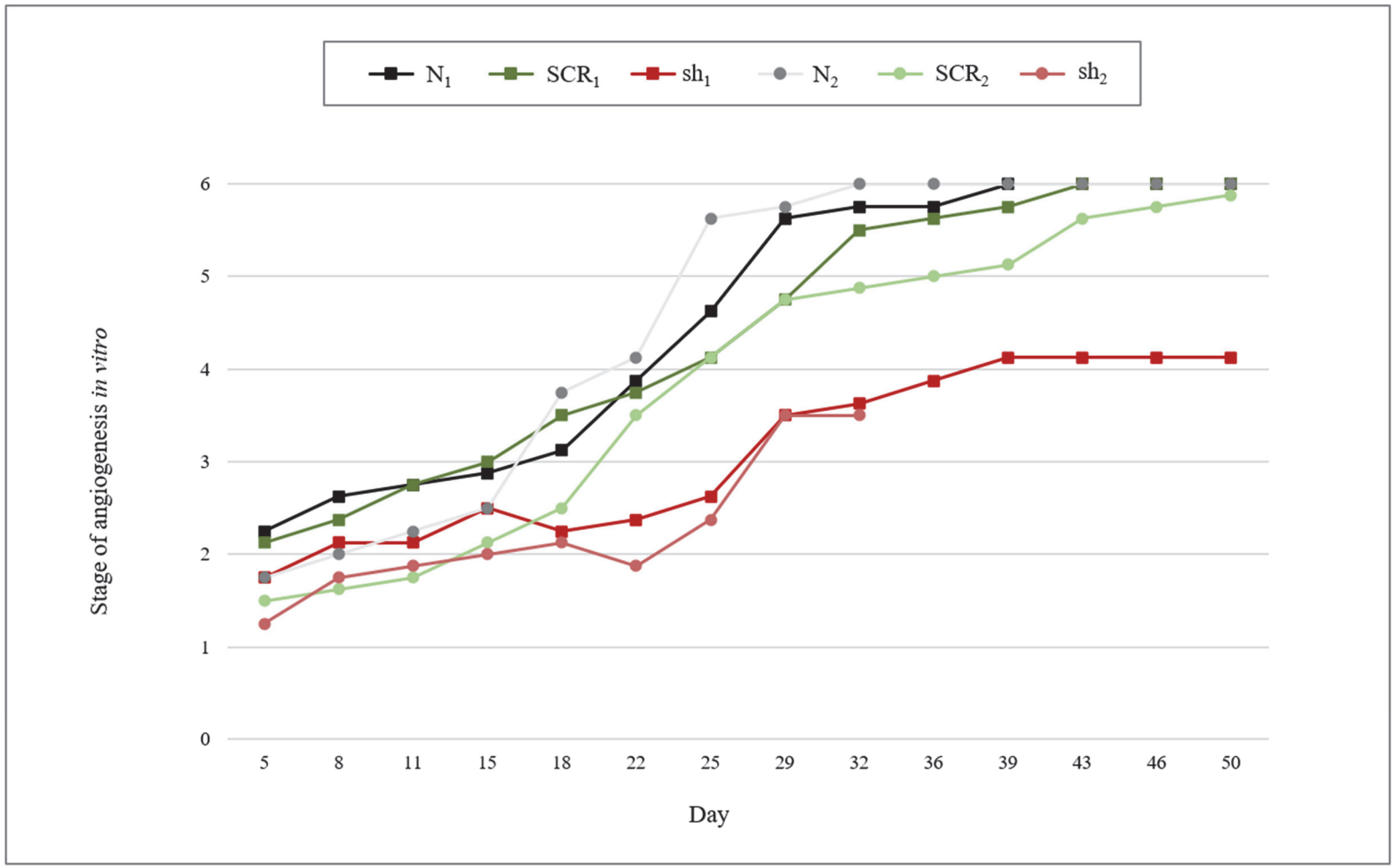

S1 Fig. Stages of angiogenesis *in vitro* of HDMECs. Native groups (N_1, N_2), control groups (SCR_1, SCR_2) and knockdown groups (sh_1, sh_2) are presented. Mean values are calculated for 4 visual fields of 4 wells per culture at 14 detection days during a cultivation period of 50 days. Native and control groups of both batches ran through all six stages of angiogenesis chronologically. Cells of sh_1 and sh_2 entered stage 4 as a maximum. Sh_2 displayed a persistence in cell death until no further staging was possible from day 36 onwards.

4. Publication II

RESEARCH ARTICLE

Knockdown of TPI in human dermal microvascular endothelial cells and its impact on angiogenesis *in vitro*

OPEN ACCESS

Authors: Christina Herre[1], Arpenik Nshdejan[1], Robert Klopfleisch[2], Giuliano Mario Corte[3], Mahtab Bahramsoltani[1]

Affiliations: **1** Department of Veterinary Medicine, Institute of Veterinary Anatomy, Freie Universität Berlin, Berlin, Germany,
2 Department of Veterinary Medicine, Institute of Veterinary Pathology, Freie Universität Berlin, Berlin, Germany
3 Department of Veterinary Medicine, Institute of Veterinary Anatomy, Universität Zürich, Zurich, Switzerland

Received: July 26, 2023
Accepted: November 10, 2023
Published: December 20, 2023

Journal: PLoS ONE 18(12): e0294933

DOI: https://doi.org/10.1371/journal.pone.0294933

Editor: Salvatore V. Pizzo, Duke University School of Medicine, UNITED STATES

Contribution of work:

Name	Type of Authorship	Contribution to Publication I
Christina Herre	First author	Correspondence with PLoS ONE Conceptualization Investigation Methodology Data curation Data analysis Formal analysis Writing
Arpenik Nshdejan	Co-author	Data curation Writing -review and editing
Robert Klopfleisch	Co-author	Supervision Writing -review and editing
Giuliano Mario Corte	Co-author	Supervision Writing -review and editing
Mahtab Bahramsoltani	Co-author	Formal analysis Project administration Supervision Writing -review and editing

PLOS ONE

RESEARCH ARTICLE

Knockdown of TPI in human dermal microvascular endothelial cells and its impact on angiogenesis *in vitro*

Christina Herre[1]*, Arpenik Nshdejan[1], Robert Klopfleisch[2], Giuliano Mario Corte[3], Mahtab Bahramsoltani[1]

1 Institute of Veterinary Anatomy, School of Veterinary Medicine, Freie Universität Berlin, Berlin, Germany,
2 Institute of Veterinary Pathology, School of Veterinary Medicine, Freie Universität Berlin, Berlin, Germany,
3 Department of Veterinary Medicine, Institute of Veterinary Anatomy, Universität Zürich, Zurich, Switzerland

* christina.herre@fu-berlin.de

OPEN ACCESS

Citation: Herre C, Nshdejan A, Klopfleisch R, Corte GM, Bahramsoltani M (2023) Knockdown of TPI in human dermal microvascular endothelial cells and its impact on angiogenesis *in vitro*. PLoS ONE 18(12): e0294933. https://doi.org/10.1371/journal.pone.0294933

Editor: Salvatore V. Pizzo, Duke University School of Medicine, UNITED STATES

Received: July 26, 2023

Accepted: November 10, 2023

Published: December 20, 2023

Data Availability Statement: All data files are available from the Harvard database (https://doi.org/10.7910/DVN/QWWGKU).

Funding: The author(s) received no specific funding for this work.

Competing interests: The authors have declared that no competing interests exist.

Abstract

Introduction

Angiogenic behaviour has been shown as highly versatile among Endothelial cells (ECs) causing problems of *in vitro* assays of angiogenesis considering their reproducibility. It is indispensable to investigate influencing factors of the angiogenic potency of ECs.

Objective

The present study aimed to analyse the impact of knocking down triosephosphate isomerase (TPI) on *in vitro* angiogenesis and simultaneously on vimentin (VIM) and adenosylmethionine synthetase isoform type 2 (MAT2A) expression. Furthermore, native expression profiles of TPI, VIM and MAT2A in the course of angiogenesis *in vitro* were examined.

Methods

Two batches of human dermal microvascular ECs were cultivated over 50 days and stimulated to undergo angiogenesis. A shRNA-mediated knockdown of TPI was performed. During cultivation, time-dependant morphological changes were detected and applied for EC-staging as prerequisite for quantifying *in vitro* angiogenesis. Additionally, mRNA and protein levels of all proteins were monitored.

Results

Opposed to native cells, knockdown cells were not able to enter late stages of angiogenesis and primarily displayed a downregulation of VIM and an uprise in MAT2A expression. Native cells increased their TPI expression and decreased their VIM expression during the course of angiogenesis *in vitro*. For MAT2A, highest expression was observed to be in the beginning and at the end of angiogenesis.

Conclusion

Knocking down TPI provoked expressional changes in VIM and MAT2A and a deceleration of *in vitro* angiogenesis, indicating that TPI represents an angiogenic protein. Native expression profiles lead to the assumption of VIM being predominantly relevant in beginning stages, MAT2A in beginning and late stages and TPI during the whole course of angiogenesis *in vitro*.

Introduction

The process of building new blood vessels due to endothelial sprouting or intussusceptive growth, is defined as angiogenesis [1]. Sprouting angiogenesis *in vivo* is based on the specialization of endothelial cells (ECs) into tip cells, stalk cells and phalanx cells. An angiogenic stimulus, e.g. vascular endothelial growth factor A (VEGF-A), induces tip cell differentiation and filopodia formation via the vascular endothelial growth factor receptor-2 (VEGFR-2). While tip cells migrate towards the stimulus, stalk cells differentiate and proliferate in order to elongate the sprout. Guidance for the sprout growth is mainly conducted by stalk cells expressing predominantly vascular endothelial growth factor receptor-1 (VEGFR-1). After lumenogenesis, phalanx cells promote vessel integrity and stabilization [2,3].

Respectively, an excessive or deficient course of angiogenesis promotes many pathological events, such as tumor growth or dysfunctional tissue repair. Currently, the research field of angiogenesis is mainly focusing on cancer treatment, tissue engineering and wound healing [4,5]. In practice, *in vitro* models are frequently used in order to reduce time and cost, be carried out expeditiously, and mainly to reduce animal experiments in the sense of the 3R principle. Nevertheless, *in vitro* models display inconsistencies regarding their reproducibility, based on the inhomogeneous use of models and the heterogeneous character of ECs [2,6–9].

Variations considering the angiogenic potency of ECs were also shown by Bahramsoltani et al. [10–13]. Several batches of capillary-derived primary cell cultures of human microvascular ECs were cultivated *in vitro* while using a newly established all-in-one assay, which comprises all phases of angiogenesis. Partially, cells were not able to enter all defined stages of angiogenesis *in vitro*, hence being classified as non-angiogenic ECs. Comparatively, angiogenic ECs ran through each angiogenic stage *in vitro* chronologically. By searching for proteomic differences between both batches of ECs, seven proteins were detected solely in angiogenic ECs and one protein in non-angiogenic ECs [14]. Three of these proteins were triosephosphate isomerase (TPI), vimentin (VIM) and S–adenosylmethionine synthetase isoform type 2 (MAT2A) [15].

TPI was one of the proteins found in angiogenic ECs [14]. It is a dimeric, non-allosteric enzyme which is primarily known for its catalytic activity in glycolytic pathways. Hereby, it facilitates the interconversion of dihydroxyacetone phosphate and D–glyceraldehyde–3–phosphate [16,17]. Recently, several additional functions were attributed to TPI which do not necessarily involve catalysis, defining TPI as a moonlighting protein [17–19]. Considering ECs, an increase in TPI expression induced by hypoxia had been demonstrated in capillary ECs [20]. Besides hypoxia, it was also shown that glycolysis can be stimulated via VEGF in ECs *in vitro* [21]. Furthermore, TPI expression and glycolic metabolism appeared to be higher in angiogenic ECs using the generated energy for cell motility and proliferation [15,22].

VIM represents an additional protein being detected in angiogenic ECs [14]. As a type III intermediate filament protein, VIM is mostly known for stabilizing intracellular structures,

influencing cell shape and contractility. Besides intracellular signalling pathways, VIM is also highly involved in extracellular regulations affecting divers physiological and pathological events, such as cell growth and differentiation, wound healing and viral infections [23–25]. By knocking down VIM, it had been shown that this protein is essential for ECs to run through all stages of angiogenesis *in vitro*. Over the course of angiogenesis *in vitro*, highest VIM expressions were detected in the beginning stages, indicating its involvement in cell migration [15,24,26]. Additionally, dynamics in VIM expression were detected in microvascular ECs, adjusting cell adhesion and motility to environmental stress [27,28]. Up until today, VIM is being analysed to reveal further molecular mechanisms that are involved in the process of angiogenesis [29].

MAT2A was the protein found in non-angiogenic ECs [14]. In most tissues, this enzyme is mainly encoded by the MAT2A-gene. Its primary function is catalysing the synthesis of S-adenosylmethionine (SAM) from methionine and adenosine triphosphate (ATP) [30–32]. SAM represents a product of the methionine cycle and thereby is involved in synthesizing polyamines, homocysteine and reduced glutathione. By being a major methyl-donor, it is highly involved in methylation reactions, e.g. protein- and DNA-methylation. Hence, it regulates cellular metabolism on genetic and molecular levels [33–35]. In ECs, it was shown that an inhibition of methylation led to an increase in VEGF-A expression followed by the differentiation of endothelial cells [36]. Moreover, a hypermethylation by supplying SAM, ECs were hindered to migrate and proliferate [37]. Currently, there is hardly any information about MAT2A and its role in angiogenesis.

This present study is based on the hypothesis of TPI being an essential angiogenic protein for angiogenesis *in vitro*. The aim of this study was to detect morphological and molecular changes in human dermal microvascular endothelial cells (HDMEC) running through *in vitro* angiogenesis after knocking down TPI. Additionally, native expression of TPI, VIM and MAT2A and expressional changes of VIM and MAT2A expression in knockdown cells were analysed.

Cells, materials and methods

Plasmids, primers and shRNA

Design and synthesis of short hairpin RNA targeting TPI-mRNA (shTPI) was executed according to previous studies [15,38,39]. In brief, four genetic shTPI sequences were generated being structured sense-loop-antisense (loop sequence `TTCAAGAGA`). First, knockdown effectiveness and the power of each hairpin construct were analyzed in HEK 293T cells *in vitro* by infecting cells with each hairpin construct individually and including a cellular induction of TPI overexpression simultaneously (TPI^+-forward `GCGGGATCCGCCACCATGGCGGAGGACG GCGAG`, TPI^+-reverse `GCGGATATCTCGTTGTTTGGCATTGATGATGTCC`). The overexpressed TPI was tagged with V5 epitope, Western Blot analysis using Rabbit polyclonal Anti-V5 tag primary antibodies (Abcam, Cambridge, UK, ab15828, 1:5,000) and donkey Anti-Rabbit IgG HRP Linked species specific F(ab')2 fragmentsecondary antibodies (GE Healthcare, Freiburg, Germany, NA9340, 1:10,000) revealed the specific construct displaying the highest knockdown efficiency (shTPI target sequence `GCTGAAGTCCAACGTCTCTGA`). Based on the shTPI sequence, a nontargeting sequence was designed consisting of the identical amount and type of nucleotides serving as control (shSCR target sequence `GCGCAGTGCCCGTACATATTA`). After attaching an U6 promotor cassette to pFUGW plasmid, containing the DNA fragments encoding the hairpins, it was used as lentiviral expression vector, additionally containing the genetic information for enhanced green fluorescent protein (eGFP). The viral particles displayed a titer in the range of 0.7–0.9 $x10^6$ IU/μl and were used in 20-fold concentration. The

amount of virus was determined after the initiation and analysis of trial runs using virus in a 10-, 20- and 30-fold concentration individually.

Cells, media and cultivation

Human dermal microvascular endothelial cells (HDMECs) were purchased from LONZA Bioscience (Basel, Switzerland, HMVEC–dBl–Neo, Cat. No. CC–2813). Distributor's analysis of CD31/105, von Willebrand Factor VIII and positive uptake for acetylated low density lipoprotein guaranteed EC population. In total, two batches (HD1 and HD2) were acquired and cultivated in EBM^{TM}–2 Endothelial Cell Growth Basal Medium–2 (LONZA, Basel, Switzerland, Cat. No. CC–00190860) as basal medium (BM). EGM^{TM}–2 MV Microvascular Endothelial SingleQuots^{TM} Kit (LONZA, Basel, Switzerland, Cat. No. CC–4147), containing Fetal Bovine Serum, growth factors, antioxidants, antibiotics, antimycotics and anti-inflammatories, was added to the BM in order to stimulate the angiogenic response in HD1 and HD2. The detailed composition of media was according to the previously described study [15]. Exchange of media were executed twice a week.

In vitro angiogenesis assay

For cultivation, 24-well-culture plates (Corning Life Sciences, Amsterdam, Netherlands, Cat. No. 3738) were used. Each well was covered with 0,5ml gelatine (Sigma Aldrich, St. Louis, MO, USA, Cat. No. G6144, 1,5% in PBS) and incubated for 20 minutes at 37˚C. Per well, 4.5 x 10^4 cells of both batches were seeded in third passage and cultivated up to 50 days at 37˚C in a 5% CO_2 humidified atmosphere (INCO2/1, Memmert GmbH & Co. KG, Schwabach, Germany). On day one, in both batches respectively, a third of cells either got infected with viral particles owning shTPI and initiating the knockdown (sh_1, sh_2), or with lentiviruses consisting shSCR serving as control group (SCR_1, SCR_2), or they remained unmodified (N_1, N_2). Twice a week, digital pictures were taken of four visual fields of each well using an inverted microscope (LEICA DMi8; Leica Microsystems, Wetzlar, Germany), LEICA MC170 HD video camera (Leica Microsystems, Wetzlar, Germany) and the imaging and analysis software Leica Application Suite X (LAS X Version 3.4.2, Leica Microsystems, Wetzlar, Germany). According to the all-in-one angiogenesis assay [10–13,40], the morphology of ECs in the micrographs were analysed and assigned to the respective stage of angiogenesis *in vitro* (Table 1. [12]). For

Table 1. Definition of stages of angiogenesis *in vitro* and description of cell morphology within the different stages [12].

Stage no.	Morphology of endothelial cells
Stage 1	Confluent monolayer Polygonal shaped cells
Stage 2	Endothelial sprouting, late phase >50% elongated shaped cells
Stage 3	Linear side–by–side arrangement, late phase >50% linearly arranged cells
Stage 4	Networking Network of linearly arranged cells
Stage 5	Three-dimensional organisation, early phase Appearance of capillary–like structures (linear structures of endothelial cells with a diameter of more than 28 μm; for these structures an internal lumen was shown by electron microscopy)
Stage 6	Three–dimensional organisation, late phase All linearly arranged cells form capillary–like structures; dissolution of cell layer on the bottom

https://doi.org/10.1371/journal.pone.0294933.t001

quantifying angiogenesis, the sum of the allocated stages of each visual field over the time was computed separately for each group of HD1 and HD2 (S^{group}). Further, the arithmetic mean of all the sums of each group was calculated and compared ($S^{\overline{group}}$).

Quantitative analysis of VIM, TPI, MAT2A transcripts via RT–qPCR

At day 5, 15, 25 and 50, harvesting of cells of each group was carried out using Hydroxyethylpiperazine Ethane Sulfonic acid, Trypsin/EDTA and Trypsin Neutralisation Solution (LONZA, Basel, Switzerland, ReagentPackTM Subculture Reagents, Cat. No. CC–5034). After centrifugation, cell pellets were deeply frozen in liquid nitrogen and stored at -76˚C. RNA isolation and digestion of remaining DNA was executed using Total RNA Kit, peqGold (Peqlab/VWR, Darmstadt, Germany, Cat. No. 12–6834) and TURBO^{TM} DNase (ThermoFisher Scientific, Bremen, Germany, Cat. No. AM2238). Applying SuperScript III Reverse Transcriptase (ThermoFisher Scientific, Bremen, Germany, Cat. No. 18091050), RNA was reverse transcribed for cDNA synthesis. Quantitative PCR was performed with triplicates of all samples, utilising Maxima SYBR Green qPCR Master Mix (2x) (ThermoFisher Scientific, Bremen, Germany, Cat. No K0223), Rotor–Gene 6000 (Qiagen, Hilden, Germany) and Rotor–Gene Q 2.3.5 software. According to the previously published article, GAPDH was shown to be the most stable reference gene and was used as normalizer gene[15]. For every gene, the respective standard curve displayed the calibrator sample and the amplification efficiency. The C_t difference between gene of interest and calibrator was determined and adjusted to the amplification efficacy. Finally, samples were normalized to GPDH. All primers are listed in the corresponding article [15].

Western blot analysis

The method of protein detection, chemicals and antibodies were applied as previously described [15]. In brief, 20μg protein per sample was deployed in triplicates and separated by 12% Bis-Tris SDS-PAGE sodium dodecyl sulfate–polyacrylamide gel electrophoresis. Proteins were transferred onto nitrocellulose membranes by electroblotting. As primary antibodies, VIM (DAKO, Hamburg, Germany, M7020, 1:500), TPI (Santa Cruz, Heidelberg, Germany, H–11, 1:200) and MAT2A (Santa Cruz, Heidelberg, Germany, B–10, 1:200) were used. Additionally, Actin (Novus Biologicals, Centennial, CO, USA, AC–15, 1:5,000) served as the internal control. For VIM and actin (ACT) detection, a further incubation in sheep anti–mouse IgG secondary antibody (GE Healthcare, Freiburg, Germany, NA9310, 1:5,000) was performed. SignalFireTM ECL Reagent (Cell Signal technology, Frankfurt, Germany, Cat No. 6883) was used for visualization. Densitometric raw volume of all samples were determined by GeneTools software version 4.03.05.0 (SynGene, Cambridge, England). Signal intensity of all values was normalised to the respective Actin.

Statistics

Statistical examination of data was performed using SPSS Statistics (SPSS Statistics 29, IBM Corporation, Armonk, NY, USA). First, the Shapiro-Wilk test was carried out revealing value distributions. Normally distributed data is presented as mean ± standard deviation, non-normally distributed as median ± standard error. By executing Student's *t* test for unpaired data or Mann–Whitney U test, two independent groups were compared. For multiple groups, analysis was done using one-way ANOVA or Kruskal-Wallis test followed by post hoc Dunn-Bonferroni test, respectively. *P*-value of 0.05 or less were defined as statistically significant.

Results

In vitro angiogenesis of N_1 and N_2, SCR_1 and SCR_2

Native cells of both batches were able to undergo the angiogenic cascade chronologically. From the beginning of cultivation, cell population of N_1 displayed a higher cell density than N_2. In N_1, endothelial sprouting was already visible at day 5, by polygonal shaped cells starting to elongate (Fig 1A). From day 25 onwards, cells displayed an early phase of three-dimensional organisation, representing stage 4 to 5 (Fig 1B). Followed by the dissolution of capillary-like structures from the bottom of the cell culture plates of stage 6, which was observed from day 39 (Fig 1C). In N_2, cells demonstrated sprouting activity from day 5 onwards (Fig 1J). In general, sprouting activity was less visible in cells of HD2 than in HD1. From day 15, linearly arranged cells generated networks (Fig 1K) and ended up building capillary-like structures after 43 days of cultivation (Fig 1L). Median and standard error of sums of assigned stages of angiogenesis (S) were calculated and compared using the Kruskal-Wallis test, followed by the post hoc Dunn-Bonferroni test. Resulting in $\bar{S}^{N_1} = 53.4 \pm 2.7$ for N_1 and $\bar{S}^{N_2} = 51.5 \pm 3.4$ for N_2 with N_2 being significantly smaller than N_1 ($p<0.001$).

Similar to N_1 and N_2, cells of SCR_1 and SCR_2 displayed a high amount of elongated shaped cells at day 5 (Fig 1D and 1M). Already at day 22, ECs of both batches reached stage 5 by networking and starting a three-dimensional organisation (Fig 1E and 1N). Finally, SCR_1 entered stage 6 after 32 days (Fig 1F) and SCR_2 after 39 days (Fig 1O). By eGFP serving as an infection control, the fluorescent signal was surveyed at each detection day. For control groups of both batches, a consistent infection was visible (Fig 1D–1F and 1M–1O). For $\bar{S}^{SCR_1}$ a value of 55.5 ± 3.0 was determined, being significantly higher than $\bar{S}^{SCR_2} = 52.1 \pm 5.1$ ($p<0.001$). No differences were detectible between native and control groups of both batches.

In vitro angiogenesis of sh_1 and sh_2

In the beginning of cultivation, no differences in sh_1 and sh_2 in comparison to native and control cells were visible considering their morphology. At day 5, cells were assigned to stages 1 and 2 (Fig 1G and 1P). However, a delay in entering next stages was visible in the following days. While native and control groups of both batches already entered stage 3 at day 8, sh_1 was able to build linear side-by-side arrangements at day 11 and sh_2 at day 15 (Fig 1H and 1Q). Stage 3 represents the furthest stage knockdown cells were able to enter during the cultivation period of 50 days. For all groups of both batches, mean values and standard deviations of all assigned stages are shown in S1 Table. The course of *in vitro* angiogenesis of respective groups are visualized in S1 Fig. A small number of cells of sh_1 started to enter stage 4 from day 18 onwards ending up in stage 5 at day 50. For these cells no fluorescence was observed, which led to the exclusion of further morphological analysis. Otherwise, eGFP signal was persistent throughout the whole cultivation in sh_1 and sh_2 (Fig 1G–1I and 1P–1R). For sh_1, a sum of $\bar{S}^{sh_1} = 44.5 \pm 3.1$ was calculated, thus a significant lower value than $\bar{S}^{N_1}$ and $\bar{S}^{SCR_1}$ ($p<0.001$). Alike, sums of N_2 and SCR_2 were significantly higher than sh_2, resulting in $\bar{S}^{sh_2} = 37.7 \pm 3.4$ ($p<0.001$). Comparing sums of knockdown groups in between batches, sh_1 showed a significantly higher value than sh_2 ($p<0.001$).

TPI, VIM and MAT2A expression in N_1 and N_2

At day 5, 15, 25 and 50 of cultivation, mRNA and protein expression of TPI, VIM and MAT2A were examined for native cells of both batches. In N_1, TPI mRNA expression was stable at first, followed by a significant increase at day 25 ($p<0.01$) and day 50 ($p<0.001$). Whereas in N_2, TPI mRNA expression decreased at day 15 ($p<0.05$) and increased on following detection

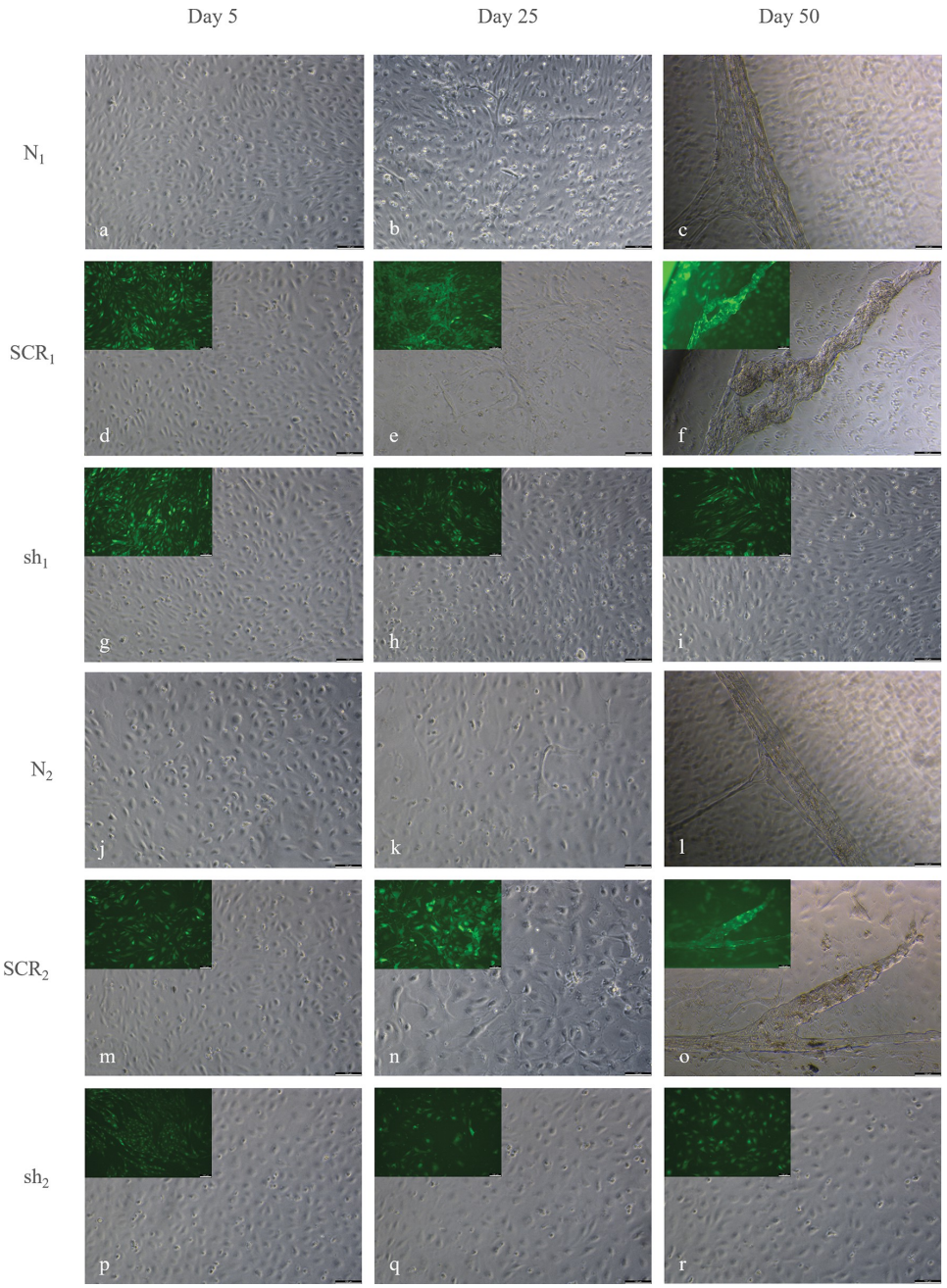

Fig 1. Morphological changes of ECs during angiogenesis *in vitro*. Native (a, b, c), control (d, e, f) and knockdown cells (g, h, i) of HD1 are presented at day 5 (a, d, g), 25 (b, e, h) and 50 (c, f, i)., followed by native (j, k, l), control (m, n, o) and knockdown cells (p, q, r) of HD2 at day 5 (j, m, p), 25 (k, n, q), and 50 (l, o, r). In the upper left corner of sh and SCR micrographs, GFP control is shown. In all groups, cells were polygonal and elongated shaped at day 5, representing stage 1–2 (a, d, g, j, m, p). At day 25, native and control cells of both batches displayed networking structures of stage 4–5 (b, e, k, n), followed by three-dimensional organisation of stage 6 (c,

f, l, o). In contrast, knockdown cells remain in stage 3, showing linear side-by-side arrangements as the furthest stage of differentiation (h, i, q, r). Scale bars = 100 μm.

https://doi.org/10.1371/journal.pone.0294933.g001

days ($p<0.001$) emerging in a significantly lower expression of TPI in N_2 at day 15 compared to N_1 ($p<0.05$, Fig 2A). On protein level, TPI was detectible during the whole angiogenic cascade *in vitro* (Fig 2B). While N_1 displayed a significant decline of VIM mRNA between day 5 and 50 ($p<0.05$), N_2 VIM expression fluctuated starting with a decrease ($p<0.001$) and an increase ($p<0.001$), followed by a down scale ($p<0.001$). At day 15, VIM mRNA expression was higher in N_1 than N_2 ($p<0.05$), whereas VIM mRNA was significantly lower in N_1 at day 50 compared to N_2 ($p<0.001$, Fig 2A). Western blot analysis showed stable protein levels of VIM (Fig 2B). Considering MAT2A, both native cell groups decreased their mRNA expression at day 15 ($p<0.01$), followed by an uprise at day 25 ($p<0.05$). Solely at day 5, MAT2A expression was observed to be significantly higher in N_1 than in N_2 ($p<0.01$, Fig 2A). Western Blot analysis displayed bright protein bands and lower protein values for N_1 at day 25 ($p<0.05$) and for N_2 at day 25 and 50 ($p<0.05$, Fig 2B, S3 Table).

Expression of TPI, VIM and MAT2A in sh_1 and sh_2

For knockdown control, eGFP was detected and TPI expression was analysed via RT-qPCR and Western blot. TPI mRNA was significantly downregulated in sh_1 compared to SCR_1 at day 5 and 15 ($p<0.001$), 25 ($p<0.01$) and 50 ($p<0.05$). Coincidentally, TPI mRNA expression in sh_2 was significantly lower than in SCR_2 at day 5 ($p<0.01$), 15 ($p<0.05$), 25 ($p<0.001$) and 50 ($p<0.05$, Fig 3A). For sh_1 and sh_2, protein expression of TPI was decreased in comparison to control groups, respectively (Fig 3D). By comparing knockdown groups of both batches, TPI mRNA expression was significantly higher in sh_1 than in sh_2 ($p<0.01$).

For assessing expressional changes in VIM and MAT2A induced by knocking down TPI, knockdown groups were compared to their respective control groups. VIM mRNA was downregulated in sh_1 at day 15 ($p<0.01$) and 25 ($p<0.05$). In contrast, an increase of mRNA was observed at day 50 ($p<0.05$). In sh_2, VIM mRNA expression was significantly downregulated at day 25 and day 50 ($p<0.05$, Fig 3B). No difference in protein expression was detected in between knockdown and control groups at any day (Fig 3D). At day 5, VIM mRNA was

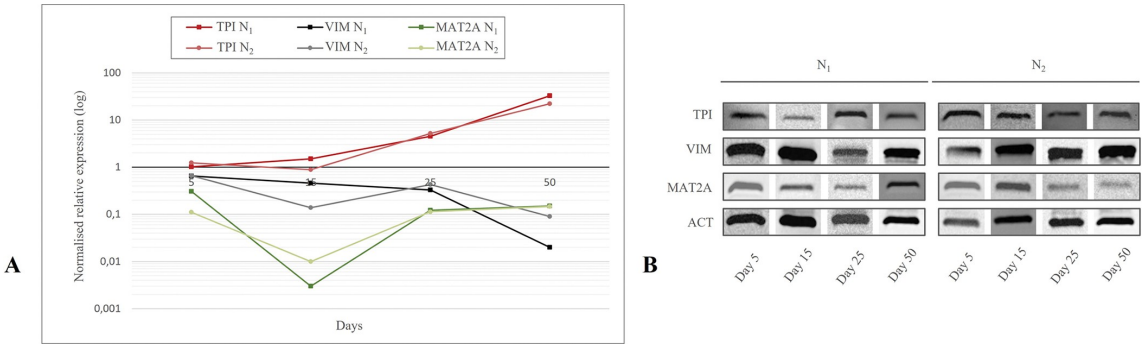

Fig 2. Expression of TPI, VIM and MAT2A in native cells. A. Changes of TPI, VIM and MAT2A mRNA expression of N_1 and N_2 in the course of angiogenesis *in vitro*. Predominantly increasing expression of TPI, decreasing expression of VIM and falling and rising expression of MAT2A was statistically analysed using Kruskal-Wallis test and post hoc Dunn-Bonferroni test ($p<0.05$). **B.** Western blot analysis of TPI, VIM and MAT2A in N_1 and N_2 at day 5, 15, 25 and 50 using ACT as internal control.

https://doi.org/10.1371/journal.pone.0294933.g002

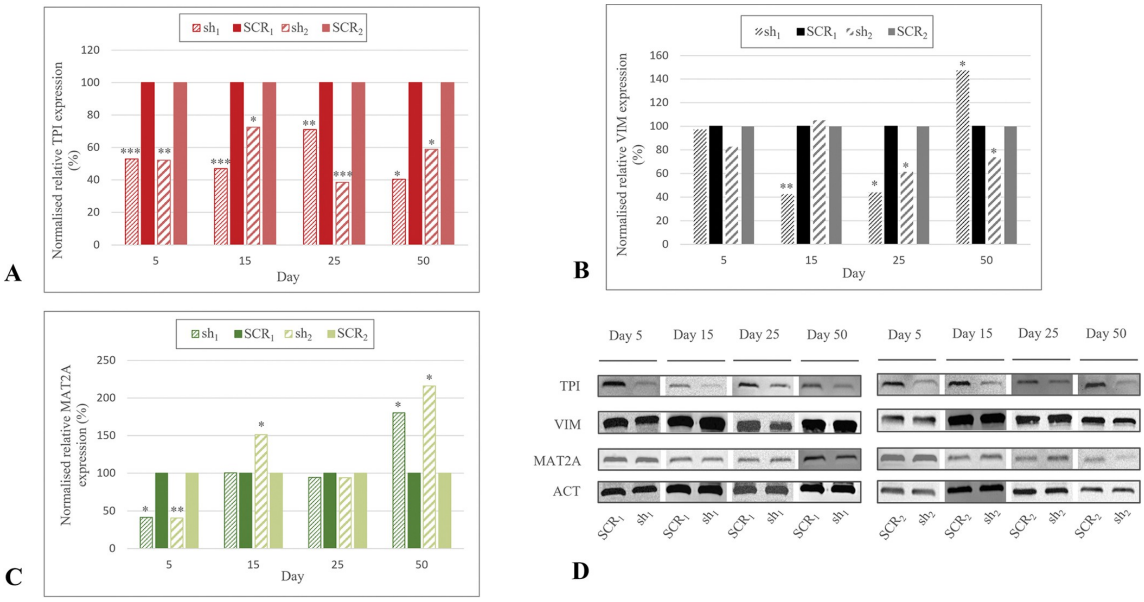

Fig 3. Expression of TPI, VIM and MAT2A in sh_1 and sh_2. Statistical analysis was performed using the Mann-Whitney U test for unpaired data. **A.** Normalised relative TPI expression of knockdown and control groups of HD1 and HD2. At each detection day, TPI expression was downregulated in sh_1 and sh_2. **B.** Normalised relative VIM expression of sh_1, SCR_1, sh_2 and SCR_2. VIM mRNA was significantly downregulated in sh_1 at day 15 and 25 and in sh_2 at day 25 and 50. Significant uprise in expression was observed in sh_1 at day 50. **C.** Normalised relative MAT2A expression of sh_1, SCR_1, sh_2 and SCR_2. MAT2A displayed a decrease in sh_1 and in sh_2 at day 5. Significantly higher expression was observed in sh_1 at day 15 and 50 and in sh_2 at day 50. **D.** Western blot analysis of TPI, VIM and MAT2A in knockdown and control groups of HD1 and HD2 at day 5, 15, 25 and 50. ACT was used as an internal control. $^{*}p<0.05$, $^{**}p<0.01$, $^{***}p<0.001$.

https://doi.org/10.1371/journal.pone.0294933.g003

expressed less in sh_1 than in sh_2 ($p<0.01$), whereas sh_1 displayed a higher VIM mRNA expression at day 50 ($p<0.001$).

For MAT2A, mRNA expression in sh_1 was less than SCR_1 at day 5 ($p<0.05$) and higher at day 50 ($p<0.05$). In sh_2, MAT2A expression was decreased at day 5 ($p<0.01$) and upregulated at day 15 ($p<0.05$) and 50 ($p<0.05$, Fig 3C). On protein level, MAT2A was detectable at each day of investigation in both batches (Fig 3D). At day 50, sh_1 and SCR_1 displayed stronger protein bands and higher values ($p<0.01$), whereas sh_2 and SCR_2 presented brighter protein bands and lower values ($p<0.001$, $p<0.05$, S3 Table). For MAT2A mRNA, no differences in between sh_1 and sh_2 were exposed. Median and standard error of mRNA expression of all three proteins is provided in S2 Table. Furthermore, S3 Table displays median and standard error of respective protein expressions.

Discussion

ECs display diversity considering their angiogenic behaviour while running through angiogenesis *in vitro* causing a lack of reliability of *in vitro* models [2,6–13]. Influencing factors on angiogenic potency of ECs must get investigated. This study is mainly focusing on the enzyme TPI and its impact on HDMECs running through angiogenesis *in vitro*. After knocking down TPI, morphological and molecular changes of VIM and MAT2A expression were examined. Additionally, native expression of TPI, VIM and MAT2A were determined during the course of angiogenesis *in vitro*.

As previously published, HD1 and HD2 are characterized as angiogenic ECs, being able to run through the whole angiogenic cascade *in vitro*. Additionally, analysis of VEGFR-1 and VEGFR-2 expression in both batches indicated a higher amount of stalk cells in the cell population of HD1 than in HD2 [15]. Endothelial stalk cells are highly proliferative in order to elongate the sprout during angiogenesis [2,3,41]. In this study, the strong proliferative character of cells of HD1 was visible by a persistently higher cell density in all groups of HD1 compared to HD2. In addition, more cells were able to enter late stages of angiogenesis, resulting in significant higher values of $S^{\bar{N}_1}$, $S^{\bar{SCR}_1}$ and $S^{\bar{sh}_1}$ than $S^{\bar{N}_2}$, $S^{\bar{SCR}_2}$ and $S^{\bar{sh}_2}$, respectively. Further, knockdown cells of HD1 were able to generate GFP-negative and therefore non-infected cells which were able to enter the angiogenic cascade and precede to further stages. In contrast, being less proliferative, sh_2 was not able to compensate manipulation and remained in early stages.

Considering native mRNA expression of TPI during angiogenesis *in vitro*, it was found to be mostly upregulated. Being a glycolytic enzyme, TPI is highly involved in energy metabolism. ATP was shown to be necessary for angiogenic stages, e.g. migration, proliferation and tube formation [21,42,43]. Furthermore, an elevation of TPI expression and of the glycolic metabolism was stated for angiogenic ECs [22]. The angiogenic character of N_1 might have caused a high expression of TPI from the beginning of cultivation, which was sufficient for cells to migrate and proliferate until day 15. Additional increase of TPI might have facilitated further differentiation of cells. For N_2, the decrease in TPI mRNA expression at day 15 might have been caused by tip cells being less glycolytically active [21]. HD2 comprises a smaller amount of stalk cells, which might have led to a significantly lower expression of TPI in HD2 in comparison to HD1. In N_1 and N_2, VIM mRNA expression decreased in the course of angiogenesis *in vitro*. The highest expression levels were detected in the beginning of cultivation, which most likely represents VIM having its major influence on the cytoskeleton of cells. Therefore, VIM is assumed to have a strong impact on early stages of angiogenesis [15,24,26]. In N_2, less sprouting and more side-by-side arrangements and networking were visible. This might have demanded a higher activity regarding cell shape and contractility, potentially causing the increase of VIM at day 25. VIM was lately identified as a positive marker for epicardial tip cells [44]. In HD2, a smaller amount of stalk cells were detected, which could have led to VIM being significantly less expressed in HD2 at day 50 compared to HD1. Furthermore, MAT2A mRNA and protein expression fluctuated in both batches during cultivation. First, a decrease was visible. Lately, MAT2A activity was associated with reducing the angiogenic potency of ECs and initiation of cell maturation via SAM [36,37,45]. Therefore, the downregulation of MAT2A in the beginning most likely caused an increase in their angiogenic potency in order to enter first stages of the angiogenic cascade. The following increased mRNA expression, which was also visible on protein level in N_1, might have initiated cells to enter final stages of angiogenesis. Infection of cells with lentiviral particles appeared to be successful and persistent during the whole cultivation period of 50 days. For SCR_1, SCR_2 as well as for sh_1 and sh_2, eGFP detection was positive at each day of investigation. No morphological or molecular differences were observed in between control and native groups. By comparing mRNA and protein expression in knockdown groups and control groups, TPI was downregulated in sh_1 and sh_2 successfully during the whole experimental period. Comparing TPI mRNA expression between sh_1 and sh_2, a higher amount was detected in sh_1. By them owning more stalk cells, the cell population of sh_1 was able to produce non-infected cells which might have increased the overall TPI mRNA expression. By excluding the non-infected cells in sh_1, knockdown groups of both batches displayed a deceleration of *in vitro* angiogenesis by not being able to precede to further stages of angiogenesis *in vitro* than stage 3. As previously described, TPI is highly contributing to cell metabolism of dividing cells [42,46], which might be the reason for

knockdown cells not being able to grow towards each other and create a network. Additionally, it has been shown that the sum of assigned stages of knockdown groups ($S^{\overline{sh}_1}$, $S^{\overline{sh}_2}$) were significantly smaller than control ($S^{\overline{SCR}_1}$, $S^{\overline{SCR}_2}$) and native groups ($S^{\overline{N}_1}$, $S^{\overline{N}_2}$). Both suggesting that TPI represents a proangiogenic protein which raises the angiogenic potency of ECs *in vitro*.

By knocking down TPI, expressional changes in sh_1 and sh_2 considering VIM and MAT2A mRNA were observed. VIM is already described as an angiogenic protein raising the angiogenic potency of HDMECs [15]. With its influence on cell shape and its involvement in Notch ligand signalling, it has a major impact on early stages of angiogenesis, especially during migration and sprouting [24,26,47,48]. Induced by TPI knockdown, cells displayed a decrease in angiogenic potency, which might have led to the downregulation of VIM expression in sh_1 and sh_2. In sh_1, the final uprise in VIM mRNA is most likely caused by non-infected cells amongst the knockdown cells. These ECs were able to enter the angiogenic cascade driven by their unaffected angiogenic potency, resulting in a significant higher VIM expression in comparison to sh_2. Based on the hypothesis that TPI has a major influence on proliferation of ECs, the knock down might have had a negative influence on their mitogenic activity. As a compensatory mechanism, sh_1 and sh_2 might have decreased their MAT2A mRNA expression in the beginning of culture, aiming the reduction of SAM levels. For SAM, a recent study stated its inhibitory influence on growth factors effecting mitosis [45]. For the following upregulation in MAT2A mRNA, both knockdown groups might have adapted to the lower angiogenic activity. MAT2A influences cellular methylation patterns via SAM, which prevents cells to undergo migration and proliferation [36,37].

Conclusion

This study presents native expression profiles of TPI, VIM and MAT2A during the angiogenic cascade of HDMECs *in vitro*. Indicative of influencing certain stages of angiogenesis *in vitro*, TPI was shown to be strongly expressed throughout angiogenesis, VIM in early stages and MAT2A mostly at the beginning and end. While knocking down TPI, cells were not able to enter late stages of angiogenic cascade *in vitro*, leading to the strong assumption of it being an angiogenic protein having a major impact on cell proliferation. By lowering the angiogenic activity of cells via TPI knockdown, it was stated that the angiogenic protein VIM was downregulated simultaneously. In contrast, MAT2A was mostly upregulated, suggesting its anti-angiogenic influence. Additionally, different batches of HDMECs displayed opposing behaviour after manipulation, despite being from the same distributor and being cultivated under the same conditions. Cell populations with a higher expression of VEGFR-1 and thus a higher amount of stalk cells were able to originate non-infected cells, which were able to enter the angiogenic cascade *in vitro* ending up in late stages. Further investigations are necessary, in order to validate the impact of the three target proteins on *in vitro* angiogenesis and the interaction in between them, e.g. knocking down MAT2A.

Supporting information

S1 Fig. Stages of *in vitro* angiogenesis. The course of angiogenesis is shown for native groups (N_1, N_2), control groups (SCR_1, SCR_2) and knockdown groups (sh_1, sh_2) during a cultivation period of 50 days. Mean values are calculated for 4 visual fields of 4 wells per culture at each detection day. Native and control groups of both batches ran through all six stages of angiogenesis chronologically. Infected cells of sh_1 and sh_2 did not precede to further stages than stage 3.
(TIF)

S1 Table. Morphologically assigned stages of angiogenesis *in vitro*. Mean values and standard deviations of native, control and knockdown groups of HD1 and HD2 are presented at each day of investigation.
(DOCX)

S2 Table. mRNA expression of VIM, TPI and MAT2A. Median and standard error of VIM, TPI and MAT2A mRNA expression of native, control and knockdown groups of HD1 and HD2 are shown at day 5, 15, 25 and 50.
(DOCX)

S3 Table. Protein expression of VIM, TPI and MAT2A. Median and standard error of VIM, TPI and MAT2A protein expression of native, control and knockdown groups of HD1 and HD2 are shown in arbitrary Oprical Densitometry units from Western Blot at day 5, 15, 25 and 50.
(DOCX)

Acknowledgments

The authors want to express their gratitude for Constance Scharff and the research group of Animal Behaviour, Institute of Biology at FU Berlin for supporting the synthesis of viral particles and acknowledges Dr. Ezequiel Mendoza for assistance in RT–qPCR analysis.

Author Contributions

Conceptualization: Christina Herre.

Data curation: Christina Herre, Arpenik Nshdejan.

Formal analysis: Christina Herre, Mahtab Bahramsoltani.

Investigation: Christina Herre.

Methodology: Christina Herre.

Project administration: Mahtab Bahramsoltani.

Supervision: Robert Klopfleisch, Giuliano Mario Corte, Mahtab Bahramsoltani.

Writing – original draft: Christina Herre.

Writing – review & editing: Arpenik Nshdejan, Robert Klopfleisch, Giuliano Mario Corte, Mahtab Bahramsoltani.

References

1. Risau W. Mechanisms of angiogenesis. Nature. 1997; 386:671–4. https://doi.org/10.1038/386671a0 PMID: 9109485
2. Ribatti D, Crivellato E. "Sprouting angiogenesis", a reappraisal. Dev Biol. 2012; 372:157–65. https://doi.org/10.1016/j.ydbio.2012.09.018 PMID: 23031691
3. Jakobsson L, Franco CA, Bentley K, Collins RT, Ponsioen B, Aspalter IM, et al. Endothelial cells dynamically compete for the tip cell position during angiogenic sprouting. Nat Cell Biol. 2010; 12:943–53. https://doi.org/10.1038/ncb2103 PMID: 20871601
4. Akbarian M, Bertassoni LE, Tayebi L. Biological aspects in controlling angiogenesis: current progress. Cell Mol Life Sci. 2022; 79:349. https://doi.org/10.1007/s00018-022-04348-5 PMID: 35672585
5. Omorphos NP, Gao C, Tan SS, Sangha MS. Understanding angiogenesis and the role of angiogenic growth factors in the vascularisation of engineered tissues. Mol Biol Rep. 2021; 48:941–50. https://doi.org/10.1007/s11033-020-06108-9 PMID: 33393005

6. Doke SK, Dhawale SC. Alternatives to animal testing: A review. Saudi Pharm J. 2015; 23:223–9. https://doi.org/10.1016/j.jsps.2013.11.002 PMID: 26106269
7. Nowak-Sliwinska P, Alitalo K, Allen E, Anisimov A, Aplin AC, Auerbach R, et al. Consensus guidelines for the use and interpretation of angiogenesis assays. Angiogenesis. 2018; 21:425–532. https://doi.org/10.1007/s10456-018-9613-x PMID: 29766399
8. Stryker ZI, Rajabi M, Davis PJ, Mousa SA. Evaluation of Angiogenesis Assays. Biomedicines 2019, 7 (2), 37. https://doi.org/10.3390/biomedicines7020037 PMID: 31100863
9. Staton CA, Reed MWR, Brown NJ. A critical analysis of current in vitro and in vivo angiogenesis assays. Int J Exp Pathol. 2009; 90:195–221. https://doi.org/10.1111/j.1365-2613.2008.00633.x PMID: 19563606
10. Bahramsoltani M, Spiegelaere W de. Quantitation of Tumor Angiogenesis In Vitro: An All-In-One Angiogenesis Assay. Methods Mol Biol. 2016; 1464:185–91. https://doi.org/10.1007/978-1-4939-3999-2_17 PMID: 27858367
11. Bahramsoltani M, Plendl J. Different ways to antiangiogenesis by angiostatin and suramin, and quantitation of angiostatin-induced antiangiogenesis. APMIS. 2007; 115:30–46. https://doi.org/10.1111/j.1600-0463.2007.apm_405.x PMID: 17223849
12. Bahramsoltani M, de Spiegelaere W, Janczyk P, Hiebl B, Cornillie P, Plendl J. Quantitation of angiogenesis in vitro induced by VEGF-A and FGF-2 in two different human endothelial cultures—an all-in-one assay. Clin Hemorheol Microcirc. 2010; 46:189–202. https://doi.org/10.3233/CH-2010-1345 PMID: 21135494
13. Bahramsoltani M, Plendl J. A new in vitro model to quantify angiogenesis. [Ein neues in vitro Modell zur Quantifizierung der Angiogenese]. ALTEX. 2004; 21:227–44.
14. Bahramsoltani M, Harms T, Drewes B, Plendl J. Searching for markers to identify angiogenic endothelial cells: a proteomic approach. Clin Hemorheol Microcirc. 2013; 55:255–69. https://doi.org/10.3233/CH-2012-1631 PMID: 23089887
15. Herre C, Nshdejan A, Klopfleisch R, Corte GM, Bahramsoltani M. Expression of vimentin, TPI and MAT2A in human dermal microvascular endothelial cells during angiogenesis in vitro. PLoS One. 2022; 17:e0266774. https://doi.org/10.1371/journal.pone.0266774 PMID: 35482724
16. Wierenga RK, Kapetaniou EG, Venkatesan R. Triosephosphate isomerase: a highly evolved biocatalyst. Cell Mol Life Sci. 2010; 67:3961–82. https://doi.org/10.1007/s00018-010-0473-9 PMID: 20694739
17. Myers TD, Palladino MJ. Newly discovered roles of triosephosphate isomerase including functions within the nucleus. Mol Med. 2023; 29:18. https://doi.org/10.1186/s10020-023-00612-x PMID: 36721084
18. Orosz F, Oláh J, Ovádi J. Triosephosphate isomerase deficiency: new insights into an enigmatic disease. Biochim Biophys Acta. 2009; 1792:1168–74. https://doi.org/10.1016/j.bbadis.2009.09.012 PMID: 19786097
19. Rodríguez-Bolaños M, Perez-Montfort R. Medical and Veterinary Importance of the Moonlighting Functions of Triosephosphate Isomerase. Curr Protein Pept Sci. 2019; 20:304–15. https://doi.org/10.2174/1389203719666181026170751 PMID: 30370845
20. Yamaji R, Fujita K, Nakanishi I, Nagao K, Naito M, Tsuruo T, et al. Hypoxic up-regulation of triosephosphate isomerase expression in mouse brain capillary endothelial cells. Arch Biochem Biophys. 2004; 423:332–42. https://doi.org/10.1016/j.abb.2004.01.003 PMID: 15001397
21. Yetkin-Arik B, Vogels IMC, Neyazi N, van Duinen V, Houtkooper RH, van Noorden CJF, et al. Endothelial tip cells in vitro are less glycolytic and have a more flexible response to metabolic stress than non-tip cells. Sci Rep. 2019; 9:10414. https://doi.org/10.1038/s41598-019-46503-2 PMID: 31320669
22. Dumas SJ, García-Caballero M, Carmeliet P. Metabolic Signatures of Distinct Endothelial Phenotypes. Trends Endocrinol Metab. 2020; 31:580–95. https://doi.org/10.1016/j.tem.2020.05.009 PMID: 32622584
23. Patteson AE, Vahabikashi A, Goldman RD, Janmey PA. Mechanical and Non-Mechanical Functions of Filamentous and Non-Filamentous Vimentin. Bioessays. 2020; 42:e2000078. https://doi.org/10.1002/bies.202000078 PMID: 32893352
24. Danielsson F, Peterson MK, Caldeira Araújo H, Lautenschläger F, Gad AKB. Vimentin Diversity in Health and Disease. Cells 2018, 7(10), 147. https://doi.org/10.3390/cells7100147 PMID: 30248895
25. Paulin D, Lilienbaum A, Kardjian S, Agbulut O, Li Z. Vimentin: Regulation and pathogenesis. Biochimie. 2022; 197:96–112. https://doi.org/10.1016/j.biochi.2022.02.003 PMID: 35151830
26. Tsuruta D, Jones JCR. The vimentin cytoskeleton regulates focal contact size and adhesion of endothelial cells subjected to shear stress. J Cell Sci. 2003; 116:4977–84. https://doi.org/10.1242/jcs.00823 PMID: 14625391

27. Liu T, Guevara OE, Warburton RR, Hill NS, Gaestel M, Kayyali US. Regulation of vimentin intermediate filaments in endothelial cells by hypoxia. Am J Physiol Cell Physiol. 2010; 299:C363–73. https://doi.org/10.1152/ajpcell.00057.2010 PMID: 20427712

28. Cesari C de, Barravecchia I Pyankova OV, Vezza M, Germani MM, Scebba F, et al. Hypergravity Activates a Pro-Angiogenic Homeostatic Response by Human Capillary Endothelial Cells. Int J Mol Sci 2020, 21(7), 2354. https://doi.org/10.3390/ijms21072354 PMID: 32231163

29. Dayekh K, Mequanint K. 3D Co-culture Model on the Role of Vimentin in Notch Signaling and Vascularization; bioRxiv 2023.03.02.530837.

30. Shafqat N, Muniz JRC, Pilka ES, Papagrigoriou E, von Delft F, Oppermann U, et al. Insight into S-adenosylmethionine biosynthesis from the crystal structures of the human methionine adenosyltransferase catalytic and regulatory subunits. Biochem J. 2013; 452:27–36. https://doi.org/10.1042/BJ20121580 PMID: 23425511

31. Firestone RS, Schramm VL. The Transition-State Structure for Human MAT2A from Isotope Effects. J Am Chem Soc. 2017; 139:13754–60. https://doi.org/10.1021/jacs.7b05803 PMID: 28880543

32. Li C, Gui G, Zhang L, Qin A, Zhou C, Zha X. Overview of Methionine Adenosyltransferase 2A (MAT2A) as an Anticancer Target: Structure, Function, and Inhibitors. J Med Chem. 2022; 65:9531–47. https://doi.org/10.1021/acs.jmedchem.2c00395 PMID: 35796517

33. Pascale RM, Simile MM, Calvisi DF, Feo CF, Feo F. S-Adenosylmethionine: From the Discovery of Its Inhibition of Tumorigenesis to Its Use as a Therapeutic Agent. Cells 2022, 11(3), 409. https://doi.org/10.3390/cells11030409 PMID: 35159219

34. Chen L, Liu X, Zhou H, Li G, Huang F, Zhang J, et al. Activating transcription factor 4 regulates angiogenesis under lipid overload via methionine adenosyltransferase 2A-mediated endothelial epigenetic alteration. FASEB j. 2021; 35:e21612. https://doi.org/10.1096/fj.202100233R PMID: 33948996

35. Zhang N. Role of methionine on epigenetic modification of DNA methylation and gene expression in animals. Anim Nutr. 2018; 4:11–6. https://doi.org/10.1016/j.aninu.2017.08.009 PMID: 30167479

36. Banerjee S, Bacanamwo M. DNA methyltransferase inhibition induces mouse embryonic stem cell differentiation into endothelial cells. Exp Cell Res. 2010; 316:172–80. https://doi.org/10.1016/j.yexcr.2009.08.011 PMID: 19715692

37. Sahin M, Sahin E, Gümüşlü S, Erdoğan A, Gültekin M. DNA methylation or histone modification status in metastasis and angiogenesis-related genes: a new hypothesis on usage of DNMT inhibitors and S-adenosylmethionine for genome stability. Cancer Metastasis Rev. 2010; 29:655–76. https://doi.org/10.1007/s10555-010-9253-0 PMID: 20821252

38. Haesler S, Rochefort C, Georgi B, Licznerski P, Osten P, Scharff C. Incomplete and inaccurate vocal imitation after knockdown of FoxP2 in songbird basal ganglia nucleus Area X. PLoS Biol. 2007; 5:e321. https://doi.org/10.1371/journal.pbio.0050321 PMID: 18052609

39. Lois C, Hong EJ, Pease S, Brown EJ, Baltimore D. Germline transmission and tissue-specific expression of transgenes delivered by lentiviral vectors. Science. 2002; 295:868–72. https://doi.org/10.1126/science.1067081 PMID: 11786607

40. Spiegelaere W de, Cornillie P, van den Broeck W, Plendl J, Bahramsoltani M. Angiopoietins differentially influence in vitro angiogenesis by endothelial cells of different origin. Clin Hemorheol Microcirc. 2011; 48:15–27. https://doi.org/10.3233/CH-2011-1393 PMID: 21876231

41. Gerhardt H, Golding M, Fruttiger M, Ruhrberg C, Lundkvist A, Abramsson A, et al. VEGF guides angiogenic sprouting utilizing endothelial tip cell filopodia. Journal of Cell Biology. 2003; 161:1163–77. https://doi.org/10.1083/jcb.200302047 PMID: 12810700

42. Qiu J, Gao H-Q, Zhou R-H, Liang Y, Zhang X-H, Wang X-P, et al. Proteomics analysis of the proliferative effect of low-dose ouabain on human endothelial cells. Biol Pharm Bull. 2007; 30:247–53. https://doi.org/10.1248/bpb.30.247 PMID: 17268060

43. Du W, Ren L, Hamblin MH, Fan Y. Endothelial Cell Glucose Metabolism and Angiogenesis. Biomedicines. 2021; 9:147. https://doi.org/10.3390/biomedicines9020147 PMID: 33546224

44. Rusu MC, Poalelungi CV, Vrapciu AD, Nicolescu MI, Hostiuc S, Mogoanta L, et al. Endocardial tip cells in the human embryo—facts and hypotheses. PLoS One. 2015; 10:e0115853. https://doi.org/10.1371/journal.pone.0115853 PMID: 25617624

45. Lu SC, Ramani K, Ou X, Lin M, Yu V, Ko K, et al. S-adenosylmethionine in the chemoprevention and treatment of hepatocellular carcinoma in a rat model. Hepatology. 2009; 50:462–71. https://doi.org/10.1002/hep.22990 PMID: 19444874

46. Lunt SY, Vander Heiden MG. Aerobic glycolysis: meeting the metabolic requirements of cell proliferation. Annu Rev Cell Dev Biol. 2011; 27:441–64. https://doi.org/10.1146/annurev-cellbio-092910-154237 PMID: 21985671

47. Antfolk D, Sjöqvist M, Cheng F, Isoniemi K, Duran CL, Rivero-Muller A, et al. Selective regulation of Notch ligands during angiogenesis is mediated by vimentin. Proc Natl Acad Sci U S A. 2017; 114: E4574–E4581. https://doi.org/10.1073/pnas.1703057114 PMID: 28533359

48. Dave JM, Bayless KJ. Vimentin as an integral regulator of cell adhesion and endothelial sprouting. Microcirculation. 2014; 21:333–44. https://doi.org/10.1111/micc.12111 PMID: 24387004

S1 Table. Morphologically assigned stages of angiogenesis *in vitro*. Mean values and standard deviations of native, control and knockdown groups of HD1 and HD2 are presented at each day of investigation.

	Day 4	Day 8	Day 11	Day 15	Day 18	Day 22	Day 25	Day 29	Day 32	Day 36	Day 39	Day 43	Day 46	Tag50
N_1	1.63	2.88	3.25	3.5	3.75	4.25	4.50	4.62	5.00	5.13	5.81	6.00	6.00	6.00
	± 0.52	± 0.84	± 0.71	± 0.53	± 0.46	± 0.71	± 0.53	± 0.52	± 0.53	± 0.64	± 0.26	± 0.35	± 0.00	± 0.00
SCR_1	1.88	3.13	3.63	3.88	4.00	4.50	4.88	5.13	5.63	5.75	6.00	6.00	6.00	6.00
	± 0.64	± 0.64	± 0.52	± 0.35	± 0.53	± 0.53	± 0.35	± 0.64	± 0.52	± 0.46	± 0.00	± 0.00	± 0.00	± 0.00
sh_1	1.63	2.38	2.88	3.25	3.00	3.00	3.13	3.38	3.38	3.75	3.75	3.75	3.88	3.88
	± 0.52	± 0.74	± 0.64	± 0.71	± 0.76	± 0.76	± 0.83	± 0.74	± 0.52	± 0.71	± 0.46	± 0.46	± 0.35	± 0.35
N_2	1.50	2.88	3.38	3.50	3.63	3.75	4.38	4.63	4.88	4.88	5.18	6.00	6.00	6.00
	± 0.53	± 0.35	± 0.91	± 0.53	± 0.52	± 0.46	± 0.52	± 0.52	± 0.35	± 0.64	± 0.26	± 0.00	± 0.00	± 0.00
SCR_2	1.75	3.00	3.38	3.63	3.63	4.50	4.63	5.00	5.00	5.13	5.50	6.00	6.00	6.00
	± 0.46	± 0.76	± 0.52	± 0.52	± 0.52	± 0.53	± 0.52	± 0.00	± 0.00	± 0.35	± 0.38	± 0.00	± 0.00	± 0.00
sh_2	1.62	2.5	2.63	2.25	2.50	2.38	2.38	2.63	3.13	3.38	3.25	3.12	3.25	2.88
	± 0.52	± 0.53	± 0.91	± 0.46	± 0.55	± 0.74	± 0.74	± 0.74	± 0.35	± 0.52	± 0.38	± 0.35	± 0.89	± 0.83

S2 Table. mRNA expression of VIM, TPI and MAT2A. Median and standard error of VIM, TPI and MAT2A mRNA expression of native, control and knockdown groups of HD1 and HD2 are shown at day 5, 15, 25 and 50.

		Day 5	Day 15	Day 25	Day 50
	VIM	0.61 ± 0.16	0.46 ± 0.21	0.37 ± 0.05	0.02 ± 0.08
N_1	**TPI**	1.02 ± 0.19	1.33 ± 0.19	4.05 ± 0.40	36.55 ± 3.22
	MAT2A	0.33 ± 0.08	0.03 ±0.03	0.12 ± 0.00	0.14 ± 0.01
	VIM	0.36 ± 0.13	0.08 ± 0.03	0.38 ± 0.02	0.07 ± 0.03
SCR_1	**TPI**	1.04 ± 0.07	4.94 ± 1.43	3.78 ± 0.22	19.23 ± 4.65
	MAT2A	0.21 ± 0.08	0.03 ± 0.01	0.08 ± 0.01	0.07 ± 0.02
	VIM	0.31 ± 0.13	0.05 ± 0.04	0.15 ± 0.24	0.26 ± 0.14
sh_1	**TPI**	0.62 ± 0.10	2.29 ± 0.74	2.24 ± 0.53	13.51 ± 4.24
	MAT2A	0.09 ± 0.03	0.01 ± 0.00	0.07 ± 0.03	0.13 ± 0.04
	VIM	0.61 ± 0.16	0.13 ± 0.03	0.40 ±0.09	0.09 ± 0.05
N_2	**TPI**	1.27 ± 0.09	0.89 ± 0.07	5.21 ± 0.48	22.68 ± 6.08
	MAT2A	0.1 ± 0.01	0.01 ± 0.00	0.10 ± 0.01	0.14 ± 0.00
	VIM	0.78 ± 0.06	0.16 ± 0.06	0.61 ± 0.08	0.03 ± 0.02
SCR_2	**TPI**	1.70 ± 0.34	0.88 ± 0.28	5.17 ± 1.05	11.56 ± 1.52
	MAT2A	0.24 ± 0.08	0.00 ± 0.03	0.09 ± 0.01	0.03 ± 0.01
	VIM	0.74 ± 0.02	0.12 ± 0.13	0.35 ± 0.06	0.01 ± 0.00
sh_2	**TPI**	0.69 ± 0.15	0.68 ± 0.00	1.93 ± 0.05	5.71 ± 1.18
	MAT2A	0.14 ± 0.06	0.05 ± 0.00	0.09 ± 0.00	0.09 ± 0.05

S3 Table. Protein expression of VIM, TPI and MAT2A. Median and standard error of VIM, TPI and MAT2A protein expression of native, control and knockdown groups of HD1 and HD2 are shown in arbitrary Oprical Densitometry units from Western Blot at day 5, 15, 25 and 50.

		Day 5	Day 15	Day 25	Day 50
	VIM	1142692.24 ± 4989.28	1260220.26 ± 3390.15	943758.15 ± 5300.33	1029055.21 ± 2904.75
N_1	**TPI**	851228.18 ± 2453.01	496761.81 ± 2029.2	792121.16 ± 6276	803933.17 ± 8192.5
	MAT2A	473978.1 ± 4906.52	449147.9 ± 2181.44	352864.7 ± 3943.76	870074.18 ± 2045.5
	VIM	204649.21 ± 7217.85	228409.23 ± 2596.18	166369.7 ± 1496.92	196495.2 ± 4118.56
SCR_1	**TPI**	164477.17 ± 4620.5	67741.7 ± 1843.71	107598.11 ± 6828.03	121995.12 ± 6590
	MAT2A	85092.8 ± 1218.76	66528.69 ± 3605.01	66775.06 ± 1978.41	149595.15 ± 1307.87
	VIM	199272.19 ± 3457.45	227384.2 ± 2860.17	157590.15 ± 2257.18	205004.22 ± 6039.28
sh_1	**TPI**	110078.11 ± 4276.05	46407.48 ± 1414	64720.67 ± 2018	107528.42 ± 5154
	MAT2A	83029.18 ± 882,97	57903.61 ± 4209.1	68621.72 ± 4476.12	135039.11 ±2100.53
	VIM	851289.13 ± 1208.5	1250745.62 ± 3110.76	934997.19 ± 5516.45	1135157.42 ± 5170.87
N_2	**TPI**	876875.18 ± 1058.5	855424.18 ± 4122	959677.2 ± 7282	877275.18 ± 3551
	MAT2A	607131.3 ± 7271.91	730563.15 ± 813	503471.01 ± 939.93	405217.8 ± 385.5
	VIM	119757.6 ± 6822	230463.31 ± 1538.25	172927.23 ± 5438.69	166129.22 ± 1331
SCR_2	**TPI**	130982.17 ± 7797.39	135644.8 ± 4570.51	144528.91 ± 8142.5	146368.20 ± 4827
	MAT2A	108279.41 ± 6095.91	77975.1 ± 3495.5	86553.21 ± 2662.17	69373.9 ± 4214.1
	VIM	127001.17 ± 2463.52	224920.3 ± 822	182753.52 ± 503.5	152240.18 ± 5867.5
sh_2	**TPI**	78908.1 ± 5755.98	74986.01 ± 3503	100268.17 ± 4798.74	92180.12 ± 9437.5
	MAT2A	103023.2 ± 4841.89	85239.11 ± 3504.18	100853.2 ± 5985	43882.06 ± 397

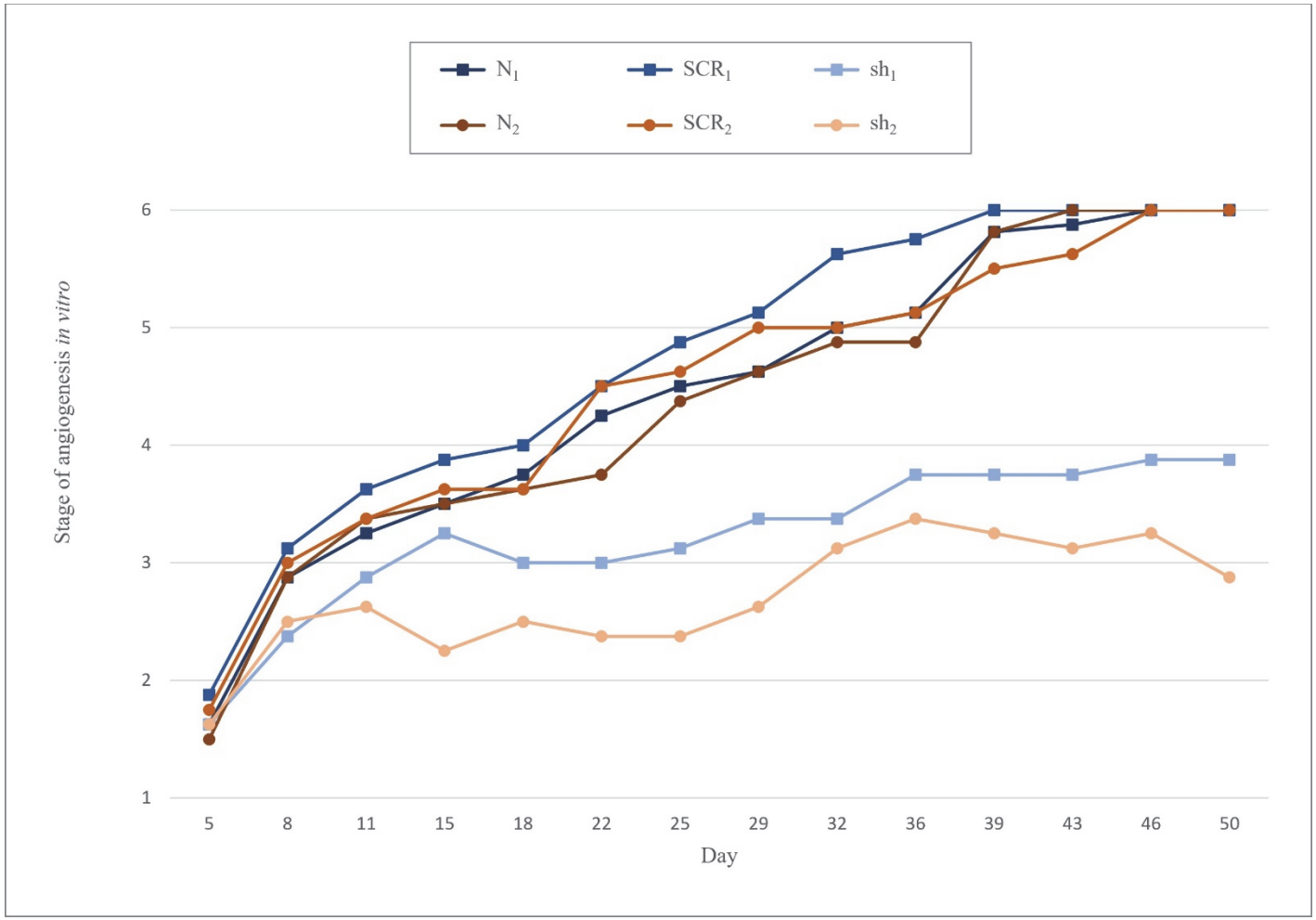

S1 Fig. Stages of *in vitro* angiogenesis. The course of angiogenesis is shown for native groups (N1, N2), control groups (SCR1, SCR2) and knockdown groups (sh1, sh2) during a cultivation period of 50 days. Mean values are calculated for 4 visual fields of 4 wells per culture at each detection day. Native and control groups of both batches ran through all six stages of angiogenesis chronologically. Infected cells of sh1 and sh2 did not precede to further stages than stage 3.

5. Discussion

This thesis aimed to analyse the connection of VIM, TPI and MAT2A expression and the angiogenic behaviour of HDMECs during *in vitro* angiogenesis. Therefore, native expression profiles were detected while cells were running through the *in vitro* angiogenic cascade. Additionally, VIM and TPI expression was downregulated individually and subsequent behavioural as well as expressional alterations were examined. Besides the impact that derived from the expression of described proteins, *in vitro* angiogenesis seemed to be affected additionally by cell differentiations among cell populations.

5.1 Endothelial protein expression and its impact on angiogenesis *in vitro*

For evaluating the mRNA and protein expression, native, control and knockdown cells of both batches were harvested at four different points in time while cells were running through the angiogenic cascade *in vitro*. Western blot and RT-qPCR analysis revealed mRNA and protein levels of each protein of each group.

5.1.1 VIM

Vim displays the first target protein which was mainly focused on in Publication I (Herre et al. 2022). By its influence on cell shape and motility, it was suggested to be a protein, which is mostly involved in angiogenic events of sprouting and migration (Danielsson et al. 2018; Antfolk et al. 2017; Dave and Bayless 2014; Tsuruta and Jones 2003).

In both studies, mRNA and protein expression of VIM was monitored while cells were running through the angiogenic cascade *in vitro*. Either experiment revealed a significant decline in VIM mRNA expression of native cells (N) of batch 1 (N_1) and batch 2 (N_2) in the course of *in vitro* angiogenesis. Coincidentally in both studies, highest C_t values were detected in cells which were assigned to stages 2 and 3. With progression to further angiogenic stages, mRNA expression of VIM was reduced in N_1 and N_2 (Herre et al. 2023; Herre et al. 2022). According to the all-in-one assay, stage 2 and 3 represent stages of sprouting and linear-side-by-side arrangements (Bahramsoltani and De Spiegelaere 2016; Bahramsoltani et al. 2010; Bahramsoltani and Plendl 2004). During these stages, cells are highly motile by changing their cell shape from polygonal to elongated with the aim to network via linear arrangements. With its influence on cytoskeleton, VIM is necessary to be highly expressed in these cells. Therefore, both studies concurringly support the assumption of VIM being highly involved in early stages of angiogenesis, i.e. sprouting and migration (Danielsson et al. 2018; Antfolk et al. 2017; Dave

and Bayless 2014; Tsuruta and Jones 2003). As it was already shown in immature precursor cells, VIM expression decreases with maturation (Nowak-Sliwinska et al. 2018; Van Beijnum et al. 2006).

Despite both studies clearly stating same tendencies in expression over the angiogenic cascade *in vitro*, in study I, N_1 and N_2 achieved overall higher C_t values each detection day than N_1 and N_2 of study II. Additionally, the decline of VIM over the cultivation period was more visible in study I in comparison to experiment II (Herre et al. 2023; Herre et al. 2022). This might indicate the sensitivity of VIM mRNA expression based on the appearance of divergent events among cultivated cell populations, such as apoptosis and environmental and osmotic stress (Cesari et al. 2020; Buchmaier et al. 2013; Liu et al. 2010).

In the first study, VIM knockdown was leading to a deceleration of *in vitro* angiogenesis and to cell death in both batches of knockdown groups (sh_1 and sh_2), concluding that VIM raises the angiogenic potency of HDMECs and represents an essential protein for cell survival and differentiation. Both indications were supported by results of the second study. Induced by knocking down TPI, a decrease of the angiogenic potency of sh_1 and sh_2 were observed. Consequently, VIM expression declined in both batches, implying the connection of angiogenic potency and VIM expression. Furthermore, it was suggested that VIM expression is necessary for cells to undergo the whole angiogenic cascade *in vitro*. VIM protein levels being consistently expressed in N_1 and N_2 in both experiments during the entire course of angiogenesis *in vitro* are strongly supporting this indication (Herre et al. 2023; Herre et al. 2022).

5.1.2 TPI

TPI represents the major target protein of Publication II (Herre et al. 2023). With its involvement in glycolic metabolism, TPI is proposed to be a protein involved in angiogenic events of migration and proliferation by generating energy for cells (Myers and Palladino 2023; Dumas et al. 2020; Wierenga et al. 2010; Qiu et al. 2007).

In both studies, the native expression profile of TPI displayed a significant increase in N_1 and N_2 over the course of *in vitro* angiogenesis. The initial increase in TPI mRNA occurred in both experiments when native cells were entering stage 3 (Herre et al. 2023; Herre et al. 2022). In this stage, cells appear mostly as linearly arranged (Bahramsoltani and De Spiegelaere 2016; Bahramsoltani et al. 2010; Bahramsoltani and Plendl 2004). Hence, cells are located in between stages of sprouting and three-dimensional organization, being characterized as highly migrative and proliferative (Sievers et al. 2011; Borselli et al. 2007; Auerbach et al. 2003). This strengthens the hypothesis of TPI being necessary for angiogenic stages of cell migration and

proliferation. Results of TPI knockdown are supportive of this assumption. Cells of sh_1 and sh_2 were not able to terminate stage 3 and proceed to further stages (Herre et al. 2023).

Additionally, in both experiments, subsequent inclines in TPI mRNA expression were visible in native cells (Herre et al. 2023; Herre et al. 2022). When comparing both studies, it was detected that each uprise in TPI mRNA was connected to an acceleration of cell differentiation by them entering further stages of *in vitro* angiogenesis shortly after. TPI is catalysing the synthesis of ATP, which was shown to be essential for ECs to enter most angiogenic stages (Du et al. 2021; Dumas et al. 2020; Yetkin-Arik et al. 2019; Qiu et al. 2007). This leads to the extended assumption of TPI not only being necessary for cell migration and proliferation but also for enabling tube formation.

TPI's impact on angiogenic stages and the deceleration of *in vitro* angiogenesis followed by knocking down TPI in study II, leads to the conclusion of TPI increasing the angiogenic potency of HDMECs. Moreover, TPI protein was observed to be steadily expressed in N_1 and N_2 of both studies over the whole cultivation period, suggesting that TPI represents an essential protein for HDMECs. Solely in study I, a decrease in TPI protein expression was detected in VIM knockdown group from batch 2. The appearance of less TPI protein was connected to a progressive cell death amongst the cell population and supports the previously described assumption of TPI being essential for cell survival (Herre et al. 2023; Herre et al. 2022).

5.1.3 MAT2A

In contrast to VIM and TPI, MAT2A is suggested to be a protein mainly having anti-angiogenic effects on ECs due to its involvement in cellular methylations via synthesizing SAM (Banerjee and Bacanamwo 2010; Sahin et al. 2010).

For both studies, an initial decrease in MAT2A mRNA expression was observed in N_1 and N_2 (Herre et al. 2023; Herre et al. 2022). As previously published, an increase in DNA-methylation by supplementing SAM was shown to inhibit cellular migration and proliferation (Banerjee and Bacanamwo 2010; Sahin et al. 2010). Cells of N_1 and N_2 were assigned to beginning stages of angiogenesis, i.e. stage 2 and 3 representing stages driven by highly motile cells starting to proliferate. By down regulating MAT2A mRNA, cells might have been enabled to undergo these stages. Furthermore, a final significant increase in MAT2A was observed in study I in N_2 on mRNA levels and in study II in N_1 on protein levels. Both cell populations were assigned to angiogenic stages of 6 (Herre et al. 2023; Herre et al. 2022). According to the all-in-one assay, stage 5 and 6 represent stages of three-dimensional organisation of ECs and appearance of capillary-like structures (Bahramsoltani and De Spiegelaere 2016; Bahramsoltani et al. 2010; Bahramsoltani and Plendl 2004). These stages involve cell maturation which was associated

with MAT2A activity and SAM synthesis (Banerjee and Bacanamwo 2010; Sahin et al. 2010; Lu et al. 2009). Both lead to the suggestion of MAT2A mainly decreasing the angiogenic potency of HDMECs by initiating cell maturation. Further indications were detectable in both studies when lowering the angiogenic potency of HDMECs by knocking down VIM and TPI respectively. Knockdown ECs displayed an overall tendency of increased MAT2A expression simultaneously, indicating an adaptation to the non-angiogenic character of ECs (Herre et al. 2023; Herre et al. 2022).

Overall, MAT2A C_t values of all groups were higher in study I than in study II, even when utilizing the same culture and detection methodologies (Herre et al. 2023; Herre et al. 2022). This might be caused by MAT2A expression being fluctuant and influenced by factors, i.e. SAM levels, metabolites and metabolic byproducts (Hunter et al. 2023; Li et al. 2022).

5.2 Cell differentiations and their impact on the course of *in vitro* angiogenesis

Two batches of human microvascular endothelial cells derived from neonatal foreskin (HD1, HD2) served equally as cellular material for both studies. Both batches were acquired from the same distributor. Cultivation substances, environment and procedures were identically applied in both experiments for both batches. Results of study I and study II have proven the angiogenic character of HD1 and HD2 by both being able to run through the entire angiogenic cascade *in vitro* chronologically (Herre et al. 2023; Herre et al. 2022). However, ECs are inhomogeneous and can display tremendous variations in their angiogenic activity resulting from only minor differences in cellular architecture (Stryker et al. 2019). It is of immense importance to characterize cell populations utilized in the lab. Therefore, gene expression of VEGFR-1 and VEGFR-2 was measured for native cells of HD1 and HD2 aiming the distribution of tip and stalk cells among the populations. With VEGFR-1 being more expressed in HD1 than in HD2, it was suggested that batch 1 comprised a higher amount of stalk cells in comparison to batch 2 (Herre et al. 2022). The difference in cell differentiations amongst cell cultures could get affiliated to divergences in angiogenic, compensatory and expressional behaviour, as follows:

During the process of angiogenesis, endothelial stalk cells are highly proliferative for elongating the newbuilt sprout (Ribatti and Crivellato 2012; Patan 2000). The highly proliferative character was visible in study I and II considering their angiogenic behaviour. HD1 displayed a higher cell density throughout the whole cultivation period than HD2. Therefore, more cells were able to enter late stages of *in vitro* angiogenesis, raising the sum of assigned stages of angiogenesis for all groups of HD1, resulting in significantly higher values compared

to HD2. Furthermore, both studies were aligned in N_2 entering stage 6 earlier than N_1 (Herre et al. 2023; Herre et al. 2022). As it was already shown, a lower expression of VEGFR-1 can lead to an acceleration of *in vitro* angiogenesis (Bahramsoltani et al. 2010). Along with an earlier maturation of N_2 in study I, MAT2A expression was significantly upregulated in comparison to N_1. This demonstrates the link between cell differentiation and expressional behaviour, as it was also shown in study I. VIM displayed significantly lower expression in N_1 than in N_2, resulting from N_2 inheriting less stalk cells and VIM being higher expressed in tip cells, as it was already demonstrated in epicardial tip cells (Rusu et al. 2015). Similarly in study II, TPI was shown to be significantly more expressed in N_1 than N_2 (Herre et al. 2023; Herre et al. 2022). As it was already shown, tip cells are less glycolytically active which might have caused the lower expression levels in HD2 owning less stalk cells (Yetkin-Arik et al. 2019).

By initiating VIM and TPI knockdown, tremendous differences regarding compensatory behaviour were observed. In both experiments, knockdown groups inheriting more stalk cells were able to compensate the infection with viral particles based on their higher proliferative character. During the second half of both studies, sh_1 displayed an uprise in cell density, a growing appearance of uninfected cells, a progression to further angiogenic stages and increase in mRNA of respective knocked down protein. In contrast, sh_2 was stagnating their differentiation in study II and even showing progressive cell death in study I (Herre et al. 2023; Herre et al. 2022). Furthermore, in study I, control group of HD2 (SCR_2) was affected more than HD1 (SCR_1). While SCR_1 was able to run through the angiogenic cascade equally to N_1, SCR_2 displayed a significant deceleration of *in vitro* angiogenesis. Additionally, expressional alterations between both batches were visible. In experiment I, sh_1 showed an upregulation of TPI mRNA which might be connected to a cellular stress response (Herre et al. 2022; Yamaji et al. 2004). In comparison, sh_2 decreased TPI mRNA expression, which might be related to cell death and the following dysregulation of metabolism (Herre et al. 2022; Kist and Vucic 2021), and downregulated MAT2A mRNA expression, suggested to aim the repair of damaged cells (Herre et al. 2022; Lu and Mato 2008).

5.3 Limitations and future solutions

Limitations of this research study address constraints of utilized cells and *in vitro* angiogenesis assay.

Overall, both batches of HDMECs were purchased from the same distributor and categorized as angiogenic ECs. The translation of present results to HDMECs from other distributors must be carried out carefully. Additionally, only angiogenic EC populations were used. For validating the angiogenic and non-angiogenic influence of proteins, experiments should get repeated

with ECs categorized as non-angiogenic. Furthermore, characterization of cell populations was only done by measuring VEGFR-1 and VEGFR-2 gene expression via RT-qPCR for both batches. To improve data integrity, it is recommended to add another detection method, i.e. immunofluorescence or Western blot.

Regarding *in vitro* testing for both experiments, the only assay used was the all-in-one assay. For validating the angiogenic and non-angiogenic effects of described proteins, more assays should be exerted (Stryker et al. 2019; Staton et al. 2004). For VIM, it is expedient to apply a migration assay and for TPI a proliferation as well as a tube formation assay. Especially the latter would be of great interest to validate TPI's impact on late stages of *in vitro* angiogenesis which could not get proven by knocking down TPI, by it resulting in a stagnation of the *in vitro* angiogenic cascade (Herre et al. 2023). Additionally, the suggested non-angiogenic influence of MAT2A must get evaluated further via knockdown.

Generally, it must be stated that this thesis provides initial information about the effects of the three target proteins on *in vitro* angiogenesis. To deliver more comprehensive results, experiments must be performed in analogy to the living system, i.e. analysis in co-cultures followed up by *in vivo* studies (Stryker et al. 2019; Nowak-Sliwinska et al. 2018; Tahergorabi and Khazaei 2012; Staton et al. 2004).

5.4 Conclusions

In this study the relation between *in vitro* angiogenesis of HDMECs and the expression of VIM, TPI and MAT2A was demonstrated.

Each protein displayed expressional fluctuation while native cells were running through the angiogenic cascade *in vitro*. VIM is highest expressed in beginning stages of *in vitro* angiogenesis followed by a downscale, indicating its impact on angiogenic stages of sprouting and migration. TPI displayed an initial uprising expression followed by further inclines implying its influence on migration, proliferation, and tube formation. In contrast, MAT2A mRNA was decreasing in beginning stages and partly uprising in end stages, leading to the suggestion of MAT2A having a non-angiogenic effect on ECs and being involved in the process of maturation (Herre et al. 2023; Herre et al. 2022).

When knocking down VIM and TPI respectively, a significant impact on the angiogenic behaviour of ECs was detected. Both knockdowns initiated a deceleration of *in vitro* angiogenesis which were accompanied by a decline of cell density in cell cultures. This led to the conclusion of VIM and TPI having pro-angiogenic effects, raising the angiogenic potency

of ECs as well as being essential for HDMECs to survive and differentiate (Herre et al. 2023; Herre et al. 2022).

Initiated by the knockdown of VIM and TPI individually, gene expression of the respective other proteins was impacted. By downregulating TPI, VIM expression followed the incline while MAT2A mRNA was uprising, leading to the conclusion of cells adapting to the lower angiogenic potency. In comparison, VIM knockdown led to an uprise of TPI and MAT2A mRNA in HD1 and a decrease in HD2. This behaviour was suggested to be connected to the different cell differentiations among cell populations (Herre et al. 2023; Herre et al. 2022).

With HD1 comprising a higher amount of stalk cells among the population than HD2, it was supposed to provide a higher proliferative activity leading to differences regarding angiogenic, compensatory and expressional behaviour. While HD1 displayed a higher cell density, HD2 presented an acceleration of *in vitro* angiogenesis. Furthermore, cells of HD1 were able to survive and recover from both knockdowns. Contrarily, cells of HD2 showed less compensatory activity by progressively dying or stagnating regarding their differentiation. Additionally, expressional differences were connected to the angiogenic and compensatory dissimilarities of both batches, i.e. decreasing expression of TPI and MAT2A in dying cells and compensational upregulation of TPI and MAT2A in surviving cells (Herre et al. 2023; Herre et al. 2022). These findings clearly constitute the tremendous impact of EC differentiations on the overall behaviour of EC populations. Leading to the conclusion of characterization of EC population being indispensable for the usage of ECs in *in vitro* angiogenesis assays and the integrity of interpretation of results.

5.5 Outlook

First, limitations of this thesis should get eradicated by repeating the experiments using HDMECs from other distributors, including non-angiogenic ECs, initiating MAT2A knockdown and implementing further single stage *in vitro* angiogenesis assays.

Overall, this thesis provides new and highly important information about VIM, TPI and MAT2A being involved in *in vitro* angiogenesis in HDMECs. It is necessary to continue this research project and explore further proteins which might affect the angiogenic potency of ECs, e.g. myozenin 2 and cAMP-specific phosphodiesterase 4D (Bahramsoltani et al. 2013). These findings are highly insightful and may serve as base for future *in vivo* studies with the aim of developing potential pro-angiogenic and anti-angiogenic substances to salutary modulate angiogenesis in living systems.

In particular, this thesis states the importance of characterization of cells used in *in vitro* assays. Further detection methods need to be established and standardized with the aim of unifying the research field of *in vitro* angiogenesis and optimize reproducibility and reliability.

6. Summary

6.1 Summary

Expression of VIM, TPI and MAT2A and their impact on *in vitro* angiogenesis in human dermal microvascular endothelial cells

Angiogenesis is the dynamic process of building new blood vessels from pre-existing ones. During sprouting angiogenesis, tip cells are mainly responsible for migration, stalk cells for proliferation and phalanx cells for maturation of the new vessel. Major research effort was directed to anti- and pro-angiogenic therapy. Therefore, *in vitro* models are frequently used. However, these assays face problems regarding reproducibility based on single stage assays and the inhomogeneous character of endothelial cells (ECs). When establishing and performing the all-in-one assay, which covers all stages of *in vitro* angiogenesis, differences regarding angiogenic potency was detected resulting in a classification of ECs into angiogenic and non-angiogenic. Proteome expression profiles of both classes exhibited one protein only found in non-angiogenic ECs, i.e. adenosylmethionine synthetase isoform type 2 (MAT2A), and seven proteins exclusively in angiogenic ECs. MAT2A represents a highly conserved enzyme being mainly involved in regulatory functions and suggested to have anti-angiogenic effects. Among the seven proteins found in angiogenic ECs, vimentin (VIM) and triosephosphate isomerase (TPI) are hypothesized to have pro-angiogenic impact on ECs. By VIM being a type III intermediate filament protein, it is highly involved in cell shape and motility. TPI is a glycolic enzyme generating energy and mainly influencing cell proliferation.

Both studies aimed to determine whether the expression of VIM, TPI and MAT2A is related to angiogenesis *in vitro* in human dermal microvascular endothelial cells (HDMECs). Therefore, two batches of HDMECs were long-term cultivated using pro-angiogenic media. Quantification of *in vitro* angiogenesis was carried out using phase-contrast microscopy twice a week. Knockdown groups got infected with lentiviral particles initiating a knockdown of VIM or TPI respectively. Additionally, a non-coding sequence was used for the infection of control groups. At days 1, 5, 25 and 50, cells of all groups were harvested and used for mRNA and protein expression analysis. The mRNA expression of vascular endothelial growth factor 1 (VEGFR-1), vascular endothelial growth factor 2 (VEGFR-2), and mRNA and protein expression of VIM, TPI and MAT2A were determined by RT-qPCR and Western Blot.

In native cells, VIM was shown to be expressed mainly in beginning stages of sprouting and migrating, which are suggested to be enabled by VIM's influence on the cytoskeleton. By knocking down VIM, cell death and a deceleration of *in vitro* angiogenesis was observed

leading to the conclusion of VIM being an essential protein for HDMECs survival and having pro-angiogenic effects on ECs. For TPI, native cells showed an overall increase in expression over the cultivation period. By TPI providing energy for cells, it is suggested to be essential for most angiogenic stages, i.e. cell migration, proliferation, and tube formation. By knocking down TPI, a deceleration of *in vitro* Angiogenesis was observed, leading to the assumption of TPI increasing the angiogenic potency of ECs. Furthermore, native TPI expression was shown to be consistent. The single decrease of TPI expression was connected to cell death, showing the essential character of TPI for HDMECs survival. Native MAT2A expression was highest at the beginning of cultivation, followed by a significant decrease. Moreover, a final increase was detected. With MAT2A owning regulatory functions via methylations, it is suggested to have anti-angiogenic effects, mainly expressed in quiescent cells and involved in maturation of HDMECs. In both knockdown studies, MAT2A displayed an overall tendency of being increased when lowering the angiogenic potency, supporting the assumption of MAT2A impacting anti-angiogenic events. By characterizing both batches of HDMECs via VEGFR-1 and VEGFR-2 expression, it was shown that HD1 comprised a higher amount of stalk cells. The difference in distribution of cell differentiation led to a divergence in angiogenic, compensatory and expressional behaviour of the batches. HD1 inherited a higher proliferative power which was visible in them having a higher cell density and higher values of sums of assigned stages. With HD1 owning more stalk cells, VIM expression was lower and TPI was significantly higher in contrast to HD2. Furthermore, HD2 displayed an acceleration of *in vitro* angiogenesis, which was connected to higher MAT2A C_t-values. Additionally, knockdown cells of HD1 were able to recover from infection by increasing their cell density and progressing to further angiogenic stages, while knockdown cells of HD2 were either stagnating their differentiation or displaying cell death. Further, control group of HD2 displayed a deceleration of *in vitro* angiogenesis while control group of HD1 was unaffected. Overall, it has been shown that the characterization of cell differentiations is of immense importance for EC application and the interpretation of *in vitro* angiogenesis assays.

Experiments should get repeated including cells from different distributors involving non-angiogenic cells, cell characterization should be extended by an additional detection method and specific assays should get employed for validating protein effects. For comprehension to living systems, subsequent experiments should involve more than one cell type, followed by *in vivo* studies. MAT2A knockdown should be initiated and further proteins influencing the angiogenic potency should be examined. Furthermore, upcoming investigations should focus on developing and optimizing the characterization of EC populations to increase reproducibility and reliability of studies in the field of *in vitro* angiogenesis.

6.2 Zusammenfassung

Expression von VIM, TPI und MAT2A und deren Einfluss auf die In-vitro-Angiogenese von humanen dermalen mikrovaskulären Endothelzellen

Als Angiogenese wird der dynamische Prozess bezeichnet, der zur Neubildung von Blutgefäßen aus bereits existierenden führt. Die sprossende Angiogenese vollzieht sich durch die Migration der Tip cells, die Proliferation von Stalk cells und die Maturation von Phalanx cells. In Rahmen der Angiogenese-Forschung kommen In-vitro-Modelle regelmäßig zum Einsatz. Sie haben jedoch häufig Probleme bezüglich ihrer Reproduzierbarkeit. Mit der Entwicklung und dem Einsatz eines all-in-one assays, wurden Unterschiede bezüglich der angiogenen Potenz von Endothelzellen (ECs) festgestellt, die eine Klassifizierung in angiogene und nicht-angiogene ECs zur Folge hatten. Eine Proteomanalyse beider Gruppen zeigte, dass das Protein Adenosylmethionine-Synthetase Isoform Typ 2 (MAT2A) ausschließlich in nicht-angiogenen ECs exprimiert wurde. Dieses Enzym weist vor allem regulatorische Funktionen auf und hat vermutlich einen anti-angiogenen Effekt auf ECs. Die Proteine Vimentin (VIM) und Triosphosphate Isomerase (TPI) wurden nur in angiogenen ECs gefunden. Deshalb wurde vermutet, dass sie pro-angiogene Effekte auf ECs haben. VIM ist ein Typ III Intermediärfilament und beeinflusst Zellform und -motilität. TPI ist ein glykolytisches Enzym, welches Energie generiert und besonders die zelluläre Proliferation beeinflussen kann.

Das Ziel beider Studien bestand darin, zu ermitteln, ob eine Verbindung zwischen der Expression von VIM, TPI und MAT2A und der In-vitro-Angiogenese in humanen dermalen mikrovaskularen ECs (HDMECs) besteht. Dafür wurden zwei Chargen an HDMECs unter Verwendung eines pro-angiogenen Mediums langzeit-kultiviert. Die Quantifizierung der In-vitro-Angiogenese erfolgte anhand phasenkontrastmikroskopischer Aufnahmen. Der Knockdown von VIM oder TPI wurde mittels lentiviralen Partikeln initiiert. Die mRNA-Expression von Vascular endothelial growth factor 1 (VEGFR-1) und Vascular endothelial growth factor 2 (VEGFR-2) und die mRNA- und Proteinexpression von VIM, TPI und MAT2A mittels RT-qPCR und Western Blot wurde an Tag 1, 5, 15, 25 und 50 analysiert.

In nativen Zellen zeigte sich die stärkste VIM-Expression hauptsächlich in den Stadien der Sprossung und Migration, die vermutlich durch VIM und dessen Einfluss auf das Zytoskelett angetrieben wurden. Während des Knockdowns von VIM, wurde ein starker Zelltod in Knockdown-Kulturen und eine Verzögerung der In-vitro-Angiogenese ermittelt. Dies führt zu der Vermutung, dass es sich bei VIM um ein für die Angiogenese essenzielles Protein handelt, das die angiogene Potenz steigert. Für TPI konnte in nativen Zellen ein allgemeiner Anstieg der Expression im Laufe der Kultivierung gezeigt werden. Da durch TPI den Zellen Energie

zur Verfügung gestellt wird, ist es nachvollziehbar, dass TPI im Prozess der In-vitro-Angiogenese notwendig für die Stadien der Migration, Proliferation und Lumenbildung ist. Der TPI-Knockdown führte zu einer Verzögerung der In-vitro-Angiogenese, was vermuten lässt, dass TPI die angiogene Potenz vom ECs erhöht. Die konstante Expression vom TPI und der mit dem Abfall der TPI-Expression assoziiert Zelltod, lässt auf den essenziellen Charakter von TPI für das Überleben der Zellen schließen. Die native MAT2A-Expression war zu Beginn und am Ende der In-vitro-Angiogenese am stärksten. MAT2A besitzt vorwiegend regulierende Funktionen durch Methylierungen und ist dadurch vermutlich ein Protein, das besonders in ruhenden ECs exprimiert wird und an deren Maturation beteiligt ist. Beide Studien zeigten die Tendenz einer verringerten MAT2A-Expression in Verbindung mit einer geringeren angiogenen Potenz, welches die Vermutung unterstützt, dass MAT2A vornehmlich anti-angiogene Effekte auf HDMECs hat. Zusätzlich wurden beide Chargen anhand ihrer VEGFR-1 und VEGFR-2 Expression charakterisiert. Es wurde gezeigt, dass HD1 eine höhere Anzahl an Stalk cells besaß, wodurch angenommen wird, dass HD1 eine höhere proliferative Kraft besitzt, welche zu einer höheren Zelldichte und zu höheren Werten bei der Quantifizierung der In-vitro-Angiogenese führte. Dies könnte auch der Grund dafür sein, dass in HD1 die VIM-Expression geringer und die TPI-Expression höher war als bei HD2. Darüber hinaus konnte in HD2 eine Beschleunigung der In-vitro-Angiogenese beobachtet werden, welche mit höheren MAT2A-C_t-Werten einherging. Des Weiteren zeigten Knockdown-Zellen von HD1 eine Erhöhung der Zelldichte und das Voranschreiten in höhere Stadien, wohingegen Knockdown-Zellen von HD2 entweder in einem frühen Stadium stagnierten oder zugrunde gingen. Zudem zeigte selbst die Kontrollgruppen von HD2 eine Verzögerung der In-vitro-Angiogenese, während die Kontrollgruppen von HD1 unbeeinflusst waren. Insgesamt wird deutlich, dass es für den Einsatz von ECs in In-vitro-Studien und die Interpretation von Forschungsergebnissen zwingend notwendig ist, Zellkulturen zu charakterisieren.

Es ist angeraten, die Experimente unter Verwendung von Zellen unterschiedlicher Hersteller und unter Einsatz von nicht-angiogenen ECs zu wiederholen, eine weitere Nachweismethode zur Zellcharakterisierung hinzuzuziehen und eine Validierung der Proteineffekte mittels spezifischer Assays durchzuführen. Um die Ergebnisse auf das lebende System zu transferieren, sind Versuche notwendig, die mehr als eine Zellart aufweisen, gefolgt von In-vivo-Studien. Es ist angeraten einen MAT2A-Knockdown zu initiieren und weitere Proteine zu untersuchen, die potenziellen pro- oder anti-angiogenen Einfluss auf ECs haben. Des Weiteren sollten zukünftige Projekte auf die Entwicklung und Optimierung der Zellcharakterisierung abzielen, um die Reproduzierbarkeit und die Zuverlässigkeit von Studien im Bereich der In-vitro-Angiogenese zu verbessern.

7. References

Adair, T. H. and J.-P. Montani (2010):
Overview of Angiogenesis.
Angiogenesis. T. H. Adair and J.-P. Montani, Morgan & Claypool Life Sciences.

Aird, W. C. (2012):
Endothelial cell heterogeneity.
Cold Spring Harbor Perspectives in Medicine 2: a006429. DOI: 10.1101/cshperspect.a006429.

Albertin, G., D. Guidolin, E. Sorato, R. Spinazzi, A. Mascarin, B. Oselladore, M. Montopoli, M. Antonello and D. Ribatti (2009):
Pro-angiogenic activity of Urotensin-II on different human vascular endothelial cell populations.
Regulatory Peptides 157: 64–71. DOI: 10.1016/j.regpep.2009.04.006.

Antfolk, D., M. Sjöqvist, F. Cheng, K. Isoniemi, C. L. Duran, A. Rivero-Muller, C. Antila, R. Niemi, S. Landor, C. V. C. Bouten, K. J. Bayless, J. E. Eriksson and C. M. Sahlgren (2017):
Selective regulation of Notch ligands during angiogenesis is mediated by vimentin.
Proceedings of the National Academy of Sciences of the United States of America 114: E4574-E4581. DOI: 10.1073/pnas.1703057114.

Antohe, F. (2006):
Endothelial cells and macrophages, partners in atherosclerotic plaque progression.
Archives of physiology and biochemistry 112: 245–253. DOI: 10.1080/13813450601094706.

Auerbach, R., R. Lewis, B. Shinners, L. Kubai and N. Akhtar (2003):
Angiogenesis assays: a critical overview.
Clinical chemistry 49: 32–40. DOI: 10.1373/49.1.32.

Bahramsoltani, M. and W. De Spiegelaere (2016):
Quantitation of Tumor Angiogenesis In Vitro: An All-In-One Angiogenesis Assay.
Methods in molecular biology (Clifton, N.J.) 1464: 185–191. DOI: 10.1007/978-1-4939-3999-2_17.

Bahramsoltani, M., W. De Spiegelaere, P. Janczyk, B. Hiebl, P. Cornillie and J. Plendl (2010):
Quantitation of angiogenesis in vitro induced by VEGF-A and FGF-2 in two different human endothelial cultures - an all-in-one assay.
Clinical Hemorheology and Microcirculation 46: 189–202. DOI: 10.3233/ch-2010-1345.

Bahramsoltani, M., T. Harms, B. Drewes and J. Plendl (2013):
Searching for markers to identify angiogenic endothelial cells: a proteomic approach.
Clinical Hemorheology and Microcirculation 55: 255–269. DOI: 10.3233/ch-2012-1631.

Bahramsoltani, M. and J. Plendl (2004):
Ein neues in vitro Modell zur Quantifizierung der Angiogenese.
ALTEX 21: 227–244.

Bahramsoltani, M. and J. Plendl (2007):
Different ways to antiangiogenesis by angiostatin and suramin, and quantitation of angiostatin-induced antiangiogenesis.
APMIS : acta pathologica, microbiologica, et immunologica Scandinavica 115: 30–46.
DOI: 10.1111/j.1600-0463.2007.apm_405.x.

Bahramsoltani, M., I. Slosarek, W. De Spiegelaere and J. Plendl (2014):
Angiogenesis and collagen type IV expression in different endothelial cell culture systems.
Anatomia, histologia, embryologia 43: 103–115. DOI: 10.1111/ahe.12052.

Banerjee, S. and M. Bacanamwo (2010):
DNA methyltransferase inhibition induces mouse embryonic stem cell differentiation into endothelial cells.
Experimental Cell Research 316: 172–180. DOI: 10.1016/j.yexcr.2009.08.011.

Blacher, S., L. Devy, M. F. Burbridge, G. Roland, G. Tucker, A. Noël and J. M. Foidart (2001):
Improved quantification of angiogenesis in the rat aortic ring assay.
Angiogenesis 4: 133–142. DOI: 10.1023/a:1012251229631.

Borselli, C., O. Oliviero, S. Battista, L. Ambrosio and P. A. Netti (2007):
Induction of directional sprouting angiogenesis by matrix gradients.
Journal of biomedical materials research. Part A 80: 297–305. DOI: 10.1002/jbm.a.30896.

Bouïs, D., Y. Kusumanto, C. Meijer, N. H. Mulder and G. A. P. Hospers (2006):
A review on pro- and anti-angiogenic factors as targets of clinical intervention.
Pharmacological research 53: 89–103. DOI: 10.1016/j.phrs.2005.10.006.

Boyden, S. (1962):
The chemotactic effect of mixtures of antibody and antigen on polymorphonuclear leucocytes.
The Journal of experimental medicine 115: 453–466. DOI: 10.1084/jem.115.3.453.

Buchmaier, B. S., A. Bibi, G. A. Müller, G. H. Dihazi, M. Eltoweissy, J. Kruegel and H. Dihazi (2013):
Renal cells express different forms of vimentin: the independent expression alteration of these forms is important in cell resistance to osmotic stress and apoptosis.
PLOS ONE 8: e68301. DOI: 10.1371/journal.pone.0068301.

Burri, P. H., R. Hlushchuk and V. Djonov (2004):
Intussusceptive angiogenesis: its emergence, its characteristics, and its significance.
Developmental dynamics : an official publication of the American Association of Anatomists 231: 474–488. DOI: 10.1002/dvdy.20184.

Cao, Y., R. Langer and N. Ferrara (2023):
Targeting angiogenesis in oncology, ophthalmology and beyond.
Nature Reviews Drug Discovery 22: 476–495. DOI: 10.1038/s41573-023-00671-z.

Cao, Z., A. Ramadan, A. Tai, F. Zetterberg and N. Panjwani (2024):
Anti-Angiogenic and Anti-Scarring Dual Effect of Galectin-3 Inhibition in Mouse Models of Corneal Wound Healing.
Am J Pathol 194: 447-458. DOI: 10.1016/j.ajpath.2023.11.018.

Carmeliet, P. and R. K. Jain (2000):
Angiogenesis in cancer and other diseases.
Nature 407: 249–257. DOI: 10.1038/35025220.

Cesari, C. d., I. Barravecchia, O. V. Pyankova, M. Vezza, M. M. Germani, F. Scebba, J. J. W. A. van Loon and D. Angeloni (2020):
Hypergravity Activates a Pro-Angiogenic Homeostatic Response by Human Capillary Endothelial Cells.
International Journal of Molecular Sciences 21: 2354. DOI: 10.3390/ijms21072354.

Chen, L., X. Liu, H. Zhou, G. Li, F. Huang, J. Zhang, T. Xia, W. Lei, J. Zhao, C. Li and M. Chen (2021):
Activating transcription factor 4 regulates angiogenesis under lipid overload via methionine adenosyltransferase 2A-mediated endothelial epigenetic alteration.
The FASEB Journal 35: e21612. DOI: 10.1096/fj.202100233R.

Danielsson, F., M. K. Peterson, H. Caldeira Araújo, F. Lautenschläger and A. K. B. Gad (2018):
Vimentin Diversity in Health and Disease.
Cells 7: 147. DOI: 10.3390/cells7100147.

Dave, J. M. and K. J. Bayless (2014):
Vimentin as an integral regulator of cell adhesion and endothelial sprouting.
Microcirculation 21: 333–344. DOI: 10.1111/micc.12111.

Dayekh, K. and K. Mequanint (2023):
3D Co-culture Model on the Role of Vimentin in Notch Signaling and Vascularization.
bioRxiv: 2023.2003.2002.530837. DOI: 10.1101/2023.03.02.530837.

De Bock, K., F. De Smet, R. L. De Oliveira, K. Anthonis and P. Carmeliet (2009):
Endothelial oxygen sensors regulate tumor vessel abnormalization by instructing phalanx endothelial cells.
Journal of Molecular Medicine-Jmm 87: 561-569. DOI: 10.1007/s00109-009-0482-z.

De Spiegelaere, W., C. Casteleyn, W. van den Broeck, J. Plendl, M. Bahramsoltani, P. Simoens, V. Djonov and P. Cornillie (2012):
Intussusceptive angiogenesis: a biologically relevant form of angiogenesis.
Journal of vascular research 49: 390–404. DOI: 10.1159/000338278.

De Spiegelaere, W., P. Cornillie, W. van den Broeck, J. Plendl and M. Bahramsoltani (2011):
Angiopoietins differentially influence in vitro angiogenesis by endothelial cells of different origin.
Clinical Hemorheology and Microcirculation 48: 15–27. DOI: 10.3233/ch-2011-1393.

Deliyanti, D., W. A. Figgett, T. Gebhardt, J. A. Trapani, F. Mackay and J. L. Wilkinson-Berka (2023):
CD8+ T Cells Promote Pathological Angiogenesis in Ocular Neovascular Disease.
Arteriosclerosis, thrombosis, and vascular biology 43: 522–536.
DOI: 10.1161/atvbaha.122.318079.
Deveza, L., J. Choi and F. Yang (2012):
Therapeutic angiogenesis for treating cardiovascular diseases.
Theranostics 2: 801–814. DOI: 10.7150/thno.4419.

Diaz-Flores, L., R. Gutierrez, M. Gonzalez-Gomez, M. D. P. Garcia, J. L. Carrasco-Juan, P. Martin-Vasallo, J. F. Madrid and L. Diaz-Flores, Jr. (2024):
Phenomena of Intussusceptive Angiogenesis and Intussusceptive Lymphangiogenesis in Blood and Lymphatic Vessel Tumors.
Biomedicines 12. DOI: 10.3390/biomedicines12020258.

Djonov, V., O. Baum and P. H. Burri (2003):
Vascular remodeling by intussusceptive angiogenesis.
Cell and Tissue Research 314: 107–117. DOI: 10.1007/s00441-003-0784-3.

Doke, S. K. and S. C. Dhawale (2015):
Alternatives to animal testing: A review.
Saudi Pharmaceutical Journal 23: 223–229. DOI: 10.1016/j.jsps.2013.11.002.

Du, W., L. Ren, M. H. Hamblin and Y. Fan (2021):
Endothelial Cell Glucose Metabolism and Angiogenesis.
Biomedicines 9: 147. DOI: 10.3390/biomedicines9020147.

Dudley, A. C. and A. W. Griffioen (2023):
Pathological angiogenesis: mechanisms and therapeutic strategies.
Angiogenesis 26: 313–347. DOI: 10.1007/s10456-023-09876-7.

Dumas, S. J., M. García-Caballero and P. Carmeliet (2020):
Metabolic Signatures of Distinct Endothelial Phenotypes.
Trends in endocrinology and metabolism: TEM 31: 580–595. DOI:
10.1016/j.tem.2020.05.009.

Engelse, M. A., N. Laurens, R. E. Verloop, P. Koolwijk and V. W. M. van Hinsbergh (2008):
Differential gene expression analysis of tubule forming and non-tubule forming endothelial cells: CDC42GAP as a counter-regulator in tubule formation.
Angiogenesis 11: 153–167. DOI: 10.1007/s10456-007-9086-9.

Esparza, A., N. Jimenez, E. A. Borrego, S. Browne and S. L. Natividad-Diaz (2024):
Review: Human stem cell-based 3D in vitro angiogenesis models for preclinical drug screening applications.
Mol Biol Rep 51: 260. DOI: 10.1007/s11033-023-09048-2.

Fan, F., A. Schimming, D. Jaeger and K. Podar (2012):
Targeting the tumor microenvironment: focus on angiogenesis.
Journal of oncology 2012: 281261. DOI: 10.1155/2012/281261.

Ferrara, N., K. J. Hillan and W. Novotny (2005):
Bevacizumab (Avastin), a humanized anti-VEGF monoclonal antibody for cancer therapy.
Biochemical and Biophysical Research Communications 333: 328–335. DOI:
10.1016/j.bbrc.2005.05.132.

Firestone, R. S. and V. L. Schramm (2017):
The Transition-State Structure for Human MAT2A from Isotope Effects.
Journal of the American Chemical Society 139: 13754–13760. DOI: 10.1021/jacs.7b05803.

Ghoochani, A., E. Yakubov, T. Sehm, Z. Fan, S. Hock, M. Buchfelder, I. Y. Eyupoglu and N. E. Savaskan (2016):
A versatile ex vivo technique for assaying tumor angiogenesis and microglia in the brain.
Oncotarget 7: 1838-1853. DOI: 10.18632/oncotarget.6550.

Gimbrone, M. A., R. S. Cotran, S. B. Leapman and J. Folkman (1974):
Tumor growth and neovascularization: an experimental model using the rabbit cornea.
Journal of the National Cancer Institute 52: 413–427. DOI: 10.1093/jnci/52.2.413.

Goodwin, A. M. (2007):
In vitro assays of angiogenesis for assessment of angiogenic and anti-angiogenic agents.
Microvascular research 74: 172–183. DOI: 10.1016/j.mvr.2007.05.006.

Guerrero, F., A. Carmona, M. J. Jimenez, T. Obrero, V. Pulido, J. A. Moreno, S. Soriano, A. Martin-Malo and P. Aljama (2021):
Passage Number-Induced Replicative Senescence Modulates the Endothelial Cell Response to Protein-Bound Uremic Toxins.
Toxins (Basel) 13. DOI: 10.3390/toxins13100738.

Guo, Y., S. Zhang, D. Wang, B. C. Heng and X. Deng (2024):
Role of cell rearrangement and related signaling pathways in the dynamic process of tip cell selection.
Cell Commun Signal 22: 24. DOI: 10.1186/s12964-023-01364-1.

Herre, C., A. Nshdejan, R. Klopfleisch, G. M. Corte and M. Bahramsoltani (2022):
Expression of vimentin, TPI and MAT2A in human dermal microvascular endothelial cells during angiogenesis in vitro.
PLOS ONE 17: e0266774. DOI: 10.1371/journal.pone.0266774.

Herre, C., A. Nshdejan, R. Klopfleisch, G. M. Corte and M. Bahramsoltani (2023):
Knockdown of TPI in human dermal microvascular endothelial cells and its impact on angiogenesis in vitro.
PLOS ONE 18: e0294933. DOI: 10.1371/journal.pone.0294933.

Hewett, P. W. (2016):
Isolation and Culture of Human Endothelial Cells from Micro- and Macro-vessels.
Methods in molecular biology (Clifton, N.J.) 1430: 61–76. DOI: 10.1007/978-1-4939-3628-1_4.

Hirschberg, R. M., M. Sachtleben and J. Plendl (2005):
Electron microscopy of cultured angiogenic endothelial cells.
Microscopy research and technique 67: 248–259. DOI: 10.1002/jemt.20204.

Huinen, Z. R., E. J. M. Huijbers, J. R. van Beijnum, P. Nowak-Sliwinska and A. W. Griffioen (2021):
Anti-angiogenic agents - overcoming tumour endothelial cell anergy and improving immunotherapy outcomes.
Nat Rev Clin Oncol 18: 527-540. DOI: 10.1038/s41571-021-00496-y.

Hunter, O. V., J. C. Ruiz, J. N. Flaherty and N. K. Conrad (2023):
Functional analysis of 3'-UTR hairpins supports a two-tiered model for posttranscriptional regulation of MAT2A by METTL16.
RNA 29: 1725–1737. DOI: 10.1261/rna.079695.123.

Jardim-Perassi, B. V., A. S. Arbab, L. C. Ferreira, T. F. Borin, N. R. S. Varma, A. S. M. Iskander, A. Shankar, M. M. Ali and D. A. P. d. Campos Zuccari (2014):
Effect of melatonin on tumor growth and angiogenesis in xenograft model of breast cancer.
PLOS ONE 9: e85311. DOI: 10.1371/journal.pone.0085311.

Jayson, G. C., D. J. Hicklin and L. M. Ellis (2012):
Antiangiogenic therapy--evolving view based on clinical trial results.
Nature reviews. Clinical oncology 9: 297–303. DOI: 10.1038/nrclinonc.2012.8.

Jeanneau, C., J.-H. Catherine, T. Giraud, R. Lan and I. About (2024):
The Added Value of a Collagenated Thermosensitive Bone Substitute as a Scaffold for Bone Regeneration.
Materials 17. DOI: 10.3390/ma17030625.

Kalluri, R. (2003):
Basement membranes: structure, assembly and role in tumour angiogenesis.
Nature Reviews Cancer 3: 422–433. DOI: 10.1038/nrc1094.

Khoury, C. C. and F. N. Ziyadeh (2011):
Angiogenic factors.
Contributions to nephrology 170: 83–92. DOI: 10.1159/000324950.

Kim, S., J. Lee, J. Ko, S. Park, S. R. Lee, Y. Kim, T. Lee, S. Choi, J. Kim, W. Kim, Y. Chung, O. H. Kwon and N. L. Jeon (2024):
Angio-Net: deep learning-based label-free detection and morphometric analysis of in vitro angiogenesis.
Lab Chip 24: 751-763. DOI: 10.1039/d3lc00935a.

Kist, M. and D. Vucic (2021):
Cell death pathways: intricate connections and disease implications.
The EMBO journal 40: e106700. DOI: 10.15252/embj.2020106700.

Kuwano, M., J. Fukushi, M. Okamoto, A. Nishie, H. Goto, T. Ishibashi and M. Ono (2001):
Angiogenesis factors.
Internal medicine (Tokyo, Japan) 40: 565–572. DOI: 10.2169/internalmedicine.40.565.

Leblanc, A. J., L. Krishnan, C. J. Sullivan, S. K. Williams and J. B. Hoying (2012):
Microvascular Repair: Post-Angiogenesis Vascular Dynamics.
Microcirculation 19: 676-695. DOI: 10.1111/j.1549-8719.2012.00207.x.

Li, C., G. Gui, L. Zhang, A. Qin, C. Zhou and X. Zha (2022):
Overview of Methionine Adenosyltransferase 2A (MAT2A) as an Anticancer Target: Structure, Function, and Inhibitors.
Journal of Medicinal Chemistry 65: 9531–9547. DOI: 10.1021/acs.jmedchem.2c00395.

Liu, T., O. E. Guevara, R. R. Warburton, N. S. Hill, M. Gaestel and U. S. Kayyali (2010):
Regulation of vimentin intermediate filaments in endothelial cells by hypoxia.
American journal of physiology. Cell physiology 299: C363-373. DOI: 10.1152/ajpcell.00057.2010.

Lopes-Coelho, F., F. Martins, S. A. Pereira and J. Serpa (2021):
Anti-Angiogenic Therapy: Current Challenges and Future Perspectives.
International Journal of Molecular Sciences 22. DOI: ARTN 3765 10.3390/ijms22073765.

Lu, H., X. Xu, M. Zhang, R. Cao, E. Bråkenhielm, C. Li, H. Lin, G. Yao, H. Sun, L. Qi, M. Tang, H. Dai, Y. Zhang, R. Su, Y. Bi, Y. Zhang and Y. Cao (2007):
Combinatorial protein therapy of angiogenic and arteriogenic factors remarkably improves collaterogenesis and cardiac function in pigs.
Proceedings of the National Academy of Sciences of the United States of America 104: 12140–12145. DOI: 10.1073/pnas.0704966104.

Lu, S. C. and J. M. Mato (2008):
S-Adenosylmethionine in cell growth, apoptosis and liver cancer.
Journal of Gastroenterology and Hepatology 23 Suppl 1: S73-77. DOI: 10.1111/j.1440-1746.2007.05289.x.

Lu, S. C., K. Ramani, X. Ou, M. Lin, V. Yu, K. Ko, R. Park, T. Bottiglieri, H. Tsukamoto, G. Kanel, S. W. French, J. M. Mato, R. Moats and E. Grant (2009):
S-adenosylmethionine in the chemoprevention and treatment of hepatocellular carcinoma in a rat model.
Hepatology 50: 462–471. DOI: 10.1002/hep.22990.

Maacha, S., H. Sidahmed, S. Jacob, G. Gentilcore, R. Calzone, J. C. Grivel and C. Cugno (2020):
Paracrine Mechanisms of Mesenchymal Stromal Cells in Angiogenesis.
Stem Cells Int 2020: 4356359. DOI: 10.1155/2020/4356359.

Makode, S., S. Maurya, S. Niknam, E. Mollocana-Lara, K. Jaberi, N. Faramarzi, A. Tamayol and M. Mortazavi (2024):
Three dimensional (bio)printing of blood vessels: from vascularized tissues to functional arteries.
Biofabrication. DOI: 10.1088/1758-5090/ad22ed.

Marin, V., G. Kaplanski, S. Grès, C. Farnarier and P. Bongrand (2001):
Endothelial cell culture: protocol to obtain and cultivate human umbilical endothelial cells.
Journal of immunological methods 254: 183–190. DOI: 10.1016/s0022-1759(01)00408-2.

Marrelli, A., P. Cipriani, V. Liakouli, F. Carubbi, C. Perricone, R. Perricone and R. Giacomelli (2011):
Angiogenesis in rheumatoid arthritis: a disease specific process or a common response to chronic inflammation?
Autoimmunity reviews 10: 595–598. DOI: 10.1016/j.autrev.2011.04.020.

Maurya, S., D. Prasad and S. Mukherjee (2024):
Matrix Metalloproteinases in Oral Cancer Pathogenesis and their Use in Therapy.
Anticancer Agents Med Chem 24: 3-17. DOI: 10.2174/0118715206270002231108071917.

Mehta, D. and A. B. Malik (2006):
Signaling mechanisms regulating endothelial permeability.
Physiological reviews 86: 279–367. DOI: 10.1152/physrev.00012.2005.

Mentzer, S. J. and M. A. Konerding (2014):
Intussusceptive angiogenesis: expansion and remodeling of microvascular networks.
Angiogenesis 17: 499–509. DOI: 10.1007/s10456-014-9428-3.

Mishra, N., R. Kant, K. Kandhari, D. A. Ammar, N. Tewari-Singh, M. B. Pantcheva, J. M. Petrash, C. Agarwal and R. Agarwal (2024):
Nitrogen Mustard-Induced Ex Vivo Human Cornea Injury Model and Therapeutic Intervention by Dexamethasone.
J Pharmacol Exp Ther 388: 484-494. DOI: 10.1124/jpet.123.001760.

Myers, T. D. and M. J. Palladino (2023):
Newly discovered roles of triosephosphate isomerase including functions within the nucleus.
Molecular Medicine 29: 1–6. DOI: 10.1186/s10020-023-00612-x.

Naschberger, E., M. Bauer and M. Stürzl (2005):
Human guanylate binding protein-1 (hGBP-1) characterizes and establishes a non-angiogenic endothelial cell activation phenotype in inflammatory diseases.
Advances in Enzyme Regulation 45: 215–227. DOI: 10.1016/j.advenzreg.2005.02.011.

Nathan, J., R. Shameera, N. Devarajan and E. Perumal (2024):
Role of berberine on angiogenesis and blood flow hemodynamics using zebrafish model.
J Appl Toxicol 44: 165-174. DOI: 10.1002/jat.4529.

Nicosia, R. F. and A. Ottinetti (1990):
Growth of microvessels in serum-free matrix culture of rat aorta. A quantitative assay of angiogenesis in vitro.
Laboratory investigation; a journal of technical methods and pathology 63: 115–122.

Nosrati, H., R. Aramideh Khouy, A. Nosrati, M. Khodaei, M. Banitalebi-Dehkordi, K. Ashrafi-Dehkordi, S. Sanami and Z. Alizadeh (2021):
Nanocomposite scaffolds for accelerating chronic wound healing by enhancing angiogenesis.
Journal of Nanobiotechnology 19: 1. DOI: 10.1186/s12951-020-00755-7.

Nowak-Sliwinska, P., K. Alitalo, E. Allen, A. Anisimov, A. C. Aplin, R. Auerbach, H. G. Augustin, D. O. Bates, J. R. van Beijnum, R. H. F. Bender, G. Bergers, A. Bikfalvi, J. Bischoff, B. C. Böck, P. C. Brooks, F. Bussolino, B. Cakir, P. Carmeliet, D. Castranova, A. M. Cimpean, O. Cleaver, G. Coukos, G. E. Davis, M. d. Palma, A. Dimberg, R. P. M. Dings, V. Djonov, A. C. Dudley, N. P. Dufton, S.-M. Fendt, N. Ferrara, M. Fruttiger, D. Fukumura, B. Ghesquière, Y. Gong, R. J. Griffin, A. L. Harris, C. C. W. Hughes, N. W. Hultgren, M. L. Iruela-Arispe, M. Irving, R. K. Jain, R. Kalluri, J. Kalucka, R. S. Kerbel, J. Kitajewski, I. Klaassen, H. K. Kleinmann, P. Koolwijk, E. Kuczynski, B. R. Kwak, K. Marien, J. M. Melero-Martin, L. L.

Munn, R. F. Nicosia, A. Noel, J. Nurro, A.-K. Olsson, T. V. Petrova, K. Pietras, R. Pili, J. W. Pollard, M. J. Post, P. H. A. Quax, G. A. Rabinovich, M. Raica, A. M. Randi, D. Ribatti, C. Ruegg, R. O. Schlingemann, S. Schulte-Merker, L. E. H. Smith, J. W. Song, S. A. Stacker, J. Stalin, A. N. Stratman, M. van de Velde, V. W. M. van Hinsbergh, P. B. Vermeulen, J. Waltenberger, B. M. Weinstein, H. Xin, B. Yetkin-Arik, S. Yla-Herttuala, M. C. Yoder and A. W. Griffioen (2018):
Consensus guidelines for the use and interpretation of angiogenesis assays.
Angiogenesis 21: 425–532. DOI: 10.1007/s10456-018-9613-x.

Omorphos, N. P., C. Gao, S. S. Tan and M. S. Sangha (2021):
Understanding angiogenesis and the role of angiogenic growth factors in the vascularisation of engineered tissues.
Molecular Biology Reports 48: 941–950. DOI: 10.1007/s11033-020-06108-9.

Orosz, F., J. Oláh and J. Ovádi (2009):
Triosephosphate isomerase deficiency: new insights into an enigmatic disease.
Biochimica et biophysica acta 1792: 1168–1174. DOI: 10.1016/j.bbadis.2009.09.012.

Orozco-Garcia, E., V. Getova, J. C. Calderon, M. C. Harmsen and R. Narvaez-Sanchez (2024):
Angiogenesis is promoted by hypoxic cervical carcinoma-derived extracellular vesicles depending on the endothelial cell environment.
Vascul Pharmacol 154: 107276. DOI: 10.1016/j.vph.2024.107276.

Pascale, R. M., M. M. Simile, D. F. Calvisi, C. F. Feo and F. Feo (2022):
S-Adenosylmethionine: From the Discovery of Its Inhibition of Tumorigenesis to Its Use as a Therapeutic Agent.
Cells 11: 409. DOI: 10.3390/cells11030409.

Pasipoularides, A. (2014):
Galen, father of systematic medicine. An essay on the evolution of modern medicine and cardiology.
International Journal of Cardiology 172: 47–58. DOI: 10.1016/j.ijcard.2013.12.166.

Patan, S. (2000):
Vasculogenesis and angiogenesis as mechanisms of vascular network formation, growth and remodeling.
Journal of Neuro-Oncology 50: 1–15. DOI: 10.1023/a:1006493130855.

Pathak, A., A. K. Pal, S. Roy, M. Nandave and K. Jain (2024):
Role of Angiogenesis and Its Biomarkers in Development of Targeted Tumor Therapies.
Stem Cells Int 2024: 9077926. DOI: 10.1155/2024/9077926.

Patteson, A. E., A. Vahabikashi, R. D. Goldman and P. A. Janmey (2020):
Mechanical and Non-Mechanical Functions of Filamentous and Non-Filamentous Vimentin.
BioEssays : news and reviews in molecular, cellular and developmental biology 42:
e2000078. DOI: 10.1002/bies.202000078.

Paulin, D., A. Lilienbaum, S. Kardjian, O. Agbulut and Z. Li (2022):
Vimentin: Regulation and pathogenesis.
Biochimie 197: 96–112. DOI: 10.1016/j.biochi.2022.02.003.

Presta, L. G., H. Chen, S. J. O'Connor, V. Chisholm, Y. G. Meng, L. Krummen, M. Winkler and N. Ferrara (1997):
Humanization of an anti-vascular endothelial growth factor monoclonal antibody for the therapy of solid tumors and other disorders.
Cancer research 57.

Pries, A. R., B. Reglin, M. W. Dewhirst and T. W. Secomb (2014):
Making microvascular networks work: angiogenesis, remodeling and pruning.
Angiogenesis 17: 716-716.

Qiu, J., H.-Q. Gao, R.-H. Zhou, Y. Liang, X.-H. Zhang, X.-P. Wang, B.-A. You and M. Cheng (2007):
Proteomics analysis of the proliferative effect of low-dose ouabain on human endothelial cells.
Biological & pharmaceutical bulletin 30: 247–253. DOI: 10.1248/bpb.30.247.

Rajabi, M., Z. Hossaini, M. A. Khalilzadeh, S. Datta, M. Halder and S. A. Mousa (2015):
Synthesis of a new class of furo3,2-ccoumarins and its anticancer activity.
Journal of photochemistry and photobiology. B, Biology 148: 66–72. DOI:
10.1016/j.jphotobiol.2015.03.027.

Rezzola, S., M. Belleri, D. Ribatti, C. Costagliola, M. Presta and F. Semeraro (2013):
A novel ex vivo murine retina angiogenesis (EMRA) assay.
Experimental eye research 112: 51–56. DOI: 10.1016/j.exer.2013.04.014.

Ribatti, D. (2008):
Judah Folkman, a pioneer in the study of angiogenesis.
Angiogenesis 11: 3–10. DOI: 10.1007/s10456-008-9092-6.

Ribatti, D. and E. Crivellato (2012):
"Sprouting angiogenesis", a reappraisal.
Developmental Biology 372: 157–165. DOI: 10.1016/j.ydbio.2012.09.018.

Ribatti, D., B. Nico, A. Vacca, L. Roncali and F. Dammacco (2002):
Endothelial cell heterogeneity and organ specificity.
Journal of hematotherapy & stem cell research 11: 81–90. DOI:
10.1089/152581602753448559.

Risau, W. (1997):
Mechanisms of angiogenesis.
Nature 386: 671–674. DOI: 10.1038/386671a0.

Rodríguez-Bolaños, M. and R. Perez-Montfort (2019):
Medical and Veterinary Importance of the Moonlighting Functions of Triosephosphate Isomerase.
Current protein & peptide science 20: 304–315. DOI:
10.2174/1389203719666181026170751.

Russell, W. M. S. and R. L. Burch (1992):
The principles of humane experimental technique.
Potters Bar, Herts., Universities Federation for Animal Welfare.

Rusu, M. C., C. V. Poalelungi, A. D. Vrapciu, M. I. Nicolescu, S. Hostiuc, L. Mogoanta and T. Taranu (2015):
Endocardial tip cells in the human embryo - facts and hypotheses.
PLOS ONE 10: e0115853. DOI: 10.1371/journal.pone.0115853.

Sacharidou, A., A. N. Stratman and G. E. Davis (2012):
Molecular mechanisms controlling vascular lumen formation in three-dimensional extracellular matrices.
Cells, tissues, organs 195: 122–143. DOI: 10.1159/000331410.

Sahin, M., E. Sahin, S. Gümüşlü, A. Erdoğan and M. Gültekin (2010):
DNA methylation or histone modification status in metastasis and angiogenesis-related genes: a new hypothesis on usage of DNMT inhibitors and S-adenosylmethionine for genome stability.
Cancer and Metastasis Reviews 29: 655–676. DOI: 10.1007/s10555-010-9253-0.

Salewskij, K. and J. M. Penninger (2023):
Blood Vessel Organoids for Development and Disease.
Circulation research 132: 498–510. DOI: 10.1161/circresaha.122.321768.

Salzinger, B., K. Lundwall, M. Evans, J. Mörtberg, H. Wallén, T. Jernberg, T. Kahan, P. Lundman, P. Tornvall, D. Erlinge, B. Lindahl, T. Baron, M. Rezeli, J. Spaak and S. H. Jacobson (2024):
Associations between inflammatory and angiogenic proteomic biomarkers, and cardiovascular events and mortality in relation to kidney function.
Clinical Kidney Journal. DOI: 10.1093/ckj/sfae050.

Sarkanen, J.-R., M. Mannerström, H. Vuorenpää, J. Uotila, T. Ylikomi and T. Heinonen (2010):
Intra-Laboratory Pre-Validation of a Human Cell Based in vitro Angiogenesis Assay for Testing Angiogenesis Modulators.
Frontiers in Pharmacology 1: 147. DOI: 10.3389/fphar.2010.00147.

Sato, T. N., Y. Tozawa, U. Deutsch, K. Wolburg-Buchholz, Y. Fujiwara, M. Gendron-Maguire, T. Gridley, H. Wolburg, W. Risau and Y. Qin (1995):
Distinct roles of the receptor tyrosine kinases Tie-1 and Tie-2 in blood vessel formation.
Nature 376: 70–74. DOI: 10.1038/376070a0.

Shafqat, N., J. R. C. Muniz, E. S. Pilka, E. Papagrigoriou, F. v. Delft, U. Oppermann and W. W. Yue (2013):
Insight into S-adenosylmethionine biosynthesis from the crystal structures of the human methionine adenosyltransferase catalytic and regulatory subunits.
The Biochemical journal 452: 27–36. DOI: 10.1042/bj20121580.

Shaw, P., S. K. D. Dwivedi, R. Bhattacharya, P. Mukherjee and G. Rao (2024):
VEGF signaling: Role in angiogenesis and beyond.
Biochim Biophys Acta Rev Cancer 1879: 189079. DOI: 10.1016/j.bbcan.2024.189079.

Sherwood, L. M., E. E. Parris and J. Folkman (1971):
Tumor Angiogenesis: Therapeutic Implications.
New England Journal of Medicine 285: 1182–1186. DOI: 10.1056/nejm197111182852108.

Sievers, H., M. Bahramsoltani, S. Kässmeyer and J. Plendl (2011):
In vitro angiogenic potency in human microvascular endothelial cells derived from myocardium, lung and skin.
Clinical Hemorheology and Microcirculation 49: 473–486. DOI: 10.3233/ch-2011-1497.

Sievers, H., R. M. Hirschberg, B. Hiebl, H. Hünigen and J. Plendl (2015):
Human microvascular endothelial cells displaying reduced angiogenesis and increased uptake of lipids during in vitro culture.
Clinical Hemorheology and Microcirculation 61: 367–383. DOI: 10.3233/ch-152002.

Silva, E. A., C. Eseonu and D. J. Mooney (2014):
Endothelial cells expressing low levels of CD143 (ACE) exhibit enhanced sprouting and potency in relieving tissue ischemia.
Angiogenesis 17: 617–630. DOI: 10.1007/s10456-014-9414-9.

Sommer, M., J. Gerth, G. Stein and G. Wolf (2005):
Transdifferentiation of endothelial and renal tubular epithelial cells into myofibroblast-like cells under in vitro conditions: a morphological analysis.
Cells, tissues, organs 180: 204–214. DOI: 10.1159/000088937.

Staton, C. A., M. W. R. Reed and N. J. Brown (2009):
A critical analysis of current in vitro and in vivo angiogenesis assays.
International journal of experimental pathology 90: 195–221. DOI: 10.1111/j.1365-2613.2008.00633.x.

Staton, C. A., S. M. Stribbling, S. Tazzyman, R. Hughes, N. J. Brown and C. E. Lewis (2004):
Current methods for assaying angiogenesis in vitro and in vivo.
International journal of experimental pathology 85: 233–248. DOI: 10.1111/j.0959-9673.2004.00396.x.

Stryker, Z. I., M. Rajabi, P. J. Davis and S. A. Mousa (2019):
Evaluation of Angiogenesis Assays.
Biomedicines 7: 37. DOI: 10.3390/biomedicines7020037.

Suprewicz, Ł., M. Zakrzewska, S. Okła, K. Głuszek, A. Sadzyńska, P. Deptuła, K. Fiedoruk and R. Bucki (2024):
Extracellular vimentin as a modulator of the immune response and an important player during infectious diseases.
Immunology and Cell Biology. DOI: 10.1111/imcb.12721.

Tahergorabi, Z. and M. Khazaei (2012):
A review on angiogenesis and its assays.
Iranian journal of basic medical sciences 15: 1110–1126.

Tsuruta, D. and J. C. R. Jones (2003):
The vimentin cytoskeleton regulates focal contact size and adhesion of endothelial cells subjected to shear stress.
Journal of Cell Science 116: 4977–4984. DOI: 10.1242/jcs.00823.

Udvadia, A. J. and E. Linney (2003):
Windows into development: historic, current, and future perspectives on transgenic zebrafish.
Developmental Biology 256: 1–17. DOI: 10.1016/s0012-1606(02)00083-0.

van Beijnum, J. R., R. P. Dings, E. van der Linden, B. M. M. Zwaans, F. C. S. Ramaekers, K. H. Mayo and A. W. Griffioen (2006):
Gene expression of tumor angiogenesis dissected: specific targeting of colon cancer angiogenic vasculature.
Blood 108: 2339–2348. DOI: 10.1182/blood-2006-02-004291.

Wang, Y., C. Muylaert, A. Wyns, P. Vlummens, K. d. Veirman, K. Vanderkerken, E. Zaal, C. Berkers, J. Moreaux, E. d. Bruyne and E. Menu (2024):
S-adenosylmethionine biosynthesis is a targetable metabolic vulnerability in multiple myeloma.
Haematologica 109: 256–271. DOI: 10.3324/haematol.2023.282866.

Wei, J., Y. Yang, Y. Li, X. Mo, X. Guo, X. Zhang, X. Xu, Z. Jiang and Q. You (2017):
Synthesis and evaluation of N-(benzofuran-5-yl)aromaticsulfonamide derivatives as novel HIF-1 inhibitors that possess anti-angiogenic potential.
Bioorganic & Medicinal Chemistry 25: 1737–1746. DOI: 10.1016/j.bmc.2016.06.021.

Werelusz, P., S. Galiniak and M. Mołoń (2024):
Molecular functions of moonlighting proteins in cell metabolic processes.
Biochimica et biophysica acta. Molecular cell research 1871: 119598.
DOI: 10.1016/j.bbamcr.2023.119598.

Wierenga, R. K., E. G. Kapetaniou and R. Venkatesan (2010):
Triosephosphate isomerase: a highly evolved biocatalyst.
Cellular and Molecular Life Sciences 67: 3961–3982. DOI: 10.1007/s00018-010-0473-9.

Yamaji, R., K. Fujita, I. Nakanishi, K. Nagao, M. Naito, T. Tsuruo, H. Inui and Y. Nakano (2004):
Hypoxic up-regulation of triosephosphate isomerase expression in mouse brain capillary endothelial cells.
Archives of Biochemistry and Biophysics 423: 332–342. DOI: 10.1016/j.abb.2004.01.003.

Yang, Y., W. Wang, G. Rademaker, M. Ravichandran, J. Hu, A. Li, J. D. Mancias, J. Y. Guo and R. M. Perera (2024a):
Abstract C053: Autophagy regulates MAT2A in response to hypoxia in pancreatic cancer cells.
Cancer Research 84: C053-C053. DOI: 10.1158/1538-7445.Panca2023-c053.

Yang, Z., X. Zhang, X. Bai, X. Xi, W. Liu and W. Zhong (2024b):
Anti-angiogenesis in colorectal cancer therapy.
Cancer Science. DOI: 10.1111/cas.16063.

Yetkin-Arik, B., I. M. C. Vogels, N. Neyazi, V. van Duinen, R. H. Houtkooper, C. J. F. van Noorden, I. Klaassen and R. O. Schlingemann (2019):
Endothelial tip cells in vitro are less glycolytic and have a more flexible response to metabolic stress than non-tip cells.
Scientific Reports 9: 10414. DOI: 10.1038/s41598-019-46503-2.

Zafer, D., T. Adams, E. Olson, L. Stenman, O. Taparli, J. Eickhoff, P. Cengiz and O. J. Mezu-Ndubuisi (2022):
Retinal vascular recovery revealed by retinal imaging following neonatal hypoxia ischemia in mice: Is there a role for tyrosine kinase receptor modulation?
Brain Res 1796: 148093. DOI: 10.1016/j.brainres.2022.148093.

Zecchin, A., J. Kalucka, C. Dubois and P. Carmeliet (2017):
How Endothelial Cells Adapt Their Metabolism to Form Vessels in Tumors.
Frontiers in Immunology 8: 1750. DOI: 10.3389/fimmu.2017.01750.

Zhang, N. (2018):
Role of methionine on epigenetic modification of DNA methylation and gene expression in animals.
Animal nutrition (Zhongguo xu mu shou yi xue hui) 4: 11–16.
DOI: 10.1016/j.aninu.2017.08.009.

Zhao, S., C. Miao, X. Gao, Z. Li, J. E. Eriksson and Y. Jiu (2024):
Vimentin cage - A double-edged sword in host anti-infection defense.
Current Opinion in Cell Biology 86: 102317. DOI: 10.1016/j.ceb.2023.102317.

Zhong, C., P. Li, S. Argade, L. Liu, A. Chilla', W. Liang, H. Xin, B. Eliceiri, B. Choudhury and N. Ferrara (2020):
Inhibition of protein glycosylation is a novel pro-angiogenic strategy that acts via activation of stress pathways.
Nature communications 11: 6330. DOI: 10.1038/s41467-020-20108-0.

Zhou, X., Q. Xia, M. Chen, X. Zhang, M. Huang, X. Zheng, S. Wang, B. Wu and Z. Du (2024):
THBS1 promotes angiogenesis and accelerates ESCC malignant progression by the HIF-1/VEGF signaling pathway.
Cell Biol Int 48: 311-324. DOI: 10.1002/cbin.12126.

Zhu, P., L. Huang, X. Ge, F. Yan, R. Wu and Q. Ao (2006):
Transdifferentiation of pulmonary arteriolar endothelial cells into smooth muscle-like cells regulated by myocardin involved in hypoxia-induced pulmonary vascular remodelling.
International journal of experimental pathology 87: 463–474. DOI: 10.1111/j.1365-2613.2006.00503.x.

Zuo, D.-P., B. Wang, Y.-Z. Liu, Z.-S. Chen, R.-J. Hu, M.-J. He, Z.-Y. Zhang, Y. Wang and C.-G. Han (2024):
The triose phosphate/phosphate translocator exports photosynthetic glyceraldehyde 3-phosphate from chloroplasts to trigger antimicrobial immunity in plants.
bioRxiv: 2024.2001.2010.574840. DOI: 10.1101/2024.01.10.574840.

8. List of publications

Peer-reviewed Publications

Herre, C.; Nshdejan, A.; Klopfleisch, R.; Corte, G. M.; Bahramsoltani, M. (2023): **Knockdown of TPI in human dermal microvascular endothelial cells and its impact on angiogenesis in vitro**. *PLOS ONE*; **18**(12), S. e0294933

Herre, C.; Nshdejan, A.; Klopfleisch, R.; Corte, G. M.; Bahramsoltani, M. (2022): **Expression of vimentin, TPI and MAT2A in human dermal microvascular endothelial cells during angiogenesis in vitro**. *PLOS ONE;* **17**(4), S. Artikel e0266774

Abstracts for Congress Contributions

Herre, C.; Nshdejan, A.; Klopfleisch, R.; Corte, G. M.; Bahramsoltani, M. (2023):
VIM, TPI and MAT2A and their role in in vitro angiogenesis
XXXIV EAVA Congress 2023
Sundvollen, Norway – 25.07. – 29.07.2023, Talk
In: The XXXIV EAVA-congress at Sundvollen hotel 2023: congress program & book of abstracts and many mor – NMBU Norwegian University of Life Sciences, EAVA, S.23

Herre, C.; Nshdejan, A.; Klopfleisch, R.; Corte, G. M.; Bahramsoltani, M. (2022):
VIM, TPI and MAT2A - pivotal proteins for angiogenesis in vitro?
11th Meeting of the Young Generation of Veterinary Anatomists
Zurich, Switzerland – 20.07.-22.07.2022, Talk
In: 11th Meeting of the Young Generation of Veterinary Anatomists, 20th – 22nd July 2022, Zurich, Switzerland, S. 12

Herre, C.; Nshdejan, A.; Klopfleisch, R.; Corte, G. M.; Bahramsoltani, M. (2021):
Specific target proteins and their role in angiogenesis in vitro.
33rd Virtual Conference of the European Association of Veterinary Anatomists
Ghent, Belgium – 28.07.-31.07.2021, Poster
In: Anatomia, histologia, embryologia; **51**(S1), S. 28

Herre, C.; Nshdejan, A.; Bahramsoltani, M. (2019):

Vimentin knock-out and its impact on angiogenesis in vitro.

12. Doktorandensymposium & DRS Präsentationsseminar "Biomedical Sciences“

Berlin - 27.09.2019, Poster

In: Doktorandensymposium & DRS Präsentationsseminar "Biomedical Sciences" Berlin:

Mensch und Buch Verlag ISBN: 978-3-96729-006-6; **Awarded with 1st Poster prize**

9. Acknowledgements

First and foremost, I want to express my deepest gratitude to everyone who has supported me throughout my PhD studies.

Above all, I am sincerely grateful for **Prof. Mahtab Bahramsoltani** and her excellent supervision. Thank you for giving me the position as research associate, enabling my first major research project and giving me the opportunity of becoming a lecturer at the Institute of veterinary anatomy. Your continuous support, guidance and trust was the most valuable help of all.

I am deeply grateful for **Dr. Giuliano Corte** and his constant support. You were there from the beginning and helped me throughout difficult times. I will forever be grateful for your encouragement.

Special thank goes to **Prof. Klopfleisch** and his excellent supervision and constructive feedback in all supervisor meetings.

I am extremely grateful for **Arpenik Nshdejan** and her great expertise in laboratory techniques. Your outstanding knowledge and technical skills made this project come alive. Thank you so much for always making time for me and giving me exceptional advice.

Further thank goes to all **technical employees** and your great advice and constant support. I am very grateful for the amazing cooperation with employees of **AG Scharff** Verhaltensbiologie, FU Berlin. Thank you for letting us use your S2 labs and protocols for virus synthesis.

I want to express extraordinary thank to all **doctoral students** at the institute. Thank you for your collegiality, good words and fantastic humour. Thank you for creating a safe and comfortable work environment. I am endlessly grateful for the friendships that have developed.

I am thankful for all **my friends** who supported me throughout, especially **Miri and Bella**. Thank you for your endless patience and your warm words!

Großer Dank geht auch an meine **Familie,** vor allem **Gabi und Klaus Herre**. Ihr wart immer für mich da und habt mich seit Beginn meiner Karriere stets bestärkt! Danke für Eure Liebe und immerwährende Unterstützung!

Steph, my lovely wife. I will forever be endlessly grateful for your daily support. No one experienced the time as intensely as you did. You were always there, listened patiently, gave me the greatest advice and always had the best for me in mind. You gave me the strength and the motivation to achieve my goal and finish up my PhD. I love you.

10. Funding Sources

The author received no specific funding for this work.

11. Conflict of Interest

The author has declared that no competing interests exist.

12. Declaration of Authorship

I hereby declare that the thesis submitted is exclusively done by me. All direct or indirect sources used are cited as references.
This thesis was not previously presented to another examination board and has not been published before.

Berlin, den 09.07.2024 Christina Nicole Herre

mbvberlin mensch und buch verlag

49,90 Euro | ISBN: 978-3-96729-258-9